Summer 2017

Maintenance and modification of mesenchymal stromal cell immunosuppressive phenotype

Alex Joseph Brown
University of Iowa

MAINTENANCE AND MODIFICATION OF MESENCHYMAL STROMAL CELL IMMUNOSUPPRESSIVE PHENOTYPE

by

Alex Joseph Brown

A thesis submitted in partial fulfillment
of the requirements for the Master of Science
degree in Biomedical Engineering in the
Graduate College of
The University of Iowa

August 2017

Thesis Supervisor: Assistant Professor James A. Ankrum

Graduate College
The University of Iowa
Iowa City, Iowa

CERTIFICATE OF APPROVAL

_____

MASTER'S THESIS

_____

This is to certify that the Master's thesis of

Alex Joseph Brown

has been approved by the Examining Committee for
the thesis requirement for the Master of Science degree
in Biomedical Engineering at the August 2017 graduation.

Thesis Committee: _____
James Ankrum, Thesis Supervisor

_____
Edward Sander

_____
Jon Houtman

To my loving friends and family. Thank you for supporting me and providing the encouragement, as well as inspiration, to undertake this journey into Science.

“We are not made of drugs, we are made of cells.”

Cade Hildreth, Bioinformant

ACKNOWLEDGEMENTS

I would first like to express my sincerest gratitude to my advisor Prof. James Ankrum for the continuous support of my Masters study and related research. I cannot thank you enough for all the help guiding my project and in the writing of this thesis. Dr. Ankrum's humor, patience, mentorship, immense knowledge, and humility has been instrumental in my training as a developing scientist and engineer. I cannot think of a better advisor and mentor for my Masters study. I will miss you dearly when I graduate.

Besides my advisor, I would like to thank the rest of my thesis committee: Prof. Ed Sander, and Prof. John Houtman, whose rigorous coursework and pointed questions served as a necessary crucible to temper my research from various perspectives. Your insight has both challenged me to widen the scope of my academic knowledge, and subsequently allowed me to focus my interests in bioengineering.

My sincere thanks also go out to Dr. Ling Yang, Dr. Al Klingelhutz, Dr. Julien Sebag, Dr. Ashutosh Mangalam, Dr. Sam Stephens, Dr. Oliver Gramlich, Dr. Markus Kuehn, Dr. Jennifier Fiegel, Dr. Michael Welsh, and Dr. Mahmoud Abou Alaiwa, who collaborated on my projects and/or gave me access to laboratory facilities and resources necessary for the completion of this thesis.

To my fellow labmates, thank you for fighting the good fight with me in the trenches of the Ankrum Lab. Thank you for all the proofreading, feedback, stimulating discussions, and friendship over the past two years. Your dedication and work ethic in the lab is truly inspiring. You are brilliant group, and I expect to see great things from you all.

Finally, I thank my family. The support and love I have received from you has shaped me into the man I am today. For that I am forever grateful.

ABSTRACT

The purpose of this study was to identify conditioning strategies for mesenchymal stromal cells (MSC) which optimize cellular immunosuppressive potency. This work identifies new treatment strategies to stimulate and maintain MSC licensing into an immunosuppressive state. These treatment strategies may be considered as the foundation for advanced licensing approaches, capable of shifting an MSC phenotype to a produce a tailored response that can be used to treat a disease specific state. We sought to determine how MSC act in response to a changing immune response or environmental condition. MSC are exquisitely sensitive to changes in their environmental conditions and we show that cellular transcriptome and secretome changes are conditionally responsive to their inflammatory stimulus. One of the main subjects of analysis here is the observations of how these cellular profiles evolve over time in the presence of an inflammatory environment. Similarly, this study observes how MSC behavior changes after an inflammatory event has been resolved to address, in part, the plasticity of MSC licensing and the ability of MSC to rapidly recall a previous immunosuppressive state upon secondary challenge with an inflammatory stimulus. Data was obtained from *in vitro* experiments with human bone marrow derived MSC and donor human peripheral blood mononuclear cells (PBMC), while *in vivo* data was obtained using C57BL6/J mice.

Overall this research demonstrated that MSC potency can be bolstered by small molecule and drug treatment conditioning, and that certain disease conditions may be more effectively paired with specific MSC conditioning strategies to improve their therapeutic effectiveness.

PUBLIC ABSTRACT

Mesenchymal stromal cells (MSC) are an extremely promising cellular therapy for numerous diseases that are characterized by disturbances in the immune system and persistent inflammation. In recent years, there has been an improved understanding of what diseases these cell therapies are most appropriate for, as well as the biology of how these cells exert their effects. Unfortunately, our increased understanding has only minimally improved issues these therapies have with batch-to-batch consistency, and potency. By improving our understanding of how MSC behave in inflammation over time, we hope to identify an exposure regiment or drug that can be used to help improve the potency of these cell therapies. My research shows that treatment of MSC with drugs and small molecules can have dramatic effect on the cell's ability to combat inflammation and suppress an immune response. Additionally, I show the utility these cells have in a mouse animal model to demonstrate this therapy has immediate potential for use as an "off-the-shelf-therapy" in eye related stroke injuries.

Overall this research demonstrated that MSC potency can be bolstered by small molecule and drug treatment conditioning, and that certain disease conditions may be more effectively paired with specific MSC conditioning strategies to improve their therapeutic effectiveness.

TABLE OF CONTENTS

LIST OF TABLES

LIST OF FIGURES

CHAPTER 1: INTRODUCTION

Mesenchymal stromal cells (MSC) are self-renewing, multipotent precursor cells originally identified in the adherent fraction of bone marrow stroma[1,2]. MSC have since been found to reside in diverse anatomical locations such as adipose tissue, mandibular molar pulp, adult muscle, corneal stroma, as well as postnatal and embryonic tissues[3]. Although their physiologic role in the body remain poorly understood, initial interest in MSC stems from their multilineage differentiation potential[4,5]. The standard for MSC multi-potency is their ability to differentiate into adipocytes, chondrocytes, or osteoblasts when placed in specific culture mediums.

While MSCs were initially used for their multilineage differentiation capacity, numerous studies have since demonstrated that these cells are also endowed with potent immunomodulatory properties. MSC are exquisitely sensitive to their environment, allowing them to evade immune response recognition in allografts, modulate responses of immune cells subtypes, and directly inhibit effector responses of T cells subtypes. The ability of these cells to sense an inflammatory environment leads to the release of soluble factors capable of modulating a local immune microenvironment such as IDO, PGE2, HGF, IL-6, TGF-β, or PDL1[6].

MSC unique combination of pro-regenerative and immunomodulatory qualities have positioned MSC therapies as the flagship therapeutic in the burgeoning fields of regenerative medicine and cellular immunotherapy. Furthermore, MSC are readily available in large numbers, promote vascularization, inhibit local inflammation and exhibit complex interactions with other immune cells[6]. MSC interact with both immune

cells of innate and adaptive origin, further complicating their immunomodulatory mode of action. MSC have been shown to alter antigen-presenting cell maturation, suppress CD34+ progenitor monocyte-derived dendritic cell (DC) differentiation, and induce macrophage polarization toward an anti-inflammatory M2 phenotype[7–12]. Furthermore, MSC are capable of altering the secretome of effector T cells, NK cells and DCs, away from a pro-inflammatory Th2 cytokine profile towards an anti-inflammatory Th2 cytokine profile[13]. Numerous studies have also demonstrated MSC have capacity to inhibit B-cell proliferation, differentiation and immunoglobulin production in vitro[14,15]. Notably, MSC also appear to promote and maintain the activity and development of differentiated regulatory T cells subsets such as Tr1, CD4+FoxP3+, CD8+FoxP3[16–18].

As a result MSC broad ranging effects in altering the immune system, they have since been used to treat numerous diseases in hundreds of small animals. Furthermore, these exciting in vitro findings have been expanded upon and become the focus of numerous successful clinical trials by both clinical research groups and companies[19]. Among these studies include several promising experimental clinical studies utilizing MSC to restore central tolerance in GvHD. Several of these clinical trials utilizing allogneic MSC products have recently gained approval in Japan and India, for the treatment of graft vs host disease (GvHD) and critical limb ischemia, respectively[20]. Similarly, rodent models have shown MSC can be used to promote long term tolerance in renal, cardiac and hepatic transplant studies[21–25]. In addition, MSCs have also been extensively studied in the context of critical limb ischemia, where their transplantation induces angiogenesis of ischemic tissues[26]. MSC have also been explored as a promising therapy for treating type one diabetes. Berman et al. recently showed that allogenic islets

and BM-MSC co-transplanted in nonhuman primates showed significant enhancement of islet engraftment and function at one-month post-transplantation, compared with animals that received islets and donor bone marrow cells[27].

Despite recent success with MSC in experimental studies, generating cells that perform in a predictable manner remains a significant challenge that must be addressed if MSC therapies are ever to be produced at full commercial scale. Batch to batch variability in MSC response to inflammatory cues limits the predictability of MSC therapy. Notably, intrinsic donor variability[28–30], changes in potency after limited passaging[28,31], and potential detrimental effects of cryopreservation on MSC potency need to be addressed[32,33]. Thus, improving predictability of MSC in vivo remains a major hurdle limiting the translation of these promising cell-based therapies from being broadly applied to numerous diseases in the clinic.

Common strategies that have been employed to address this issue of MSC variability in MSC potency have relied on selection of potent MSC donors[30], culture of MSC under hypoxic conditions, using pooled MSC from multiple allogenic donors[34], and utilizing cells only at low passage numbers; continual expansion of MSC has diminishing returns on cell potentcy[31]. While each of these strategies have their own promise, many are only effective for small proof-of-concept studies. Understanding the mechanisms that make a donor or batch of MSC highly potent is necessary to facilitate commercial scale-up of MSC therapy and to design MSC therapies tailored to treat specific conditions.

In addition to issues associated with MSC variability, there is an essential need to understand how MSC react in various disease environments. While MSC donor variability remains a consistent hurdle in developing a reliable MSC therapy, the problem

is further complicated by patient variability factors which influence the success of the therapy. Although, MSC have been shown to be promising in treating many different conditions, large percentages of the patient populations remain non-respondent to the cell therapy[35,36]. For example, MSC therapy can lead to a dramatic increase in two year survival rate in patients with severe steroid-refractory GvHD. While this is a dramatic improvement for patients who have exhausted all other clinical recourses, only 40-70% of patients show an increased two year survival rate, compared to standard of care control treatment[34,36,37].

Decreased levels of naïve T cell populations and subtle differences in cytokine profiles, or within disease microenvironments could, in part, account for altered clinical outcomes between respondent and non-respondent severe steroid-refractory GvHD patient pools. MSC constitutively express a large repertoire of growth factors and a subset of immunomodulatory factors. However, many of the most potent angiogenic and immunomodulatory genes are inducible. To control MSC phenotype, extensive research has been done on characterizing physical, environmental, and biochemical cues that activate inducible gene pathways which control MSC response. Because of this, MSC may in fact require a minimal threshold of inflammatory cues to exert regenerative and immunomodulatory functions. This then begs the question of whether these cells can be manipulated or 'primed' prior to transplantation in order deliver a more predicable response.

Typically, these priming regiments have relied on licensing MSC to become immunomodulatory via stimulation with cytokines such as interferon-γ (IFN-γ) and tumor necrosis factor-α (TNF-α). Recent evidence suggest that the global gene expression

profiles of these cells are dramatically altered post exposure to these inflammatory cues. Furthermore, treatment of MSC with IFN-γ, TNF-α, or IFN-γ + TNF-α yields distinctly different phenotypes[38]. While cytokine simulation appears to uniformly polarize MSC to different phenotypes, the kinetics and long term effects of these responses on MSC phenotype remain unknown. MSC activation in a disease microenvironment is likely to result in a gradient of gene expression profiles and be influenced by a number of different factors outside of these two traditional listening cytokines. Macrophages for instance were first described as polarizable only along a linear continuum with M1 and M2 at opposite ends. However systematic characterization of distinct macrophage activating conditions have identified as many as 13 polarizable activation profiles[39]. In a similar way MSC preconditioning strategies to maintain predictability and potency can still be considered in its infancy. Cytokine mediated polarization may also be coupled with small molecule stimulation to either enhance or block gene pathways and more specifically tune MSC into a desired phenotype[28,40].

MSC therapies face many challenges including donor potency variability, non-respondent patient populations, limited capacity of cells to target and engraft to target tissue, and limited persistence in vivo. While many groups have begun to address these important barriers facing MSC therapies, few reports have identified how MSC phenotype may be altered post transplantation. Although in vitro studies show that MSC are sensitive to their environment, little is known about how MSC respond to environmental cues post transplantation. To bring light to this topic, the following chapters will focus on understanding how transitions to new environments impact MSC function. Here I will explore how MSC immunomodulatory potency is regulated to

develop a strategy to predictably polarize MSC into a therapeutic phenotype before transplantation into a host tissue. These strategies will explore the effect of both cryopreservation and traditional licensing approaches as well as new unexplored cytokines and small molecules to tune and optimize MSC phenotype. The goal of this research is to tailor in vitro priming and engineering strategies that optimize and prolong an immunomodulatory phenotype within MSC to improve efficacy and predictability in future MSC therapies.

In chapter 2, I address the impact of cryopreservation on MSC function. Cryopreservation utilizes very low temperatures and crypotectants to efficiently preserve structurally intact living cells. However, the cryopreservation process subjects MSC to extreme temperature changes during the storage and reconstitution procedure. While cryopreservation has utility in a clinical setting for immediate use as an "off the shelf therapy", risk of freezing damage due to ice crystal formation may impair the therapeutic efficacy of MSC compared to cell-culture derived fresh MSC[32,41–43]. Here we investigate the effects of a cryopreservation pretreatment scheme in an acute retinal ischemia/ reperfusion injury model designed to replicate a clinical model scenario of an ischemic stroke injury. The findings reported here highlight the applicability of using cryopreserved MSC with minimal impact on phenotype and therapeutic potency in vitro or in vivo. This work also emphasizes the notion that cryopreservation of MSC, and priming strategies utilizing inflammatory cytokines might require being tailor fitted to each targeted disease.

In chapter 3, I explore how MSC maintain their immunosuppressive phenotype long-term. This chapter looks at how transitioning MSC into an environment containing

inflammatory cytokines polarizes them into an immunosuppressive phenotype. Results of this study suggest that priming MSC with IFN-γ, TNF-α, and IFN-γ / TNF-α results in a durable profile that can be used to predict how MSC will respond and modify their response over time. Here we also highlight that polarizing MSC into an immunosuppressive phenotype is highly dependent on the duration and timing of pre-licensing exposure.

Finally, chapter 4 explores how MSC immunosuppressive phenotype be altered or enhanced. To promote a response that is both heightened and targeted, we investigate the possibility of utilizing small molecules to enhance MSC immunoregulatory properties. We report for the first time that a cyclic AMP (cAMP) agonist potently enhances MSC immunosuppressive activity. Further we observe that the effects of this small molecule have no significant effect on reducing immune cell proliferation, and its enhanced immunosuppressive effects are contingent upon COX-2 activity and dose dependent.

CHAPTER 2: CRYOPRESERVATION OF MSC[44,45]

Chapter 2: Preface

One of the major challenges facing the translational use of MSC therapies is the logistics of maintaining large populations of cells on-site capable of being rapidly deployed to an acute injury. The ability to cryopreserve MSC would be particularly advantageous in conditions like stroke, myocardial infarction, ischemic injury, sepsis, or toxic shock syndrome, that require treatment within hours of the onset of the condition. Deployment strategies for MSC that do not rely on cryopreservation are carried out by experienced technicians in dedicated cell processing facilities that require infrastructure that few hospitals have or could afford. This not only leads to quality control issues, but dramatically increases the cost associated with a given therapy and limits the possibility of these therapies from being used in the majority of healthcare facilities. Therefore, it is critical to identify cryo-preservation and pretreatment conditions that preserve MSC function and potency post-thaw for MSC therapies to be broadly utilized as an 'off the shelf' therapy.

Although multiple studies have investigated the impact of cryopreservation on MSC phenotype, results have been conflicting and have yet to reach agreement on whether cryopreservation impacts the long term therapeutic efficacy and phenotype of MSC. Several groups have reported that cryopreservation can have detrimental effects on MSC in vitro, resulting in changes to MSC proliferation, viability, adhesion capacity, and immunosuppressive potential[32,33,41]. Cryopreservation of MSC has also been shown to increase susceptibility to destruction by instant blood mediated inflammatory reaction and complement activation. Despite these findings, it remains unclear as to whether an

altered phenotype cause by cryopreservation leads to any meaningful impact on therapeutic efficacy[46]. Thus, we sought to determine if cryopreservation derived impairments observed in vitro stretched to impede in vivo function.

In this chapter, my team and I investigated the effects of a cryopreservation pretreatment scheme in an acute retinal ischemia/ reperfusion injury model designed to replicate a clinical model scenario of an ischemic stroke injury. The findings reported here highlights the ability of these cells to be maintained throughout the cryopreservation process with minimal impact on phenotype and therapeutic potency in vitro or in vivo. This work also emphasizes the notion that cryopreservation of MSC, and priming strategies utilizing inflammatory cytokines might require being tailor fitted to each targeted disease. The following chapter is an adaptation of two peer-reviewed articles published on May 23, 2016 in *Scientific Reports*, and November 10, 2016 in *Stem Cells*:

1. Gramlich, O. W.; Burand, A. J.; Brown, A. J.; Deutsch, R. J.; Kuehn, M. H.; Ankrum, J. A. *Sci. Rep.* **2016**, *6* (May), 26463.

2. Burand, A. J.; Gramlich, O. W.; Brown, A. J.; Ankrum, J. A. *Stem Cells* **2016**, 0–2.

In contributing to this work, I played a supporting role in designing the research study, writing the manuscripts, carrying out research experiments and analyzing data. In this project, I specifically carried out in vitro experiments that involved maintaining MSC cultures for analysis via western blot, assessing IDO activity, and assessing MSC immunosuppressive capacity by direct co-culture with isolated PBMCs.

Introduction

Mesenchymal stromal/stem cells (MSC) have been explored in hundreds of clinical trials for the treatment of dozens of conditions[47,48]. While MSC can be harvested from nearly any tissue[49], they are a rare cell type[50] and thus typically require significant *ex vivo* expansion to generate therapeutic doses of cells. Allogeneic MSC are used in most clinical trials as MSC are immune evasive, allowing them to avoid immediate immune detection and clearance[48]. Allogeneic MSC are typically expanded in culture, cryopreserved, and banked for future use, creating the opportunity for an 'off-the-shelf' therapy.

Many proposed applications of MSC therapy would require on demand access to therapeutic doses of MSC and therefore necessitate access to cryopreserved MSC stocks. Acute conditions including acute graft versus host disease (GvHD), acute kidney injury, acute lung injury, and sudden onset ischemic events such as myocardial infarction, acute limb ischemia, retinal and optic neuropathies, and stroke would all benefit from rapid MSC administration within hours after the onset of symptoms. The mechanism of action of MSC in these conditions is thought to be mediated through both modulation of inflammatory reactions as well as secretion of protective growth factors[51]. Even if a disease indication could accommodate a post-thaw recovery period ranging from hours to days, logistically, use of MSC immediately post-thaw would still be preferable, since post-thaw recovery needs to be carried out by experienced technicians in dedicated facilities. This not only leads to quality control issues but also adds significant infrastructure requirements that will prevent the use of MSC therapies in many hospitals. Therefore, identification of conditions that preserve MSC function throughout

cryopreservation as well as disease indications that allow MSC to be applied directly post-thaw is critical to the development of truly 'off-the-shelf' MSC therapies.

Although multiple groups have investigated the impact of cryopreservation on the phenotype of MSC, studies to date have yielded conflicting results and many questions remain. Most importantly, do changes in phenotype caused by cryopreservation have a meaningful impact on therapeutic efficacy? Luetzkendorf *et al.* examined changes in MSC proliferation, viability, and immunosuppressive potential after cryopreservation[52]. In this study cryopreserved MSC showed no difference in proliferation or viability post-thaw. When co-cultured with PHA-stimulated peripheral blood mononuclear cells (PBMC), MSC' immunosuppressive potency after thaw varied depending on MSC donor. Two donors exhibiting enhanced suppression after cryopreservation, one donor exhibited reduced potency, and a fourth donor had highly variable function[52]. Galipeau and colleagues recently reported freshly thawed MSC exhibit significantly diminished viability compared to cells that had been in culture for greater than 7 days[32]. In addition, freshly thawed MSC showed reduced response to interferon-γ (IFN-γ). Notably, maintenance in culture for 7 days restored MSC sensitivity to IFN-γ and indoleamine 2,3-dioxygenase (IDO) expression, suggesting the observed impairment was transient. The reduced viability and expression of immunomodulatory factors in freshly thawed MSC also resulted in reduced suppression of activated T-cells and, in some cases, actually led to hyper-proliferation of T-cells in co-culture assays. The authors hypothesized that these phenomena are due to the presence of large numbers of dead cells[32]. The same group subsequently reported that the actin cytoskeleton of freshly thawed MSC is disrupted, leading to reduced adhesion to endothelium and poor engraftment following intravenous

infusion. Again, recovery in culture for 48 hours restored this aspect of MSC function[33]. Moll *et al.* recently compared the propensity of freshly thawed MSC to activate the complement cascade and induce an instant blood mediated inflammatory reaction (IBMIR)[41]. In their study, freshly thawed MSC were more susceptible to destruction by IBMIR and complement activation. They also demonstrated that freshly thawed MSC had lower levels of IDO transcripts after IFN-γ stimulation and had diminished immunosuppressive potency in co-cultures with activated PBMCs isolated from whole blood.

In contrast to the Galipeau paper[32] and in agreement with the Leutzkendorf paper[52], the viability of freshly thawed MSC was observed to be similar to the viability of MSC harvested from continuous cultures, likely a consequence of differences in MSC donors and/or cryopreservation/thaw procedures used in the respective labs. In addition to *in vitro* analysis, Moll *et al.* also compared the clinical response of acute GvHD patients receiving intravenous injections of thawed MSC versus MSC collected from continuous cultures. Overall patients receiving fresh MSC, particularly early passage fresh MSC, had a much improved clinical response compared to patients receiving cryopreserved MSC[41].

Herein we seek to determine the effect of cryopreservation on human MSC's suitability to treat acute ischemic and inflammatory conditions. MSC phenotype, including viability, growth potential, growth factor secretion, expression of immunomodulatory factors, and ability to suppress activated inflammatory cells are analyzed in passage and donor matched MSC with and without cryopreservation. Finally,

we test an 'off-the-shelf' MSC therapy treatment paradigm in a retinal ischemia/reperfusion injury model designed to replicate a clinical scenario.

Results

Cryopreservation marginally impairs MSC viability and metabolic activity

Cryopreservation is an inherently stressful process for cells and it is not surprising to see detrimental effects on the viability and growth kinetics of cells immediately after thawing. Viability of MSC after thawing has been one of the most variable metrics in recent papers examining the use of cryo-MSC, ranging from as low as 50%[32 7] to greater than 90% viability[41,52]. These disparate finding could be related to the fact that pores form in membranes following exposure to DMSO[53] that could lead to false staining with traditional cell death markers including PI and Annexin V. Thus, here we sought to characterize the viability and growth kinetics of MSC following cryopreservation by directly labeling double stranded DNA breaks characteristic of cell death in MSC in the hour immediately post-thaw. In addition, we measured viability and metabolic activity 24, 48, and 72 hours after thawing to determine if cryopreservation has any lasting impact on MSC. Staining for double strand breaks with TUNEL immediately after thawing and after 1 hour of storage on ice revealed that MSC viability is not significantly reduced by cryopreservation when carried out as described herein (0.1–0.2% of cells stained positive by TUNEL in all groups, (Figure 1A). In contrast, when viability was assessed by PI staining cryo-MSC displayed a minor, but statistically significant, reduction in viability both 24 and 48 hours after thawing (2.8% and 1.9% reduction respectively, $n = 5$, $p < .05$, (Figure 1B). Differences in viability were no longer significant 72 hours after thawing (1.3% reduction, (Figure 1B). Similarly, while cryo-MSC displayed slightly

lower metabolic activity than fresh MSC at 24 (18% lower), 48 (17% lower), and 72 hours (4% lower) after thawing, as measured by XTT, differences were not statistically significant at any time point (Figure 1C). Overall, cryopreservation and cell handling, as performed in this study, appears to only marginally reduce MSC viability and metabolic activity.

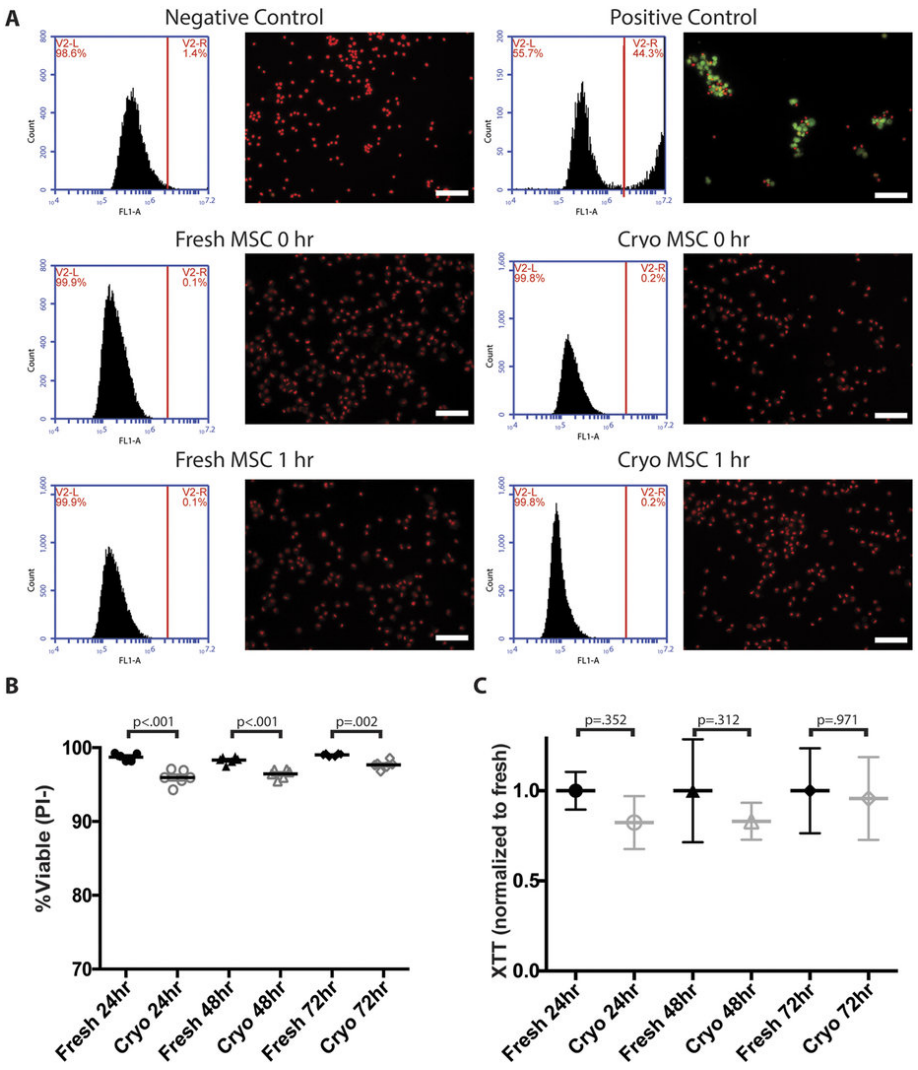

Figure 1: Cryopreservation marginally affects MSC viability and metabolic activity.

(**A**) MSC harvested from culture or thawed directly out of cryostorage were assayed for double strand DNA breaks by TUNEL staining. MSC were analyzed immediately after thawing or after 1 hour of storage on wet ice by flow cytometry and fluorescence imaging. The percent of positive and negative stained cells is reported in the upper right and left corners of each plot respectively. Cells were fixed, stained with PI (red) and FITC-dUTP (green). Double positive cells were considered dead. (Scale Bar = 100 μm). (**B**) Viability of MSC plated after thawing was compared to donor and passage matched MSC from fresh cultures 24, 48, and 72 hours after thawing. Cells were stained with Hoechst 33342 and PI and imaged with a fluorescence microscope. Cells double positive for Hoechst 33342 and PI were considered dead. (One-way ANOVA with Sidak correction for multiple comparisons, $p < 0.05$ considered significant, $n = 5$). (**C**) The metabolic activity of MSC after cryopreservation was compared to donor and passage matched MSC from continuous cultures using XTT (mean ± SD, One-way ANOVA with Sidak correction for multiple comparisons, $p < 0.05$ considered significant, $n = 6$). All experiments performed with MSC from donors 8002L and 7083 at passages P3–P5.

Cryopreserved MSC Maintain Immunomodulatory Potential

Sterile inflammation following ischemia/reperfusion injury leads to the destruction of cells in the tissue that would otherwise survive the ischemic insult. MSC can prevent this untargeted damage by inducing neutrophil apoptosis through the expression of IDO, which produces kynurenine metabolites known to be toxic to neutrophils[54,55]. In addition, MSC express a variety of factors that have been demonstrated to directly suppress T-cell activation and proliferation[56]. Thus, we sought to determine if MSC's immunomodulatory potency was impaired during cryopreservation.

We have previously described that IDO expression varies significantly by MSC donor and passage[28], and consequently all experiments here were completed with donor and passage matched MSC. MSC exposed to IFN-γ immediately after thawing expressed similar levels of IDO as MSC maintained in fresh cultures (Figure 2A). Very little IDO was detectable in either fresh or cryo-MSC after 24 hours of cytokine stimulation, but IDO levels increased similarly in both groups 48 and 72 hours after stimulation. In addition, both fresh and cryo-MSC stimulated for 48 hours with either IFN-γ or IFN-γ and TNF-α displayed high levels of IDO protein expression (Figure 2B) and concomitant IDO activity as measured by kynurenine production (Figure 2C). Next, to determine if cryo-MSC maintain their ability to suppress T-cell activation, we performed a co-culture experiment with primary human PBMCs. Unstimulated PBMCs and PBMCs stimulated with CD3/CD28 dynabeads served as unactivated and activated controls, respectively (Figure 2D). Both fresh and cryo-MSC were able to suppress proliferation of PBMCs when cultured at MSC:PBMC ratios of 1:3, 1:6 and 1:12 (Figure 2E). Mean PBMC proliferation rates in the presence of fresh MSC were 21%, 35%, and 57%, respectively,

whereas PBMC in the presence of cryo-MSC proliferated at 31%, 43%, and 59%, respectively (Figure 2F). None of the differences were statistically significant (1:3 and 1:6 n = 4, 1:12 n = 3). Thus, in our hands, cryopreservation did not significantly impair MSC's immunomodulatory potential.

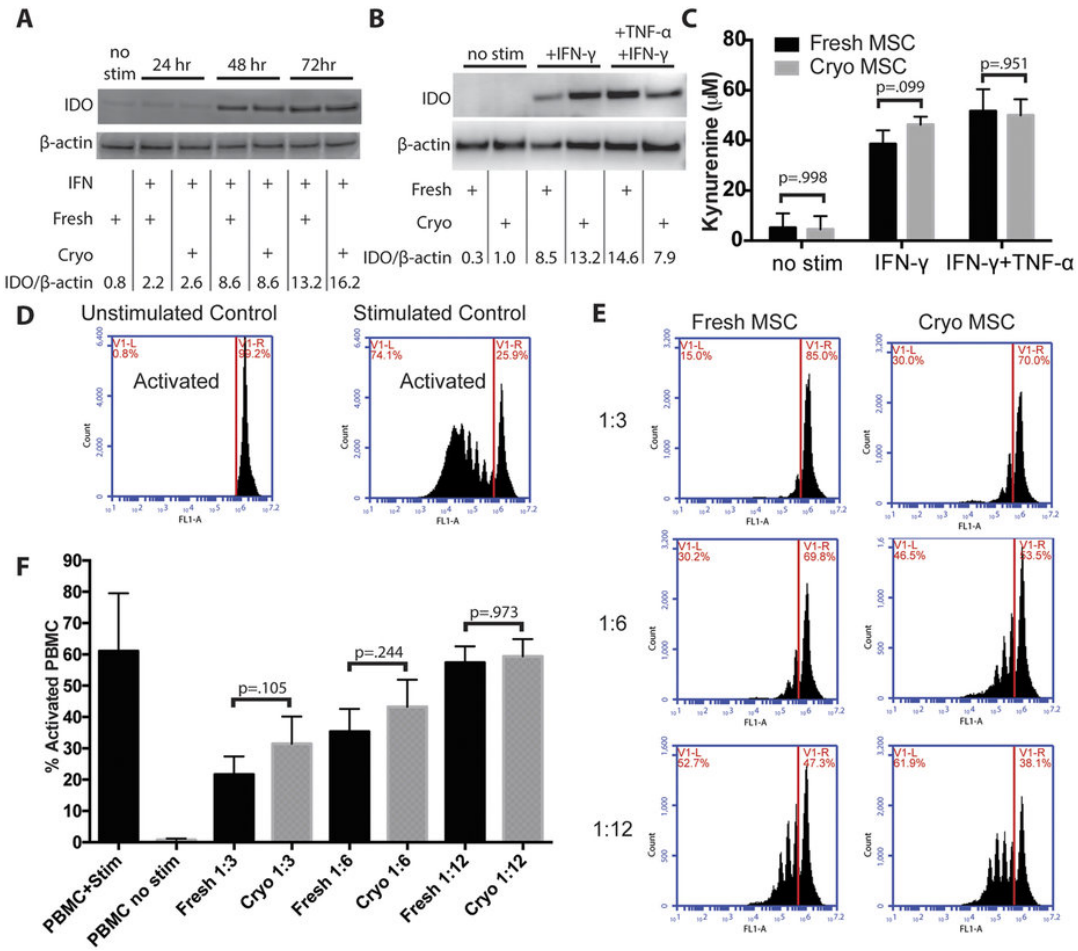

Figure 2: Cryopreserved MSC maintain immunosuppressive potential.

(**A**) Representative Western blot of IDO protein in fresh and cryo-MSC after exposure to IFN-γ for 24, 48, or 72 hours. β-actin provided as a loading control. (**B**) Representative Western blot of IDO in fresh and cryo-MSC after exposure to IFN-γ or TNF-α/IFN-γ for 48 hours. β-actin provided as a loading control. (**C**) IDO activity as measured by the concentration of kynurenine in the conditioned media collected from fresh or cryo-MSC exposed to IFN-γ or TNF-α/IFN-γ for 48 hours (mean ± SD, One-way ANOVA with Sidak correction for multiple comparisons, $p < 0.05$ considered significant, $n = 6$). (**D**) Example unstimulated and stimulated PBMC controls used for gating and setting the activation threshold. PBMCs stained with CFSE remain as a single population in unstimulated conditions but upon stimulation with CD3/CD28 dynabeads become activated and proliferate. (**E**) Example flow cytometry histograms of stimulated CFSE stained PBMCs co-cultured with fresh or cryo-MSC at MSC:PBMC ratios of 1:3, 1:6 or 1:12. (**F**) Quantification of the percent of activated PBMCs in each co-culture condition compared to unstimulated and stimulated controls. No statistical differences between fresh MSC and cryo-MSC at each ratio. (mean ± SD, One-way ANOVA with Sidak correction for multiple comparisons, $p < 0.05$ considered significant, 1:3 and 1:6 $n = 4$, 1:12 $n = 3$). All experiments performed with MSC from donors 8002L and 7083 at passages P3–P5.

Effect of Cryopreservation on MSC Secretome

In addition to blunting a T-cell mediated inflammatory response, the ability of MSC to support cell survival in ischemia/reperfusion could also involve the synthesis of growth factors that prevent cell death and aid the reestablishment of the vasculature. Indeed, VEGF secreted from MSC has previously been shown to reduce neuronal loss in a rat stroke model[57] and PDGF secreted from MSC has been implicated as being neuroprotective for retinal ganglion cells[58]. Thus, we sought to identify any potential changes in the MSC growth factor secretome that arises due to cryopreservation. The quantity and composition of the MSC secretome is heavily dependent on MSC donor and over 10-fold differences in expression and secretion levels have been observed by multiple groups when comparing individual donors subjected to identical culture conditions[28–30,59]. Thus, we analyzed fresh and cryopreserved passage matched MSC derived from a single donor, #7083, in order to isolate the impact of cryopreservation on the MSC secretome. Fresh or cryo-MSC, from donor #7083, were plated in reduced serum (1% FBS) growth media with or without a cytokine cocktail selected to mimic *in vivo* inflammatory conditions. After 48 hours, the media was collected and analyzed for the presence of 40 growth factors. Of the 40 screened factors, only 14 were detectable in at least 2 of the 4 conditions tested, and their concentrations are displayed in Figure 3A,C. In addition, as a statistical measure of the impact of cryopreservation on the production of each growth factor, the effect size, displayed as fold change compared to fresh MSC is plotted in Figure 3B,D. Overall, the profile and magnitude of growth factor expression was similar when comparing cryo-MSC to fresh MSC in both the unstimulated (Figure 3A,D) and stimulated conditions (Figure 3C,D). Expression of

PDGF which is known to be anti-apoptotic and pro-angiogenic, was slightly elevated in cryo-MSC compared to the fresh MSC while VEGF levels remained similar in both groups. Cytokine stimulation resulted in marked increase in secretion of both stem cell factor receptor (SCF R/c-kit) and TGF-β1 in both fresh and cryo-MSC. BMP-7 exhibited the most striking difference between cryo-MSC and fresh MSC. It was robustly expressed in both unstimulated and stimulated cryo-MSC, but was undetectable in both forms of fresh MSC. Overall, differences in secreted factors between fresh and cryo-MSC were subtle and the impact of these differences must be considered in the context of specific therapeutic applications. Thus, we turned to an *in vivo* model of retinal ischemia reperfusion injury to determine if MSC's therapeutic potency was impaired by cryopreservation.

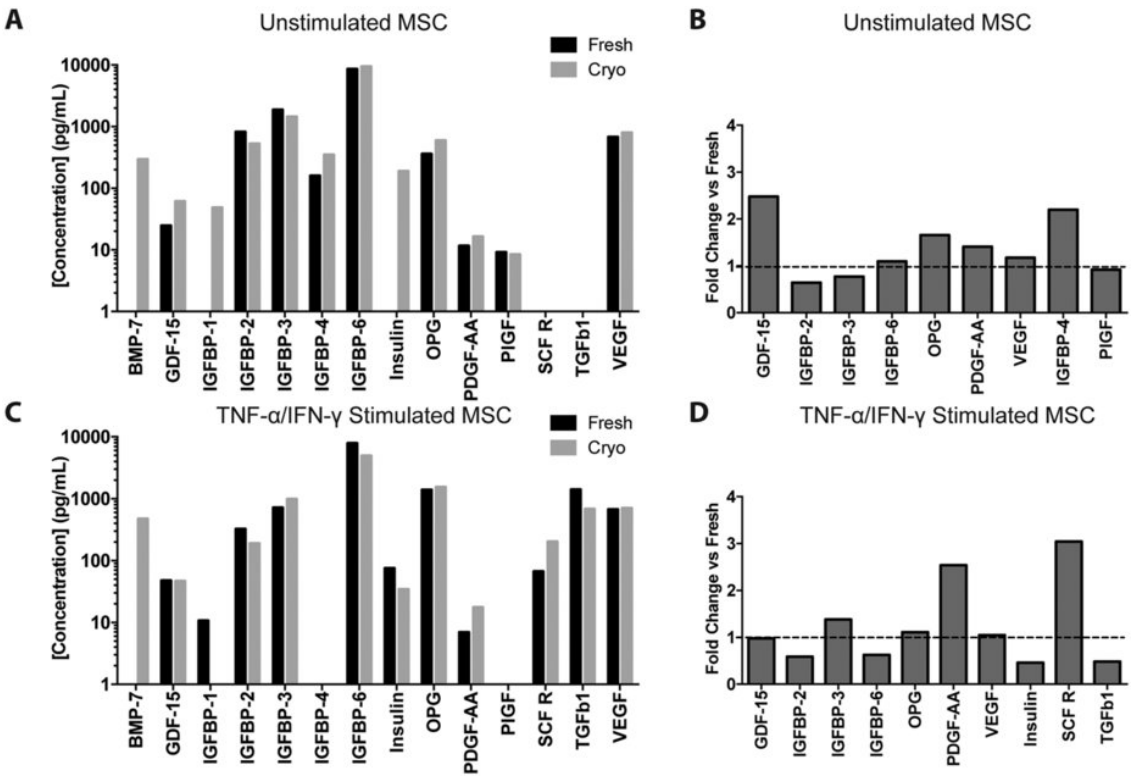

Figure 3: Cryopreservation minimally impacts baseline or stimulated growth factor secretion by MSC.

Fresh and cryo-MSC, both passage 4 MSC from donor 7083, were cultured for 48 hours in reduced serum media with or without stimulation by TNF-α/IFN-γ, the media was collected, and screened for 40 growth factors. Of the 40 proteins, 14 were detectable in at least 2 of the tested conditions and are reported here. Values represent measured concentration after background subtraction (unconditioned control media. (**A**) The concentration of each growth factor produced by fresh and cryo-MSC over 48 hours in unstimulated conditions. (**B**) Fold change in concentration in unstimulated MSC, [Cryo]/[Fresh] (**C**): The concentration of each growth factor produced by fresh and cryo-MSC over 48 hours in stimulated conditions. (**D**) Fold change in concentration in stimulated MSC, [Cryo]/[Fresh]. Dashed line at 1 corresponds to no-change between groups.

In order to assess whether cryo-MSC retain their neuroprotective potential *in vivo* we employed retinal ischemia/reperfusion (I/R) as a model of central nervous system (CNS) injury (Figure 4A). As expected, 1 hour of ischemia induced significant retinal damage as measured by retinal ganglion cell (RGC) loss. Eyes in the vehicle-only control group displayed a loss of approx. 88% of RGC seven days after I/R injury when compared to the non-ischemic contralateral eyes (I/R + PBS: 309 ± 308 RGC mm^2; non-ischemic: 2413 ± 413 RGC mm^2; $p < 0.001$, Figure 4B,C). Loss of RGC was significantly ameliorated in the presence of fresh MSC. Transplantation of these cells resulted in survival of 829 ± 405 RGC mm^2 ($p = 0.0019$). Moreover, transplantation of cryo-MSC provided an equivalent effect on RGC survival (845 ± 320 RGC mm^2) and is also statistically significant when compared to the RGC density of the vehicle group ($p = 0.024$).

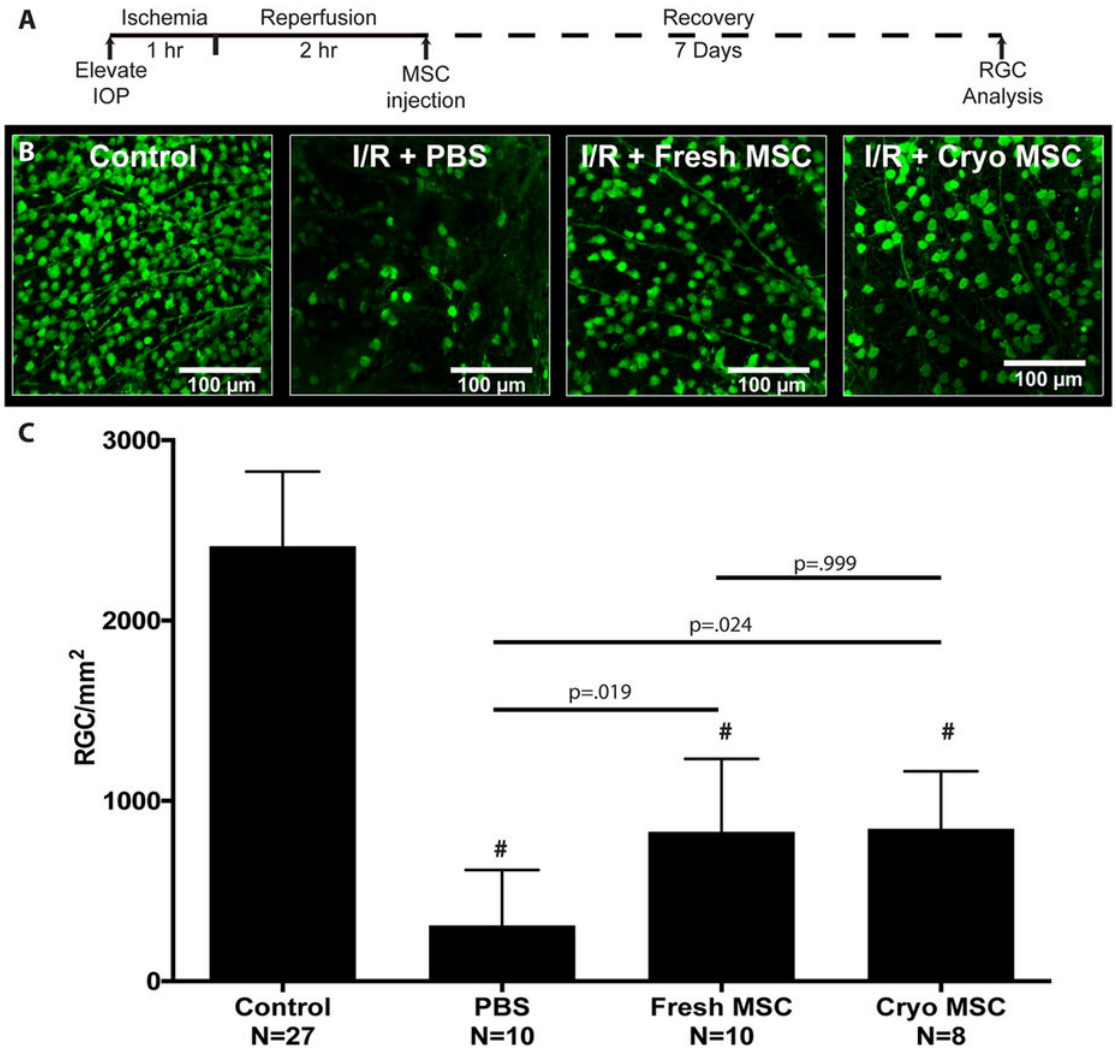

Figure 4: Cryopreserved MSC prevent RGC loss after ischemia/reperfusion injury in vivo.

(**A**) Injury and treatment timeline for all retinal ischemia/reperfusion model. Intraocular pressure (IOP) was elevated to blanch the fundus for 1 hour, after which perfusion was restored. 2 hours after reperfusion, eyes were injected with one of the MSC groups or PBS as a vehicle control. 7 days later, animals were sacrificed and eyes were analyzed for RGC counts. (**B**) Representative images of γ-synuclein immunostaining of whole-mounted retina from non-ischemic retinas (control) and retinas after I/R treated with vehicle (I/R + PBS), fresh MSC (I/R + Fresh MSC) or cryo-MSC (I/R + Cryo-MSC). (**C**) Quantitative analysis of RGC survival in eyes after I/R revealed a significant rescue effect after transplantation of both fresh MSC and cryo-MSC (mean ± SD, One-way ANOVA with Tukey honest significant difference post hoc test to correct for multiple comparisons, $p < 0.05$ considered significant). #denotes $p < 0.001$ in comparison to healthy control. Both cryo-MSC and fresh MSC were from donor 7083.

Rescue of RGC did not appear to depend on engraftment or persistence of MSC in the eye. Staining the human cell surface antigen Tra 1–85 has been used successfully to identify human cells, including MSC, in xenogenic transplant experiments[60,61]. By staining retina sections for Tra 1–85, a small portion of surviving MSC could be consistently detected in I/R eyes three days after transplantation (Fig. 5A,B). The remnant of MSC were found either in the vitreous, on the surface of the nerve fiber layer, or partially integrated, in the retinal ganglion cell layer (Fig. 5B). After 7 days, no MSCs were detected and furthermore, no signs of tumor formation were observed in any of the eyes by histological analysis (n = 7). To confirm MSC did not persist in the eye and no human derived tumors had formed, RT-PCR was performed. PCR amplification of genomic DNA extracted from the retinas of treated eyes did not indicate the presence of human DNA within the mouse tissue 7 days after transplantation (Fig. 5C). These data indicate that all of the tested samples contained fewer than 17 cells, which was the lowest concentration included in the standard curve, and support our immunohistochemical findings suggesting that MSC do not persist in the retina at 7 days. The absence of human genomic DNA also demonstrates the absence of MSC derived tumors. Thus our data not only demonstrate that use of human MSC is safe and effective in this mouse model of retinal I/R injury but are also congruent with our *in vitro* data indicating that cryopreservation does not significantly diminish the function of MSC. These findings show that fresh MSC and cryo-MSC equally rescue retinal ganglion cells following I/R injury.

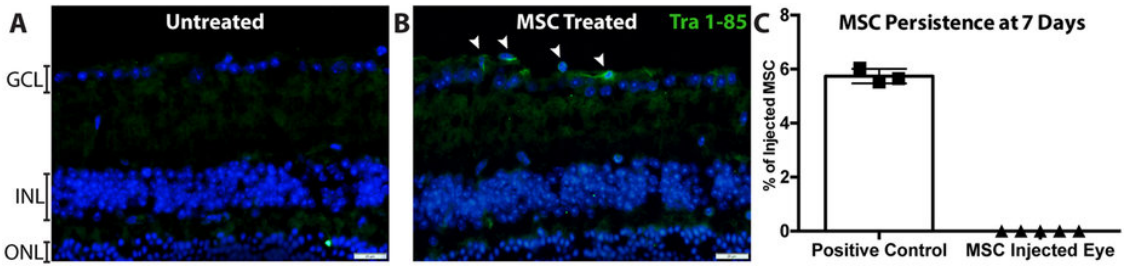

Figure 5: Cryopreserved MSC do not persist in the eye following ischemia/reperfusion injury.
Human cells, identified by human specific Tra 1–85 immunostaining and counterstained with DAPI were undetectable in (**A**) untreated eyes and rare in (**B**) treated eyes at 3 days, white arrows indicate positive cells atop the ganglion cell layer. (**C**) Quantitative PCR for human genomic DNA remaining in mouse retina seven days after transplantation. Human DNA was not detected in any of the tested eyes (n = 5, mean ± SD). Data normalized as % of injected as 30,000 MSC were delivered to each eye. Donor 7083 used for all mice. Positive control is DNA extracted from 1,670 MSC, corresponding to 5.6% of the total injected MSC). GCL: Ganglion cell layer, INL: Inner Nuclear Layer, ONL: Outer Nuclear Layer.

We then sought to improve the therapy further by prelicensing MSCs with IFN-γ prior to freezing. Using a similar strategy to Chinnadurai et al., we pretreated MSCs with IFN-γ for 24 or 48 hours and froze the MSCs as reported[62]. We then examined the level of IDO expression after thawing and plating MSC in IFN-γ containing media. Both batches of primed MSCs were evaluated for IDO protein content 8, 24, and 48 hours after thaw or until they had been exposed to IFN-γ for a total of 72 hours (Figure 6A). At 8 and 24 hours after thawing, the 24-hour prelicensed group had less IDO content compared to fresh MSC but the discrepancy in IDO content was no longer noticeable at 48 hours after thawing (72 hours of total IFN-γ exposure). The 48-hour prelicensed group performed considerably better in this assay, displaying comparable levels of IDO content at both 8 and 24 hours after thawing. We then took the 48 hour prelicensed cryo-MSC and tested to see if they would outperform fresh MSCs in an ischemia/reperfusion model *in vivo*. To

our surprise, the IFN-γ prelicensed cryo-MSCs lost effectiveness *in vivo*, rescuing fewer RGC than either fresh or unlicensed cryopreserved MSC (Figure 6B).

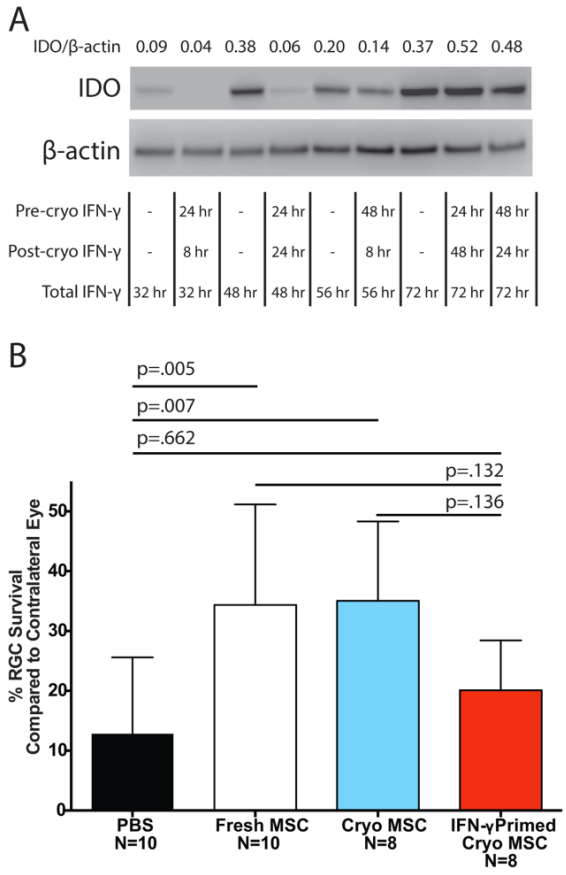

Figure 6: IFN-γ priming increases IDO expression of cryopreserved MSCs in vitro but is detrimental to MSC performance in an ischemia/reperfusion injury in vivo.
(A): Representative Western blot of IDO protein in human MSCs pretreated with 100 ng/ml rhIFN-γ for 24 hours or 48 hours prior to cryopreservation (Pre-cryo IFN-γ), followed by restimulation for an additional 8, 24, or 48 hours (Post-cryo IFN-γ), compared to fresh MSC cultures grown in 100 ng/ml IFN-γ. β-Actin served as a loading control. **(B)**: Quantitative analysis of retinal ganglion cells (RGC) survival in eyes after retinal I/R injury revealed a significant rescue effect after transplantation of fresh MSC and cryo-MSC, while cryo-MSC preconditioned in 100 ng/ml IFN-γ for 48 hours show diminished rescue of RGCs (mean ± SD, One-way ANOVA with Tukey honest significant difference post hoc test to correct for multiple comparisons, $p < .05$ considered significant).

Discussion

Successful application of MSC to treat numerous conditions in animal models has led to a rapid increase in clinical trials exploring MSC therapy[48]. The safety of MSC therapy in clinical trials to date has only hastened the exploration of MSC for more and more conditions[7]. While most studies using animal models and even small clinical trials have utilized fresh MSC cultured on-site, cryopreservation of MSC is essential to the widespread application of MSC-based therapies. Cryopreservation allows for MSC to be prepared by specialized facilities, in large batches under the application of accepted quality control measures. Preservation and storage is already routine for other tissue engineered products: Organogenesis' Apligraf can be stored for 15 days at 20–23 °C and Orthofix's Trinity Elite bone allograft can be stored for weeks at −80 °C allowing off-the-shelf use as the need arises and eliminating the need for on-site GMP cell culture facilities.

Importantly, the availability of cryo-MSC enables administration of large doses of cells without time delay caused by culture expansion. While development of cryopreservation techniques for MSC that minimize loss of therapeutic function is a critical step to advancing MSC-therapy for all applications, many acute-onset conditions such as ischemic events or acute GvHD would specifically benefit from an off-the-shelf MSC therapy. Tissue damage in these conditions is often rapid and without immediate treatment, the desired therapeutic effect may not be fully realized. For example, in the retinal ischemia/reperfusion model employed herein almost all damage occurs within the first 72 hours after the insult and little additional damage is observed 7 days after reperfusion[63].

To date, studies focused on the impact of cryopreservation on MSC function have yielded mixed results[64]. Cryopreservation of MSC has become routine and MSC stored for extended periods of time have been shown to have low tumourigenic potential[65], maintain growth kinetics upon thawing[66], and remain capable of multilineage differentiation[66–69]. When MSC were examined for their ability to differentiate to form bone, cryopreservation did not significantly impact the differentiation capacity of the cells in *in vitro* assays[66] or after *in vivo* transplantation[67–69]. Subcutaneously implanted scaffolds in primate[67] and murine[68,69] models have revealed no statistical difference between fresh and cryo-MSC's osteogenic potential. In contrast, studies focused on the use of MSC for their secreted trophic factors have reported detrimental effects from cryopreservation. Most notably, MSC have been reported to have poor viability after cryopreservation which reduces the number of cells capable of responding to inflammatory cues[32]. In addition, cellular debris in one study induced hyperproliferation of T-cells in co-culture experiments[32]. While MSC function in *in vitro* potency assays are informative, the critical question is whether cryopreservation impairs MSC function *in vivo*. While the first MSC clinical trials, for pediatric osteogenesis imperfecta (OI)[70] and graft versus host disease (GvHD)[21], utilized fresh cultured MSC, the majority of clinical trials and companies developing commercially available MSC-based products today utilize cryopreserved MSCs. Until now, data comparing the efficacy of cryo-MSC compared to fresh MSC *in vivo* and in humans has been limited. A post-hoc analysis of clinical outcomes in acute GvHD patients receiving intravenous injection of fresh or cryo-MSC revealed patients receiving fresh MSC tended to respond better than patients receiving cryo-MSC[41]. It is then important to note that while cryopreservation simplifies

logistics of cell therapy, it is not without potential drawbacks. Cryopreserved MSCs may be suboptimal and inappropriate for the treatment of some conditions, while being adequate and necessary for others. As our understanding of the disease specific therapeutic mechanisms employed by MSCs grows, so too will our ability to identify culture conditions and cryopreservation techniques that maintain or enhance rather than hinder MSC potency. At present, however, the full impact of cryopreservation on MSC function in specific disease contexts is not well understood (Figure 7).

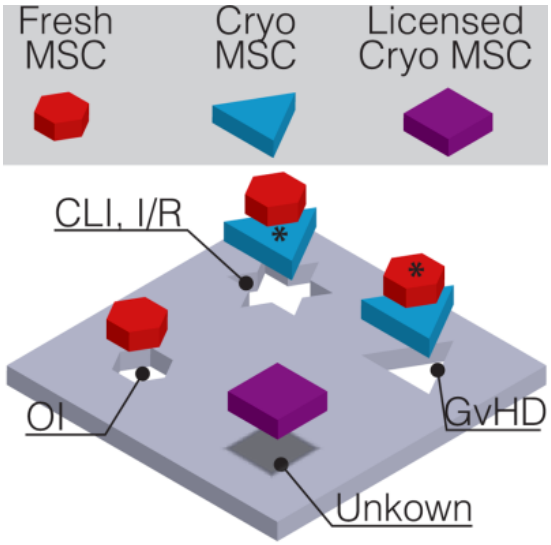

Figure 7: Tailoring MSCs to fit the disease.

Fresh, cryopreserved and, prelicensed cryopreserved MSC are all being explored to treat numerous diseases, but all are not suitable to treat all conditions. injury. "*" denotes preferred therapeutic strategy when both fresh MSC and cryo-MSC have shown utility in treating the disease but one is more efficacious or logistically suitable. Abbreviations: CLI, critical limb ischemia; GvHD. graft versus host disease; I/R, ischemia reperfusion (I/R); OI, osteogenesis imperfecta.

We sought to determine whether cryopreservation would impact the therapeutic potency of MSC intended to combat I/R injury. Multiple mechanisms lead to cell death in the context of ischemia/reperfusion injury in the CNS. In addition to hypoxic insult, reperfusion of the ischemic tissue results in the generation of damaging reactive oxygen species and an influx of inflammatory cells that cause sterile inflammation[71]. While inflammation benefits clearance of damaged cells, activated neutrophils in sterile inflammation often contribute to damage, and viable cells are indiscriminately killed while cellular debris is cleared. Sterile inflammation has been well documented to significantly contribute to tissue damage following ischemic events in a variety of tissues[72]. For example, inhibition of neutrophil function by knocking out Nlrp3 prevented inflammosome activation and significantly reduced the extent of tissue damage in a model of acute renal ischemia[73]. In addition, antigen presenting cells such as dendritic cells are exposed to antigens from dying cells and damage associated molecular patterns (DAMPs) released by necrotic cells that serve as adjuvants[74]. These activated dendritic cells can then migrate to lymph nodes where they stimulate a T-cell response to antigens in the ischemic tissue[75]. Thus, preservation of both cell viability and MSC immunomodulatory properties is critical to the successful use of cryo-MSC to treat ischemia/reperfusion injury.

Numerous cryopreservation techniques and cryoprotectants have been used to preserve MSC with variable effects on the phenotype of cells post-thaw. Recent reviews by Yong *et al.*[64] and Marquez-Curtis *et al.*[76] provide an in depth overview of emerging cryopreservation technology. As viability of cells post-thaw appeared to be a predictor of MSC function in past studies, we used a cryopreservation media and method that has

worked well in our lab and others[77] for maximizing post-thaw recovery. MSC were frozen in serum-free, xeno-free CryoStor CS5 media containing 5% DMSO at a concentration of 1×10^6/ml using a controlled-rate freezing cell at 1 °C/min. This process consistently yields MSC with >95% viability post-thaw. Cryo-MSC had an overall similar profile of secreted growth factors compared to passage and donor matched fresh MSC. MSC preserved and thawed using our protocol responded to exposure to IFN-γ by synthesizing IDO and converting tryptophan to kynurenine at the same rate as fresh MSC. In addition, these cryo-MSC remained suppressive of anti-CD3/anti-CD28 activated PBMCs in co-culture assays. While these findings stand in contrast to previous studies that reported impaired immunosuppressive properties using cryopreservation techniques that yielded 40–50% dead cells after thawing[32], they are consistent with the notion that post-thaw viability is critical for post-thaw immunomodulatory function. Thus, viability, and not cryopreservation per se, appears to be a predictor of MSC function. Our study demonstrates that when viability is maintained, MSC remain functional in *in vitro* potency assays regardless if they are fresh or cryopreserved. This is in agreement with a recent study from RoosterBio which reported cryopreservation in CryoStor CS5 results in MSC with high viability, IDO activity, and similar cytokine secretion compared to fresh MSC[77].

We demonstrated cryo-MSC remain therapeutic when injected immediately after thawing in a retinal model of I/R. Retinal I/R leads to rapid destruction of RGCs, neurons on the surface of the retina that transmit signals received from photoreceptor cells via bipolar and amacrine cells to visual processing centers of the brain through long axons that form the optic nerve[78]. The inner layer of the retina, were the RGC cell bodies reside,

have been demonstrated to be particularly sensitive to hypoxia[79], thus the ability to salvage RGC in the setting of I/R is critical if some degree of vision is to be preserved. In addition, retinal I/R injury not only resembles various ophthalmologic disorders causing visual impairment such as ischemic optic neuropathies and glaucoma, but also recapitulates many aspects of CNS injury, in particular stroke[80–82]. The analogy in the pathobiology with respect to hypoxia, oxidative stress and inflammation makes the animal model of retinal I/R extremely suitable to determine whether transplantation of cryo-MSC into the ischemic retina improves RGC survival as an off-the-shelf therapy. The rapid onset of reactive oxygen species and inflammatory cells in the ischemic tissue following reperfusion requires any mitigating treatment to be applied quickly if ganglion cells are to be salvaged. Thus, cell therapy strategies that require *in vitro* culture prior to infusion are not suitable for treating I/R injury.

To enhance the immediate impact transplanted cryopreserved MSC would have on salvaging RGC in our I/R injury model, we prelicensed MSC with IFN-γ prior to cryopreservation. A recent article by Chinnadurai et al. evaluated of the fitness of cryopreserved MSCs, and demonstrating that thawed MSCs are susceptible to lysis by cytotoxic T lymphocytes (CTL) in coculture assays[62]. However, prelicensing MSCs with IFN-γ was shown to lead to induce high levels of IDO mRNA and protein. Prelicensed cryo MSC also recovered their ability to avoided CTL mediated lysis and suppress PBMC proliferation equally as well as fresh MSCs.

While MSCs licensed with IFN-γ are known to increase expression of immunosuppressive factors, treatment also dramatically increases surface expression of MHC-I and MHC-II molecules[28] which may accelerate the detection and clearance of

MSC via xeno-recognition. Notably, in our ischemia/reperfusion model all human MSC were cleared from the mouse eyes by day 7[44]. Further analysis is needed to determine if the reduced effect of prelicensed MSC was due to hastened immune detection and clearance of MSC or changes in secreted factors that support RGC survival. While a syngeneic or autologous transplant model would allow for analysis of the fate of prelicensed cryo-MSC independent of rejection mechanisms, it would not be without significant drawbacks. Notably, MSC biology diverges significantly between human and mice, with documented differences in chemokine receptors[83] as well as their use of central immunomodulatory mechanisms, with murine MSC utilizing iNOS while human MSC employ IDO[84]. In addition, since the goal of our work was to move toward an off-the-shelf therapy for I/R injury that can be administered within hours of the onset of an ischemic event, the analogous human application would likely employ allogeneic MSC, and thus MSC would likely suffer from enhanced allo-recognition in a prelicensed state. Our current data are insufficient to fully conclude that prelicensed cryo-MSC have no place in the world of cell-therapy, but highlight the need for future work in this area to proceed cautiously with careful attention paid toward *in vivo* immune detection and clearance.

Chinnadurai et al.'s report[62] that cryopreserved MSCs can be killed via CTL mediated lysis is further evidence that MSCs are immune evasive in nature, but only evade destruction if their immunosuppressive facilities are intact[48]. Both the Chinnadurai et al. report[62] and our observed negative impact of prelicensing on MSCs *in vivo* highlight the need to understand in greater detail the multiple mechanisms by which MSCs are cleared *in vivo* and how cryopreservation and other preconditioning regimens

extend or shorten their persistence *in vivo*. In addition, our observation that prelicensed cryopreserved MSCs performed worse in the retinal ischemia/reperfusion model demonstrates the need to evaluate the suitability of cryopreserved or otherwise manipulated MSCs in a disease specific context. MSC exert multiple mechanisms including immune suppression, secretion of growth factors[85], and even donation of mitochondria[86]. However, each can be differentially impacted by cryopreservation and preconditioning strategies and the appropriateness of such strategies cannot be determined outside of the context of a specific pathology.

Studies in animal models to date have shown that cryopreserved MSC are effective in treating disease models of colitis[87], allergic airway inflammation[88], and ischemia/reperfusion injury to the eye. In contrast, cryo-MSC failed to induce a chondrogenic response in a mouse-based chondrocyte-responsive bioassay suggesting cryo-MSC may be unsuitable for treatment of OI[89]. In humans, cryopreserved MSC have elicited positive responses in clinical trials for critical limb ischemia[90] while retrospective analysis of GvHD patients receiving fresh versus thawed MSC suggest fresh MSC are more efficacious[91].

In our model, we demonstrated that MSC could be taken directly from cryostorage, thawed, washed, and injected into the ischemic tissue without impairing the therapeutic potency of the MSC. These findings are similar to those of earlier studies that suggested that retinal transplantation of MSC improves RGC survival after injury[58,92]. However, these studies relied on experimental designs that employed fresh MSC transplanted prior to injury. Herein we significantly extend these findings by demonstrating that transplantation of human MSC taken directly from cryostorage and

injected two hours after reperfusion is significantly protective. This is a crucial difference from a translational point of view as our model recapitulates a clinical scenario, in which patients seek treatment in the hours following an ischemic event, receive reperfusion therapy, and would then be able to receive an off-the-shelf therapy to prevent secondary damage from the I/R injury. Our finding that MSC can be cryopreserved without an apparent loss in efficacy suggests that storage and use of MSC in a clinical setting may be feasible for I/R injury to the eye and CNS.

Materials and Methods

MSC Cultures and Cryopreservation

Pre-characterized human MSC were provided by the Texas A&M Health Science Center College of Medicine Institute for Regenerative Medicine at Scott & White through a grant from NCRR of the NIH, Grant # P40OD011050, resource ID SCR_005522. Two donors of MSC, #7083 and #8002L, were obtained from Texas A&M and both were accompanied by a complete analysis of MSC surface marker expression and differentiation capacity in accordance with the ISCT minimal criteria for MSC[93]. Specifically, MSC from both donors were >95% positive for CD73a, CD90, and CD105, <2% positive for CD11, CD14, CD19, CD34, CD45, CD79a, and HLA-II, and capable of multilineage differentiation. MSC were plated at a density of 5,000 cells/cm^2 in MEM-alpha supplemented with 15% fetal bovine serum (Premium Select, Atlanta Biologicals), 1% penicillin/streptomycin, and 1% L-glutamine unless otherwise stated. Cells were passaged when cells reached 70–80% confluence, which typically corresponded to 2.5 population doublings. All MSC were between population doubling levels of 6–11 at the time of use (Passage 3–5). MSC were cryopreserved using CryoStor CS5

cryopreservation media (Sigma, St. Louis, MO) and a CoolCell controlled rate freezing container (Biocision, San Rafael, CA). Briefly, MSC were harvested from cultures, pelleted, and resuspended in 4 °C Cryostor CS5 at a concentration of 1×10^6/ml and aliquoted into cryovials. Vials were then placed in a CoolCell pre-chilled to 4 °C and placed in a −80 °C freezer for at least 90 minutes. Vials were then rapidly transferred to a pre-chilled liquid nitrogen storage box and maintained in liquid nitrogen vapor for 7–30 days before thawing. For thawing, all vials were removed from liquid nitrogen and placed directly in a 37 °C water bath until a small ice pellet remained. Cells were then gently pipetted into 4 ml pre-warmed media, centrifuged at 500 × g for 5 min and resuspended in 1 ml pre-warmed media for use in downstream applications. For *in vivo* transplantation, cryopreserved MSC (cryo-MSC) were thawed, resuspended in room temperature PBS−/− (without calcium and magnesium), counted, centrifuged, and resuspended in ice cold PBS−/− at a concentration of 10×10^6/ml and placed on ice. All intraocular MSC injections occurred within 1 hour of thawing. 'Fresh' MSC in this study were all maintained in culture for at least 7 days. Cryo-MSC were used immediately after thawing unless otherwise noted. All experiments used donor and passage matched MSC to isolate the effect of cryopreservation on MSC phenotype and function.

Viability and Metabolic Activity Assays

For viability analysis, terminal deoxynucleotidyl transferase dUTP nick end labeling (TUNEL) staining was performed on fresh MSC and MSC thawed directly from cryopreservation. In both cases, cells were washed twice, resuspended in PBS, and either analyzed immediately or after 1 hour of storage on wet ice. TUNEL staining was performed using the Apo-Direct Apopotosis Detection Kit (BD Biosciences, Franklin

Lakes, NJ) according to the manufacturer's instructions. Briefly, cells were fixed in 2.5% neutral buffered formalin (Sigma, St. Louis, MO) for 60 minutes, washed three times, fixed, and permeabilized in 70% ethanol at −20 °C for 3 days. Post thawing, double strand breaks were stained by incubation with FITC-dUTP followed by staining of all nuclei with propidium iodide (PI). The samples were analyzed by an Accuri C6 flow cytometer, with positive and negative control cells used for gating and color compensation. Fluorescent images of all samples were also acquired as validation. For viability analysis of fresh and cryo-MSC in the days after thawing, 30,000 MSC were seeded into a 24-well plate in triplicate for each experiment and cultured for 24, 48, and 72 hours. At each time point, media was removed from wells and 200 μL of staining media containing Hoechst and PI (Invitrogen, Carlsbad, CA) was added to each well. After 20 minutes of staining at 37 °C, four random fields were imaged to detect PI positive nuclei and total nuclei. Cells incubated with 1 μM staurosporine (Tocris, San Diego, CA) for 3 hours served as a dead control to verify the staining procedure and set the acquisition settings. Images were captured using an inverted phase contrast and fluorescent microscope with a 10x objective (DMI6000B, Leica Microsystems, Wetzlar, Germany). ImageJ (NIH) was used for nuclei counting.

Metabolic activity in the days following thawing was measured using an XTT assay (ATCC, Manassas, VA) after 24, 48, and 72 hours. Here, 15,000 MSC were placed in wells of a 96-well plate in 100 μL of culture media. Both fresh MSC, cultured for >7 days, and cryo-MSC were plated in duplicate or triplicate for each time point and metabolic activity was measured according to the manufacturer's instructions. Wells with

half the cell starting density with XTT, media only with XTT, and MSC alone without XTT were used as controls for each experiment (n = 4).

Growth Factor Array

Growth factor secretion from fresh and cryo-MSC was assessed using the Human Growth Factor Array Q1 (RayBiotech, Norcross, GA). Here, either 200,000 fresh or cryo-MSC were cultured in 2 mL of 1% (v/v) FBS, 1% (v/v) Penicillin/Streptomycin, and 1% (v/v) L-glutamine supplemented MEM-α media in T25 flasks for 48 hours with or without 100 ng/mL human IFN-γ (PeproTech, Rocky Hill, NJ) and 50 ng/mL human TNF-α (Invitrogen, Carlsbad, CA). Media was collected and frozen at −20 °C along with cell lysate for western blot and IDO activity analysis. The array was performed per the manufacturer's instructions using the growth factor standards provided in the kit and the media was loaded into the array with no dilution and at a 4x dilution. The slide was read and data extracted by RayBiotech. The total concentration of each growth factor in basal media and MSC conditioned media was interpolated using the standard curves for each factor. To determine growth factor concentration contributed by the MSC, the concentration of growth factor in the basal media was subtracted from the concentration measured in the MSC conditioned media.

Western Blot

Cell lysates were collected from MSC by washing T25 plates in chilled PBS three times to remove media followed by addition of 80 µL chilled RIPA buffer with protease inhibitor cocktail (Santa Cruz Biotechnology, item# sc-24948A) and agitation with a cell scrapper. Tubes were incubated on ice for 15 minutes and lysate was clarified by pelleting precipitate at 8,000 × g at 4 °C for 10 minutes. Prior to loading, total protein

content was measured by microBCA (Thermo Scientific, Waltham, MA). 10–20 μg of protein was loaded into each well of a precast Bolt 4–12% Bis-Tris gels. After transfer, the membranes were blocked with 5% non-fat dry milk and stained with their respective primary antibodies (1:1000 rabbit anti-IDO (12006S, Cell Signaling, Danvers, MA), 1:20,000 mouse anti-β-actin (1406030, Ambion, Thermo Scientific, Waltham, MA)). Horseradish peroxidase conjugated antibodies (1:10,000 goat anti-rabbit (A2315), 1:10,000 goat anti-mouse (H2014), Santa Cruz Biotechnology, Dallas, TX) were used as a secondary followed by incubation with SuperSignal West Femto chemiluminescent substrate (Thermo Scientific, Waltham, MA). Western blot images were visualized using an Odyssey C-Digit scanner and processed using Image Studio software (LI-COR Biosciences, Lincoln, NE). All Westerns were repeated 2–3 times and representative blots are displayed.

IDO Activity Assay

Media collected from fresh or cryo-MSC stimulated with or without human IFN-γ/TNF-α was analyzed for kynurenine content as a marker of IDO activity[94]. L-kynurenine (Sigma Aldrich, St. Louis, MO) was dissolved in culture media and used to create a standard curve. 100 μL of conditioned media or standards were placed in a 96-well plate. 50 μL of 30% (w/v) trichloroacetic acid was added to each well to precipitate out proteins. The plate was heated for 30 minutes at 52 °C to facilitate the conversion of N-formylkynurenine to kynurenine and then centrifuged at 1,200 × g for 15 minutes. 75 μL of supernatant from each sample or standard was mixed with 75 μL of Ehrlich's reagent (0.8% (w/v) 4-(Dimethylamino)benzaldehyde in acetic acid), and incubated at

room temperature for 10 minutes. The plate was then read at 492 nm and the concentration of kynurenine in each sample was interpolated from the standard curve.

PBMC Co-cultures

MSC immunosuppressive capability was assessed by direct co-culture with isolated PBMCs from leukapheresis reduction cones obtained from the DeGowin Blood Center at the University of Iowa Hospital and Clinics. MSC to PBMC ratios (1:3, 1:6, and 1:12) were established by seeding 250,000 PBMCs in wells containing 83,300 MSC, 41,600 MSC, or 20,800 MSC of a 48-well plate. MSC were plated 1 hour prior to addition of PBMCs in RPMI supplemented with 10% (v/v) FBS, 1% (v/v) Penicillin/Streptomycin, and 1% (v/v) L-glutamine. PBMCs were labeled with CellTrace CFSE Cell Proliferation Kit (Invitrogen, Carlsbad, CA) at a final dye concentration of 1 μM. The PBMCs were then stimulated with 250,000 Human T-activator CD3+/D28+ Dynabeads (Invitrogen, Carlsbad, CA) in each well and cultured for 6 days. PBMC only with or without Dynabeads served as activated and un-activated controls respectively for all experiments. After 6 days, PBMCs were dispersed by gentle pipetting, collected, centrifuged at 500 × g for 5 minutes, and resuspended in 100 μL RPMI before analysis on an Accuri C6 flow cytometer. Unstimulated control PBMCs were used to set the gating threshold for each experiment (n = 4).

Retinal Ischemia/Reperfusion Injury and MSC Transplantation

All animal experiments were carried out in accordance with the ARVO Statement for the Use of Animals in Ophthalmology and Vision Research and were approved by the IACUC committee of the University of Iowa. Unilateral retinal damage was induced by Ischemia/Reperfusion (I/R) injury as described earlier[63,95,96]. Briefly, male and female

two-month old C57BL6/J (The Jackson Laboratory, Bar Harbor, ME) were anaesthetized by intraperitoneal injection of Xylazin/Ketamine (10 mg/kg and 100 mg/kg, respectively). Eyes received 0.5% proparacaine eye drops for topical analgesia, pupils were dilated with 0.5% tropicamide (both Akorn, Lake Forest, IL), and corneas were kept moist until animals had fully recovered (GenTeal, Alcon, Fort Worth, TX). The anterior chamber was cannulated with a sterile 30-gauge needle, which was connected to a saline reservoir by a perfusion line. Intraocular pressure (IOP) was elevated to 80 mmHg in left eyes by setting the saline reservoir to an equivalent height (108 cm) above the mouse's head. Retinal ischemia was confirmed by blanching of the fundus and stasis within retinal vessels using fundus imaging. After one hour of IOP elevation, the cannula was carefully removed and reperfusion was evident by resumption of retinal blood and recovery of pulsation.

Two hours after I/R, animals underwent isoflurane sedation and I/R eyes were treated with either fresh MSC (I/R + Fresh MSC, N = 10) or cryo-MSC (I/R + Cryo-MSC, N = 17). 3×10^4 MSC in 3 µl PBS were transplanted into the vitreous cavity using a Hamilton syringe equipped with a 33-gauge needle. A vehicle control group received an equivalent volume of PBS (I/R + PBS, N = 10). The right eyes of all mice received no manipulation and served as controls. Animals were euthanized at either three or seven days after I/R injury by CO_2 inhalation followed by cervical dislocation.

Detection of transplanted MSC

Eyes of animals having received cryopreserved MSC were harvest three (N = 5) days after transplantation, fixed in 4% paraformaldehyde for 2 hours, sucrose embedded and processed for traversal sectioning. Eyes (N = 7) obtained seven days after MSC

transplantation were spilt in half; DNA was extracted from freshly isolated retinas for RT-PRC experiments from one half of the eye while the other half was processed for immunostaining. 7 μm sections were blocked in 1% BSA/PBS for 30 min, washed and incubated with goat anti-human Tra 1–85 antibodies (1:50 in 0.3% Triton X-100/PBS, R&D Systems, Minneapolis, MN) overnight. Slides were washed with PBS and an Alexa Flour 488 donkey anti-goat secondary antibodies (1:400 in PBS) was applied for 3 hours. After final rinses, nuclei were visualized using DAPI. Sections were coversliped and images were taken using an Olympus BX41 microscope.

Detection of human DNA

Genomic DNA was extracted from the posterior retina of five eyes seven days after MSC transplant using DNeasy columns (Qiagen, Valencia, CA). 250 ng of this DNA was used in a quantitative PCR reaction using primers specific for human genomic DNA (forward: GAGAGCGTTTGGAAATTGGA, Reverse: TGGCTGCTGTTTCATGTCTC). Samples were amplified in a quantitative PCR reaction for 45 cycles using a CFX96 thermal cycler (BioRad, Hercules, CA). Data were compared against a standard curve was constructed using genomic DNA extracted from a known quantity of human MSC (17 to 16,750 cells). A positive control containing DNA from 1,675 MSC and a negative control (water only) were included. All measurements were taken in triplicate.

Analysis of Retinal Ganglion Cell Survival

All animals were euthanized seven days after I/R injury by CO_2 inhalation followed by cervical dislocation. Eyes were enucleated and fixed in 4% paraformaldehyde for 2 hrs. As previously described[97,98], retinas were immunostained for

γ-synuclein, a marker for retinal ganglion cells (RGC), and the number of surviving RGC was determined. Briefly, retinas where incubated overnight with mouse anti-γ-synuclein primary antibody solution (1:400, Abnova Corporation, Walnut, CA, USA), followed by several rinses in PBS and incubation with an Alexa Fluor 488 donkey anti-mouse secondary antibody (1:300, Life technologies, Grand Island, NY). After another PBS wash, retinas were whole-mounted, cover slipped and imaged. Twelve images (318 × 318 μm, 40X magnifications) were taken at predetermined mid-peripheral locations using a Nikon Eclipse i80 confocal microscope (Nikon Instruments Inc, Melville, NY). γ-synuclein positive RGC were counted in a masked fashion by an independent observer using the cell counter plugin in ImageJ software (NIH).

Statistical Analysis

For statistical comparisons *in vitro* between fresh and cryo-MSC, One-way ANOVA with Sidak correction for multiple comparisons with significance set at $p < 0.05$ was used in Prism 6 (GraphPad, San Diego, CA). For *in vivo* experiments, averaged RGC data was analyzed using Tukey's honest significant difference (HSD) post hoc tests (with unequal *N*) in Statistica software (Dell, Round Rock, TX). P-values < 0.05 are considered as statistically significant. All data are given as mean ± standard deviation (SD).

Acknowledgements

Financial support for this work was provided in part by the NIDDK Diabetic Complications Consortium (DiaComp), grant DK076169. Start-up funding provided by the Fraternal Order of Eagles Diabetes Research Center to was supported in part by Merit Review Award Number I01 RX001163-02 from the United States (U.S.) Department of Veterans Affairs Rehabilitation R&D (Rehab RD) Service.

CHAPTER 3: PRE-LISCENCEING MSC

MSC possess a potent ability to modulate the immune system and have been seen to exert their effects on both innate and adaptive immune cell subsets including T-cells, B-cells, NK cells, monocyte, dendritic cells, and neutrophils[99]. Measured outcomes of suppression assays involving MSC and PBMC have uncovered a broad panel of non-redundant effector molecules that attribute to MSC immune regulatory effects, including transforming growth factor-β1 (TGF-β1)[100–102], indoleamine-2,3-dioxygenase (IDO)[103–105], IL-6[106,107], IL-10[11,108], prostaglandin-E2 (PGE-2)[16,109,110], hepatocyte growth factor (HGF)[111,112], nitric oxide (NO)[113–115], heme oxygenase-1 (HO-1)[114,116,117], HLA-G5[118,119] and TNF-α stimulated gene 6 (TSG-6)[30,120,121]. MSC activation by means of inflammatory cytokines such as IL-17, IL-1α/β, IFN-γ, or TNF-α, generated following T-cell activation or activation of tissue macrophages and dendritic cells, is typically considered a pre-requisite for MSC-mediated immune modulation. MSC engagement with inflammatory cytokines, toll-like receptors[122,123], or danger associated molecular patterns[124] results in licensing. Licensing can result in MSC adopting anti-apoptotic, or pro-inflammatory characteristics depending on the nature of the stimulatory response. Although these auxiliary licensing strategies exist, priming efforts are primarily focused on directing MSC phenotype towards transiently promoting an immunoregulatory state. Pre-activated MSC strategies focused on enhancing immune-modulation hold enormous potential for obtaining more predictable clinical outcomes.

While pre-treated MSC have yet to be applied in a clinical setting, established enhancements to immunosuppression is widely reported in vitro. IFN-γ pre-treatment has

garnered particular attention, and has recently been shown to enhance reduction of colitis and GvHD mortality in mice[125,126]. Continued application of MSC in animal models and clinical trials is likely to result in cell therapies that enhance MSC immunomodulatory ability, as well as their capacity to survive and engraft in target tissues post-transplantation. Approaches to overcome persistence limitations post-transplantation are currently being explored through hypoxic preconditioning[127], and surface engineering methods to enhance MSC engraftment[128,129]. Despite these efforts to extend persistence of viable MSC, *in vivo*, it remains unknown as to whether MSC immunosuppressive phenotype can also be maintained post-transplantation.

One way to ensure MSCs make the most of their short persistence is through pre-activation, or priming, of MSC. While we and other groups have shown that IFN-γ primed MSC potently enhances their immunosuppressive capacity, it is unknown whether MSC would benefit from prolonged licensing. If MSC are capable of persisting long-term it would also be essential to know if surviving cells would remain functionally immunosuppressive. Given the complex and multifactorial roles MSC play in regulating inflammation, we sought to understand how long of pre-licensing is necessary for MSC to elicit a maximally immunosuppressive response. In parallel with this, we also aimed to identify how durable the MSC prelicensed phenotype is after removal of the pre-licensing media.

Using IDO as a marker for MSC licensing into an immunomodulatory state, we initially focused on identifying how MSC phenotype persists after prolonged exposure to an inflammatory environment. While many groups have delivered MSC to inflammatory

environments, these exposure regimens have typically treated the cells for 6-72 hr. However, these time points, while experimentally convenient, may not reflect the characteristic time frame native MSC are exposed to an inflammatory stimulus. We sought to observe MSC beyond this initial 72 hr time window and determine how these cells respond to prolonged stimulation of inflammatory cytokines (50 ng/mL IFN-γ). Our initial hypothesis was that MSC would get 'fatigued', after prolonged inflammatory stimulus. Fatigued cells would be identified by a loss in the ability to continually respond to stimulation via production of immunomodulatory factors. We expected the MSC to remain in a functional immunosuppressive state for a finite period, and ultimately enter a refractory phase where their immunosuppressive phenotype would be diminished.

This hypothesis was educated by the fact that MSC potency is highly variable with significant differences observed between donors[130] and a progressive loss of potency as cells are passaged[131]. *In vitro* cell expansion is routine practice for MSC therapy as thousands of harvested cells are expanded into lots of hundreds of millions of cells (15-20 population doublings). With each passage event, changes in MSC morphology and phenotype have been observed including a gradual increase in cell size and reduced expression of immunomodulatory factors[50,132]. A retardation of immunosuppressive properties in exhausted cells may then contribute to an increase in detection and clearance. Thus, we reasoned that these age-related changes to MSC might influence fatigue after continual inflammatory exposure. Parallel to the idea of continual stimulation, it would also be desirable to identify how MSC phenotype persists after an inflammatory event has been resolved.

To determine if MSC phenotype persists after an inflammatory event has been resolved, MSC were first pretreated with IFN-γ. During pre-treatment cells were either exposed to 6hr, 1d, 2d, 3d, or 4d of IFN-γ, followed by 6 days of rest in IFN-γ free media. We also wanted to know if MSC maintain their phenotype long-term, and we administrated a sustained course of IFN-γ stimulation for 10 days without rest. MSC were analyzed via western blot and cells were harvested on successive days after initial pretreatment (Figure 8A). IDO is an inducible enzyme in MSC, and is not basally expressed in MSC[133]. Despite this, withdrawal of inflammatory stimulus from MSC cultures did not result in rapid degradation of IDO. Instead IDO expression is steadily increased for days (Figure 8B). Notably, IDO protein levels appeared to be maintained over the course of several days, in the absence of stimulation. IDO presence also appeared to be contingent on the duration of pretreatment, as persistence of IDO in the cytosol can be maintained for several additional days after withdrawal of initial stimulation by subjecting MSC to longer pretreatment regiments. Sustained stimulation of IFN-γ revealed the highest levels of IDO, observed over a 10-day period. Interestingly, this finding is in direct opposition to our initial hypothesis. This implys that MSC immunomodulatory capacity does not fatigue after prolonged stimulation. Densitometry of western blots would also suggest that IDO reaches a maximum plateau over the course of a 10-day exposure to IFN-γ. The lasting effect of an IFN-γ priming strategy was also determined not to be due to upstream Jak/Stat phosphorylation of the IDO pathway. Upstream dephosphorylation of phosphotyrosine on STAT1 dimers occurs rapidly after withdrawal of IFN- γ, suggesting prolonged maintenance of IDO expression occurs downstream (Figure 9).

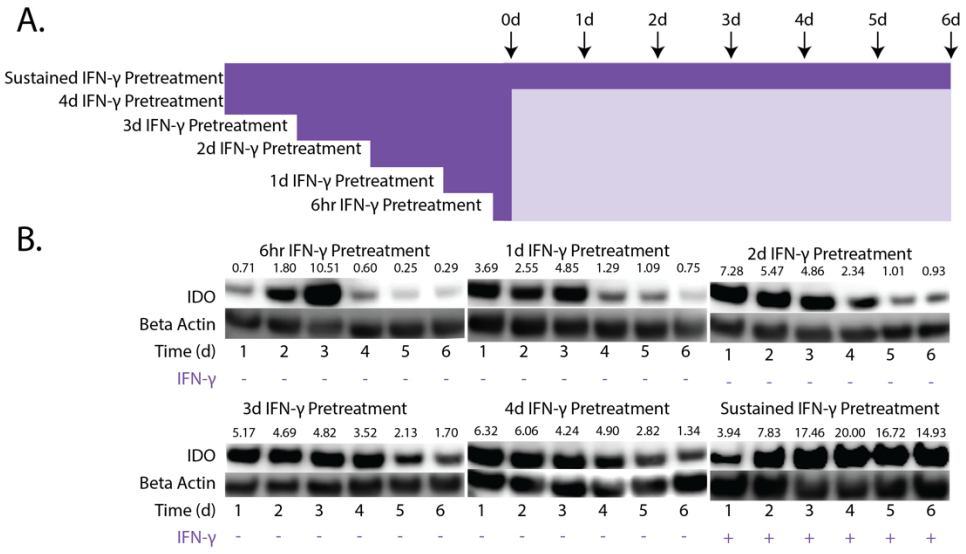

Figure 8: Kinetics of IDO expression after IFN-γ challenge.
(A) Timing of MSC exposure to IFN-γ and withdrawal of inflammatory stimulus. (B) Western blot of IDO protein content measured from MSC exposed to 50ng/mL IFN-γ. Beta actin shown as a loading control.

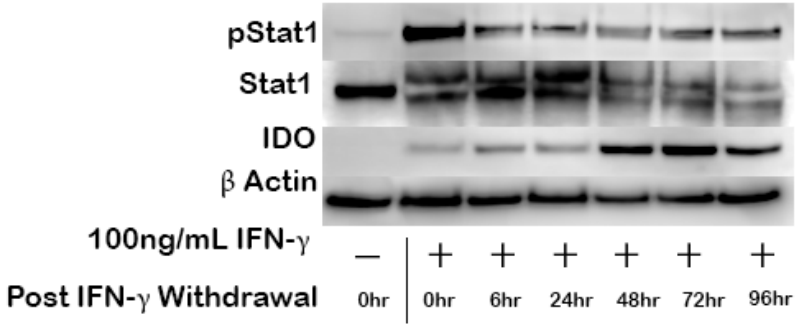

Figure 9 : IDO presistance is not due to prolonged Jack/Stat phosphorylation.
After 72 hours of treatment, IFN-γ was removed from MSC cultures. IDO protein expression continues to rise for days after inflammatory event has been resolved, while phospho-Stat1 is not maintained past 6 hours.

Knowing that IDO is highly sensitive to IFN-γ stimulation, I wanted to see if other secreted factors increased during this initial stimulation that could account for the subsequent persistence of IDO after inflammatory removal. The persistence of IDO, on a protein level, suggested that there may be a positive feedback loop present to maintain and augment IDO expression in MSCs. The idea of a positive feedback loop or co-dependency of multiple immunomodulatory factors has been suggested to exist in MSC. A larger body of evidence to support a feedback loop has emerged out of the related fields of cancer cell biology and dendritic cell literature[134–137]. Within dendritic and cancer cells, HGF, PGE2, TGF-β1, IL-6, and IDO have all been linked to playing a role in promoting autocrine feedback loops that may influence long term immunomodulation. For instance, IL-6 secretion has been shown to be dependent on PGE2 secretion by MSC[115]. Similar studies in human cancer cells suggest that constitutive IDO expression is sustained by and IL-6 autocrine loop[134]. While several other reports suggest IDO maintenance in tolerogenic dendritic cell is sustained by a TGF-β and HGF feedback loop and or possible codependency[135–137]. By identifying potential interdependencies and redundancies present in these pathways one might be able to better understand how cell behavior changes after an inflammatory event has been resolved. Alternatively, developing an understanding of how key molecular factors in MSC immune modulation are controlled, could help identify exposure regiments that could enhance MSC immune suppressive ability. Downstream, these exposure regiments could be used to prime cells to be hyper therapeutic in specific disease environments or be coupled with drug delivery strategies that could provide a local surplus of a crucial factor to maintain MSC phenotype post transplantation.

Here we specifically focused on the possible co-dependency of IDO, PGE2 and HGF, as reports on feedback loops involving these factors appear to be closely tied to priming with IFN-γ. To assess the potential of a possible feedback loop, MSC were either stimulated with IFN- γ, TNF- α, IFN-γ / TNF-α, for 72 hr (Figure 10). Both IDO and cyclo-oxygenase 2 (COX-2) are inducible enzymes. PGE2 is a catabolite of arachidonic acid and is generated by COX-2. Normalizing to MSC expression after 24 hours of IFN-γ/TNF-α licensing, analysis of all three trophic factors, IDO, COX-2, and HGF revealed dramatic changes in profiles that depend both on the combination of cytokines and duration of exposure. IDO is dramatically upregulated in presence of IFN-γ and acts synergistically with TNF-α to further enhance expression.

Interestingly, we see that while COX-2 is not induced by IFN-γ or TNF-α alone. When primed with both IFN-γ and TNF-α, the same kind of synergistic relationship observed in IDO expression profiles also appears with COX-2. While HGF levels are strongly upregulated upon stimulation with IFN-γ, priming with IFN-γ and TNF-α only moderately enhanced HGF expression.

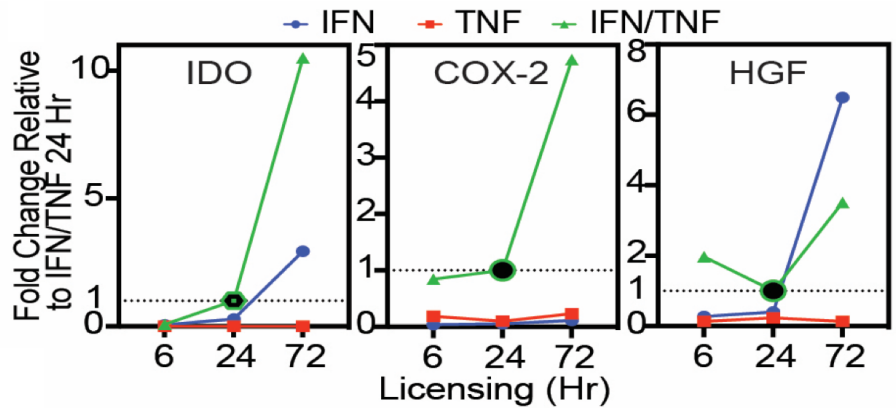

Figure 10: qRT-PCR analysis of IDO, COX-2, and HGF transcript levels after licensing MSCs for 6, 24, or 72 hours in IFN-γ, TNF-α, or IFN-γ/TNF-α licensing media. RNA extracted by Trizol followed by RNA column purification. Fold change calculated using $2^{-\Delta\Delta CT}$ relative to MSC expression after 24 hours of IFN-γ/TNF-α exposure using GAPDH as an internal control (4 replicates, representative of 2 MSC donors).

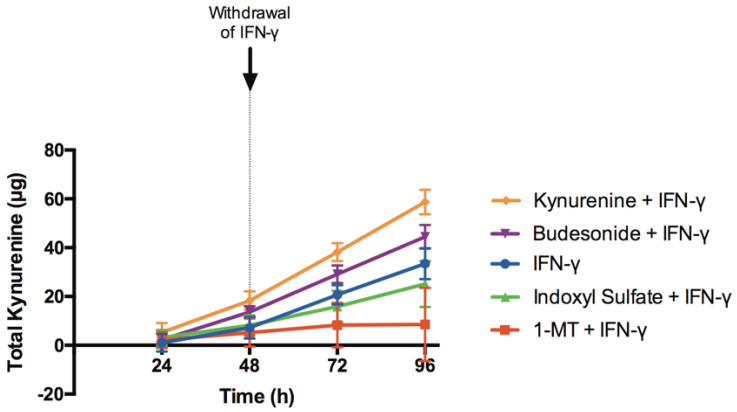

Figure 11: IDO-catabolism of tryptophan generates endogenous ligands capable of enhancing IDO.
MSC were pre-treated with IFN-γ stimulation for 48 hours with or with out addition of kynurenine (100µM), budesonide (1µM), indoxyl sulfate (10µM), or 1-DL-MT (500µM). IFN- γ was removed from media after 48 hours cells were continued to grow with drug or small molecule stimulation for an additional 48 hours. Cell media was collected daily and assessed for kynurenine presence using a colorimetric analysis.

While the persistence of IDO and COX-2 further suggested that there may be a positive feedback loop present to maintain and augment IDO expression in MSCs, additional factors may be at work to maintain prolonged IDO levels. Previous reports in cancer cell lines, dendritic cells, as well as MSC have suggested that the catalytic activity of IDO is linked to the signal transduction of the ligand-operated transcription factor aryl hydrocarbon receptor (AHR)[138–142]. Tryptophan catabolites such as kynurenines, are believed to augment MSC immunomodulation independent of IDO via acting as endogenous ligand of AhR[138,142]. To test if this feedback loop could be manipulated we stimulated MSC with IFN-γ in the presence of kynurenine, a tryptophan metabolite (Figure 11). Using kynurenine production as a colorimetric marker for IDO activity, we found IDO activity to increase significantly over baseline after withdrawal of IFN-γ. Accounting for the added levels of kynurenine doped into MSC media stimulated with IFN-γ, we found that kynurenine conditioning actually outperformed treatment of budesonide, a corticosteroid previously shown to enhance IDO production in MSC[28], treatment at all time points. However, an AHR agonist indoxyl sulfate appeared to not have an effect on promoting kynurenine over baseline.

It is still unclear whether AHR plays a direct role in enhancing IDO catabolism of tryptophan after an inflammatory event has been resolved. However small molecule stimulation appears to enhance IDO activity, as both Kynurenine and Budesonide treatment enhanced production of additional kynurenine in MSC, post withdrawal of IFN-γ. Although small molecules have potential in effectively evoking an enhanced immunomodulatory response in dendritic cells[143], few reports have utilized small molecules as priming agents to augment MSC immunomodulatory potency. The few

reports utilizing small molecules to enhance MSC immunosuppressive potential, have primarily focused on pretreatment with immunosuppressive drugs. MSC primed with the immunosuppressive drugs rapamycin, everolimus, FK506 or cyclosporine A showed an increase capacity to inhibit the proliferation of T-lymphocytes *in vitro*[144]. Akin to pretreatment strategies, non-genetic approaches to augment MSC have utilized engineered poly-lactide-co-gylcolic acid (PLGA) particles for a stable internalized delivery of glucocorticoid steroids[28,145].

Strategies utilizing small molecules could also be coupled with existing cytokine based licensing approaches. Small molecules often have the added benefit of being highly specific to a target gene or protein, while cytokines stimulation results in a wide range of inducible genes being activated[38]. Ranganath *et al*. recently developed a particle-in-cell approach has also been used to deliver TPCA-1, an NF-κB inhibitor, to regulate secretion of pro-inflammatory components of the MSC secretome[40,146]. Similarly, a priming strategy for MSC that could specifically enhance or suppress gene or protein products could further be used to maintain a potential positive feedback loop by specifically enhancing IDO or PGE2. To this end, we screened a short list of candidate small molecules that could be used to enhance a possible MSC immunosuppressive feedback loop centered around IDO and PGE2. Candidate regulators of IDO and PGE2 production included the hormone progesterone, as it has well documented immunomodulatory activity in maintaining maternal-fetal tolerance[147–149]. In this screen we also evaluated the AHR agonist indoxyl sulfate[150,151], the glucocorticoid budesonide[28], in addition to a cyclic AMP (cAMP) agonist forskolin[143] and an inducing agent, retinoic acid, which can facilitate development of adaptive Tregs[152–154].

To test for the effect of modulators of the IDO and PGE2 pathways on MSC potency, I set up co-cultures with MSCs and PBMCs at a 1:4 ratio and directly added the agent into the co-culture. Additionally, I ran PBMC only controls for all the drug treatments to determine if there were any direct consequences of the agents on PBMC proliferation (Figure 12A). Activated PBMC controls had CD3+/CD28+ Dynabeads and rh-IL2 added but were not treated with any agent – this condition was used as the maximum positive control. An MSC + activated PBMC control was used in the co-culture assay to determine this particular MSC donor's baseline immunosuppressive potency at a 1:4 ratio (Figure 12B) – this condition was used as the reference for enhanced immunomodulatory ability for each drug treatment (as represented by the dotted line). In the PBMC only controls, both indoxyl sulfate and progesterone had a significant effect on PBMC proliferation. Indoxyl sulfate caused about a 10% drop in PBMC proliferation compared to the activated control, while progesterone caused >50% reduction.

Interestingly, direct cytokine addition – and not pre-licensing, which has been shown to be effective in enhancing MSC immunosuppression – only moderately enhanced MSC's immunosuppressive ability. Budesonide did not appear to enhance MSC immunosuppression when added directly in co-culture, though it has been shown to be an effective strategy for enhancing IDO production when delivered internally as a drug loaded microparticle[28]. However, pretreatment with budesonide may be an ineffective strategy to enhance MSCs, as previous reports of stimulating MSC with immunosuppressive drugs suggests that any enhanced effect on MSC potency is likely due to adsorption of the drug by MSC during pre-treatment[144]. The adsorbed agent is

believed to exert its effect by subsequently diffusing into co-culture, resulting in inhibition of T-cell proliferation rather than directly augmenting the MSC immunosuppressive profile.

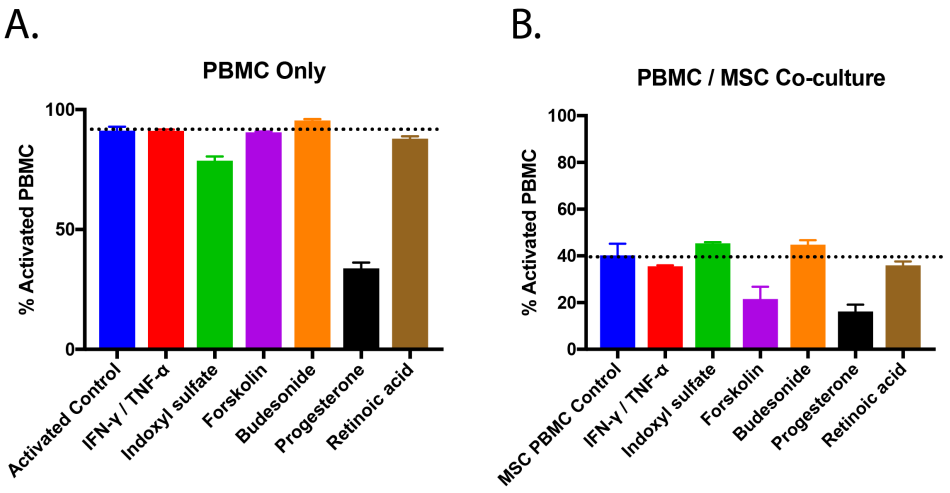

Figure 12: Small molecule screen identifies forskolin as a regulator of the PGE2 pathway that enhances MSC potency.
Co-cultures with a 1:4 ratio with drug treatments added directly into culture with (A) PBMC only, or (B) PBMC and MSC.

In co-culture, the most potently immunosuppressive conditions involved MSCs that were those treated with forskolin within the co-culture. Forskolin has been shown to increase cAMP levels, which is similar to PGE2 acting as an agonist at the EP2, EP3, and EP4 receptors. Recent literature has shown that forskolin's PGE-2-mimetic-like effects are predominantly mediated through the EP2 pathway versus EP3 or EP4 pathways[143]. To investigate whether forskolin's enhanced immunosuppressive effects are dependent upon

PGE2, I ran the same co-culture experiments treating with forskolin and indomethacin, which is an inhibitor of COX-2 the rate-limiting enzyme in PGE2 production.

In PBMC only controls, forskolin and indomethacin have no independent effects on PBMC proliferation, nor do they if used in combination (Figure 13A). In co-culture, forskolin once again enhanced MSC immunosuppressive potency – making the MSCs nearly twice as potent as baseline. When forskolin and indomethacin were used together in co-culture, this blocked the enhanced immunomodulatory effects of forskolin bringing the suppressive level back to baseline (Figure 13B). Indomethacin treatment alone caused a decrease in the immunosuppressive potency of the MSCs, implicating that COX-2 dependent factors are necessary for the baseline suppression of PBMCs. Restoring the signaling downstream of EP2 via treatment with forskolin and indomethacin brings the immunosuppressive level back to baseline, but does not account for the enhanced immunosuppression.

We then sought to investigate if forskolin's effects could be enhanced in a dose dependent way. In addition to increasing the dose of forskolin to enhance its effect, Braun *et al*. reported that forskolin has an added effect in promoting IDO in dendritic cells when co-administered with TNF-α[143]. To test this, PBMC and MSC co-cultures were set up in a 1:16 ratio. As before drug treatments added at the start of co-culture. In the PBMC only controls the highest does of forskolin combined with TNF-α resulted in a significant reduction in PBMC proliferation, causing >25% reduction compared to stimulated controls (Figure 14A). Interestingly, co-culture conditions suggest that forskolin's impact on enhancing MSC potency are dose dependent (Figure 14B).

Forskolin treatment in combination with TNF-α showed a minor enhancement in PBMC suppression, compared to equivalent dose forskolin treated groups. While TNF-α co-administration with forskolin shows a mild enhancement, high dose treatment of 20μM and 100μM forskolin potently suppressed PBMC proliferation at levels, exceeding suppression levels of microparticle approaches combined with glucocorticoids and cytokines[28]. To our surprise, forskolin's effects were eliminated when administered as a pre-treatment strategy alone (Figure 15), while pretreating MSC with 100ng/mL IFN-γ did show an enhanced reduction in PBMC proliferation.

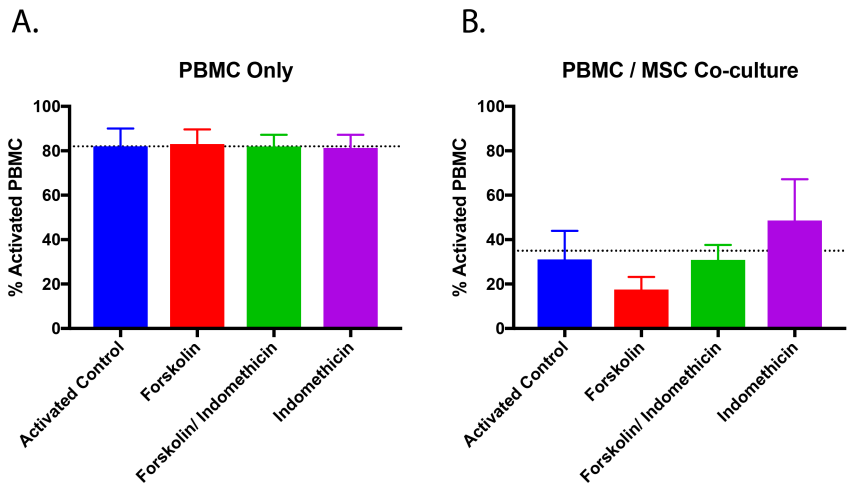

Figure 13: PBMC suppression is due to Forskolin's effects on MSCs and appears to be dependent COX2 activity.
Co-cultures with a 1:4 ratio with drug treatments added directly into culture with (A) PBMC only, or (B) PBMC and MSC.

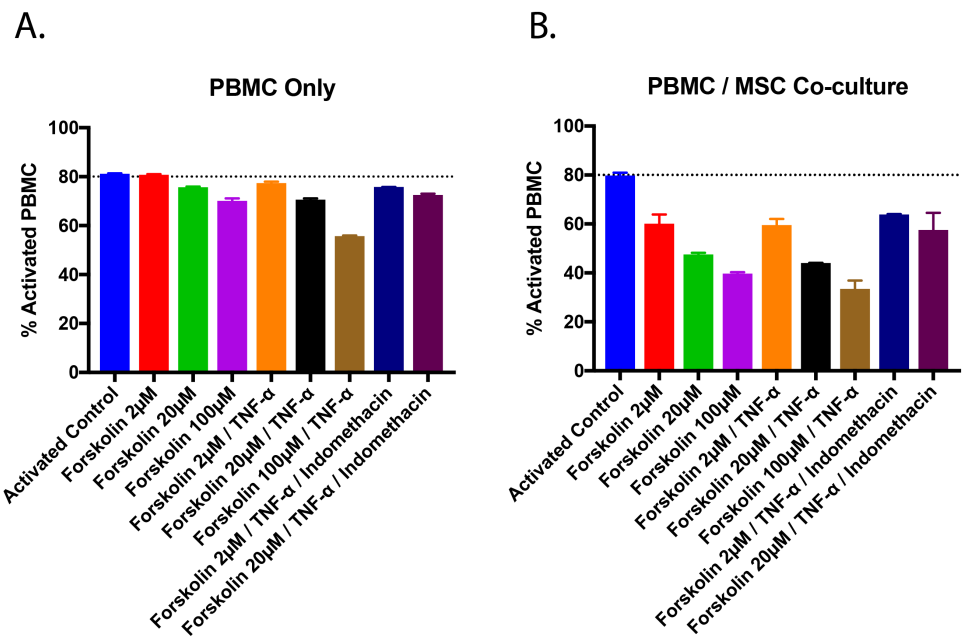

Figure 14: Forskolin effects are dose dependent and enhanced by TNFα.
Co-cultures with a 1:16 ratio with drug and cytokine treatments added directly into culture with (A) PBMC only, or (B) PBMC and MSC.

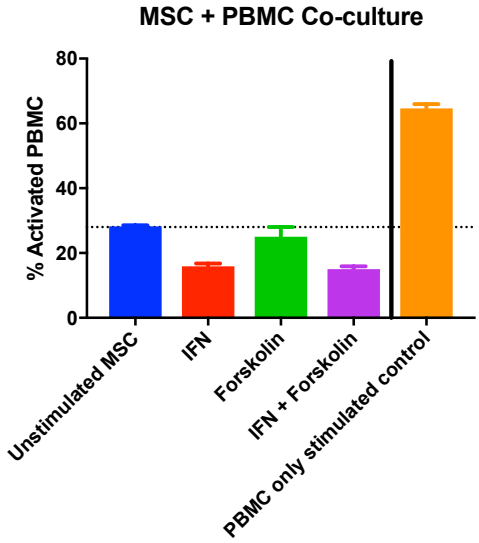

Figure 15: Forskolin's effects are eliminated when administered as a pretreatment strategy.
MSC pre-treated for 72 hr IFN-γ, 20µM forskolin, or 100ng/mL IFN- γ and 20µM forskolin. MSC were removed from pretreatment prior addition with PBMCs at a 1:8 ratio.

Discussion

IFN-γ and TNF-α treatment is known to enhance expression of trophic immunomodulatory factors in MSC, however duration and timing of exposure have dramatic influence over the immunosuppressive profile of MSC. Furthermore, IFN-γ treatment polarizes MSC into a stable phenotype that is capable of maintaining immunosuppressive properties days after initial stimulating agents are removed. Our results are also in accordance with other reports suggesting that MSC immunosuppressive capacity may be tied to a positive feedback loop; which facilitates in maintaining a robust phenotype in the absence of continual stimulation. Here in we demonstrated the potential of using pre-licensing to control MSCs post-transplantation and the critical need to identify optimal cytokine compositions and timings that preserve MSC's therapeutic functions. Future directions for this work aim to identify if pre-licensing time has a functional impact on the immunosuppressive capacity of MSC. While we show that increasing the duration or priming results in a monotonically increasing production of IDO, other groups have also shown that histone acetylation and chromatin remodeling changes of previously licensed MSC appears to make donors more responsive to a secondary inflammatory stimulus[155]. In future experiments, we hope to assess what effects donor variability have on IDO production. We suspect that, a poor IDO producing donor maintains the same intrinsic capacity to produce high levels of IDO as a high preforming donor, but is delayed in its responsiveness to IDO.

In addition to small molecules and IFN-γ and TNF-α, we also challenged MSC to other cytokine stimuli that might influence this enhanced and persistent state of IDO. Both kynurenine and budesonide where capable of enhancing IDO activity above cells that were stimulated with IFN-γ alone. Although a specific agonist of AHR did not enhance kynurenine output, AHR is also a known ligand dependent transcription factor with known to interact with a diverse range of agonists and antagonists, which influence its ultimate functional activity[156–158]. While AHR may be playing a role in enhancing IDO production via a kynurenine-dependent mechanism, the specific agonist of AHR indoxyl sulfate may only influence AHR-mediated transcription in an IDO independent process.

This data also highlights the potential small molecules have as an advanced treatment strategy to enhance MSC potency by targeting a single factor. The current study supports the idea that forskolin is dependent upon a COX-2 derived factor being present to allow for maximal immunosuppressive enhancement via either directly acting on forskolin or via a synergistic combination of downstream signaling. Forskolin's effects are also capable of being enhanced by co-administration with TNF-α, and suppress PBMCs in a dose dependent manner. While forskolin's effects are MSC specific, MSC require a constant signal of forskolin in order to maintain an augmented level of immune suppression. Future experiments on this topic will identify whether PGE2 and IDO levels are enhanced in forskolin treated conditions, the potential role forskolin plays in inducing surrogate MSC-educated myeloid-derived immune suppressive cells, as well as understanding if forskolin's effects can be mimicked by stimulating PKA or EP-2.

Methods

Human MSC Culture

Pre-characterized human MSCs (donor #7083) were acquired from Texas A&M Health Science Center College of Medicine Institute for Regenerative Medicine at Scott & White through a grant from NCRR of the NIH, Grant #P40OD011050, resource ID SCR_005522. Two additional pre-characterized sets of human donor MSCs (#00081, #00082, and #00055) were acquired from RoosterBio. All MSCs were acquired from healthy donors after informed consent with characterization conforming to MSC minimal criteria of the International Society for Cellular Therapy - all donors were >95% positive for CD73a, CD90, and CD105, but <2% positive for CD11, CD14, CD19, CD34, CD45, CD79a, and HLA-II with trilineage differentiation ability. Upon acquisition, MSCs were expanded using StemPro MSC SFM (Life Technologies) media supplemented 1% (v/v) penicillin/streptomycin, and 1% (v/v) L-glutamine at a density of 5000 cells/cm^2 until 70-80% confluence. MSCs were subsequently cryopreserved at a concentration of 1 x 10^6 cells/mL using CryoStor CS5 cell preservation media (Sigma Aldrich) and a CoolCell controlled rate freezing container (BioCision) and stored in liquid nitrogen until experimental use. All cells used for experiments were maintained for at least two passages out of cryostorage in MEM-alpha (Invitrogen) supplemented with 15% fetal bovine serum (Premium Select, Atlanta Biologicals), 1% (v/v) penicillin/streptomycin, and 1% (v/v) L-glutamine before being used for experiments at P3-6, representing ~6-11 population doublings.

IDO Protein and Activity Assays

To assess the effect of palmitate exposure on IDO protein levels, western blot analysis was conducted as previously prescribed. MSC were plated at a density of 5,000 cells/cm^2 in MEM-alpha supplemented with 15% fetal bovine serum (Premium Select, Atlanta Biologicals), 1% penicillin/streptomycin, and 1% L-glutamine unless otherwise stated.. Cell lysates were harvested at the indicated timeponts by washing wells with ice cold PBS three times to remove media followed by addition of 40 µl ice cold RIPA buffer (10 µl/ml PMSF solution, 10 µl/ml sodium orthovanadate, and 10 µl/ml protease inhibitor cocktail). Cells were then lifted using a cell scraper, collected in Eppendorf tubes, and incubated on ice for 5 min. Lysate was then clarified by centrifugation at 8000 rcf at 4°C for 10 min. The supernatant was then transferred to clean tubes and total protein concentration was determined by microBCA (Thermo Scientific). 10-20 µg of protein was added to a 4-12% Bis-Tris gradient gel followed by electrophoresis and transfer. Following transfer, the membrane was blocked with 5% nonfat dry milk in TBS with 0.01% Tween. Primary antibodies – rabbit anti-IDO (1:1000) and mouse anti-β-actin (1:20000) (Cell Signaling) - were then used to probe for protein bands. Horseradish-peroxidase-conjugated secondary antibodies (goat anti-rabbit IgG HRP and goat anti-mouse IgG HRP, Fisher Scientific) and WesternBright ECL HRP Substrate (Advansta) were used to visualize protein bands followed by densitometric quantification using the LI-COR C-Digit Scanner. Supernatants from the wells were collected to determine the effect of palmitate on IDO activity levels by assessing kynurenine production as previously described[44]. Protein in the supernatant was removed by addition of 100 µl of tricholoracetic acid (30%, w/v) and incubated at 52°C for 30 min to facilitate conversion

of N-formylkynurenine to kynurenine. Samples were then centrifuged at 2500 rcf for 10 min to pellet proteins, and 100 µl of the resultant supernatant for each sample was added to a 96-well plate. 100 µl of Ehrlich's reagent (0.8% p-dimethylaminobenzaldehyde in glacial acetic acid) was added to each well to induce a colorimetric change. Samples were then incubated at room temperature for 10 min follow by absorbance reading on a microplate reader at 490 nm.

MSC-PBMC Direct-Contact Co-culture

PBMCs from three de-identified blood donors were retrieved from leukopheresis reduction cones provided by the DeGowin Blood Center at the University of Iowa Hospitals and Clinics. For co-culture plating, MSCs were harvested and 15,625 or 62,500 MSCs were added to each well of a 24-well plate and allowed to attach for 2h. During the time for MSC attachment, PBMCs were labeled using a CFSE Cell Proliferation Kit (Invitrogen) at a final dye concentration of 1 μM. Prior to being added to each well, PBMCs were incubated for 15 min with an equal concentration of Human T Activator CD3+/CD28+ Dynabeads (Invitrogen). After this time, 250,000 PBMC and 250,000 Dynabeads were added to wells containing 15,625 or 62,500 MSCs, to achieve a 1:16 or 1:4 ratio of MSC to PBMC respectively. Total culture volume of each well was standardized to 750 μL of RPMI supplemented with 10% FBS, 1% (v/v) L-Glutamine, and 1% (v/v) penicillin/streptomycin. 30 µl of 20% w/v BSA and/or 10mM palm-BSA were added to each coculture once MSCs and PBMCs were plated, as well as recombinant human IL-2 to ensure T cell activation. Stimulated and unstimulated PBMCs without addition of glucose or palmitate were used as controls in both the co-culture and PBMC only plates. MSC-PBMC co-cultures were maintained for 6 days, after which time

the media from the wells (containing the suspended PBMCs) was collected and centrifuged to pellet the PBMCs. Supernatants from all wells were collected and analyzed in subsequent bead-based cytokine arrays. PBMC pellets from cultures with and without MSCs were re-suspended in RPMI followed by analysis via an Accuri C6 flow cytometer to assess for PBMC proliferation in the presence and absence of MSCs and/or palmitate.

RNA Extraction and Quantitative Reverse Transcription-Polymerase Chain Reaction (RT-PCR)

Total RNA was extracted using TRIZOL (Invitrogen) and reverse transcribed using a High-Capacity cDNA Reverse Transcription kit (Thermo Fisher Scientific). Quantitative real-time PCR reactions were performed with an ABI PRISM 7000 Sequence Detection System (Applied Biosciences) using the SYBR Green PCR Master Mix assay (Applied Biosciences). Gene expression values were normalized to the expression of GAPDH housekeeping gene.

CHAPTER 4: CONCLUSIONS AND FUTURE DIRECTIONS

The success of MSC clinical therapy will ultimately depend on the availability of a rapidly accessible source of reliably effective cells. An essential step in this process is understanding how MSC viability and potency is affected by changing environmental conditions.

Cryopreservation greatly simplifies the logistics of cell therapy, by allowing centralized GMP facilities to grow and characterize MSC phenotype. Cryopreservation allows MSC to be used on-demand, eliminating the need to wait for cells to be expanded or acclimated in culture prior to use. However, cryopreserved cells only have therapeutic utility if their potency is preserved in the process. The work presented here outlines a simple and effective method for cryopreserving MSC that maintains >95% viability, expression of immunomodulatory factors and growth factors, and the ability of MSC to suppress activated immune cells. In addition, we demonstrate cryo-MSC perform as well as fresh MSC in a retinal model of I/R injury. Thus, we observed no major detriment in MSC phenotype or potency in *in vitro* and *in vivo* assays following cryopreservation making cryo-MSC a feasible off-the-shelf therapy for some indications. Further studies warrant targeting additional disease indications and delivery routes to fully elucidate conditions and modes of delivery that are compatible with freshly thawed cryo-MSC. Furthermore, this work highlights the need to better understand how MSC priming strategies coupled with cryopreservation techniques must give appropriate consideration to the disease targeted for treatment. This work importantly highlights that the efficacy of priming and cryopreservation is disease specific and context dependent.

Most MSC priming strategies to date have focused on using licensing cytokines, which lead to dramatic shifts in MSC phenotype. However, many of these reports focus on the effect these factors have on enhancing a single factor. This work explores these priming strategies more holistically and seeks to examine both how these cells respond after an inflammatory stimulus has been resolved and the potential for licensed cells to maintain their phenotype through positive feedback loops involving multiple factors. While our initial work has focused on the effect kynurenine metabolites have on enhancing an IDO feedback mechanism our continued work in this area leads us to believe that a similar feedback mechanism may exist between kynurenine metabolites and PGE2, and may explain how MSC phenotype is able to persist long after initial stimulating signals are removed. Furthermore, this work uniquely identifies a cAMP agonist, forskolin, as a potent small molecule candidate to enhance MSC immunosuppressive properties alone or in combination with TNF-α.

As a whole, this thesis work contributes to the field of MSC therapy by furthering an understanding of how an immunomodulatory phenotype may be altered and maintained under different environmental conditions. Specifically, this work has reviled the following important points:

- MSC viability is maintained throughout the cryopreservation process.
- MSC retain their therapeutic potency in both in vitro potency assays, and an in vivo ischemia/reperfusion model.
- The function of cryopreserved MSC with and without IFN-γ prelicensing is context dependent.

- Cryopreserved MSC may serve as an appropriate delivery strategy for certain disease settings. Continued work in this field requires the identification of culture conditions capable of being paired with cryopreservation techniques to enhance MSC potency.
- MSC maintain their immunosuppressive potency in the absence of continual stimulation.
- MSC immunosuppressive potency is highly dependent on the timing and duration of its initial stimulus.
- Small molecules can be used as an effective conditioning strategy to enhance MSC immunosuppressive phenotype.
- The small molecule forskolin, potently enhances MSC mediated suppression of PBMC.
- The effects of forskolin are MSC specific, dose dependent, and require COX2 activity.

Results from these experiments may be used as a model for future studies to educate how MSC gene profiles evolve overtime in response do different inflammatory environmental stimulus. Understanding of how MSC phenotype is controlled during and after an inflammatory event is critical as this may lead research groups to make educated decisions on how pathway interactions, or new licensing strategies can be used to tune MSC into a hyper therapeutic profile by skewing pathways onto one another or accelerating transcription of several related immunomodulatory gene simultaneously.

APPENDIX A: MSC APPLICATIONS IN MULTIPLE SCLEROSIS

In addition to the primary work on maintaining and modifying a persistent immunosuppressive phenotype in MSC, we also explored the development and application of these tuned cells as a potential therapeutic in a closely associated mouse model of multiple sclerosis (MS) – experimental autoimmune encephalomyelitis (EAE). MS affects the central nervous system and afflicts approximately 350,000 Americans. MS is characterized by autoreactive T cells demyelinating nerve axons, which severely disrupts communication between the brain and the body. Current treatments manage neural inflammation caused by T cells, but are not capable of slowing the progression of the disease. Clinical trials utilizing MSC therapies have shown considerable promise in slowing or reversing the disease by decreasing effector T cell populations and promoting T regulatory cells (Treg)[159–161]. MSCs are capable of suppressing chronically inflamed environments and locally suppressing immune response through the secretion of soluble paracrine mediators and direct cell-cell contact. This makes them an exceptional cell therapy candidate for treating autoimmune diseases such as MS. A major knowledge gap facing MSC therapies for MS is understanding the cellular mechanisms of how MSCs mediate immunosuppression. Recent studies have highlighted the importance of MSC ability to inhibit serum levels of inflammatory markers such as IL-17A, Il-6, and IL-23[161]. Similarly, MSC appear to secrete neuroprotective factors such as hepatocyte growth factor (HGF), that play a critical role in mediating a functional recovery in animal models of multiple sclerosis[112]. However, the MSC ability to alter the inflammatory cell infiltration and promote remyelination can only be partially attributed to secreted factors alone. Success of future MSC therapies in MS hinges on the ability to understand how

multiple therapeutic mechanisms deployed by MSC can be synchronized to deliver predictable outcomes across patients.

Emerging evidence shows a strong correlation between MS disease recovery and MSCs secreting soluble factors to promote inducible regulatory T cells (iTreg); which in turn suppress pathogenic Th-1 and Th-17 cells. While Th-17 cells are a pro-inflammatory T cell subset that play an important role in anti-tumor response and extracellular microbial clearance at microbial barrier sights. Moreover, Th-17 cells produce unique inflammatory cytokines that drive nueroinflammation in MS. Th-17 cells are also strangely flexible in their developmental specialization. Interestingly, their differentiation lineage is closely linked to iTreg subsets, which act as an elegant ying and yang between immune homeostasis and pathogenic clearance. Numerous studies have indicated that an imbalance in the ratio of T cell subsets, Th17 and Treg, can play a key role in the pathogenesis and development of MS and other autoimmune diseases[162]. MSCs may alleviate MS pathology by skewing T cell polarization towards iTregs. MSC ability to secrete soluble factors may work to directly antagonize Th-17 cells and shift the balance in favor of Tregs by decreasing Th-17 dependent IL-6 levels while subsequently promoting Treg dependent TGF-β[163].

Promotion of endogenous Tregs can have profound and long-term effects on maintaining tolerance in an autoimmune environment. While this cell population may only represent a 1-5% of all lymphocytes, Tregs isolated from MSC cocultures have been found to strongly inhibit lymphocyte proliferation at a ratio of one Treg for every 100 responder Tcells[17]. While several non-cytokine cofactors and co-signaling receptors have been implicated in the promotion of Treg subsets, cognate antigen recognition by Treg T

cell receptors appears to be required for Treg activation. Immature dendritic cells expressing IDO have been shown capable of activating Tregs in an MHC restricted manner[164], and similar promotion of auto regulatory CD8 T cells in EAE also appears to be dependent on the recognition of specific antigenic determinates.

While MSC have been directly shown to promote Treg subsets in vitro, we also suspect that MSC transplanted in an autoimmune environment, such as MS, may present encephalitogenic antigen on major histocompatibility complexes (MHC) to promote Tregs. MSC, while not classically thought of as antigen presenting cells are capable of presenting and cross-presenting soluble antigen after being licensed into an immunoregulatory phenotype via IFN-γ[165,166]. Characteristic of this phenotype is high surface expression of MHC-I and MHC-II[167]. Despite high surface expression of MHC-II, it has been shown to not enhance the immunogenicity of MSC[168,169]. Importantly, hMSCs do not express crucial ACP receptors, like CD80, CD86, or CD40 normally used to drive effector T cell expansion[102,170]. MSC instead express PDL-1, ICAM-1, and HLA-G, which may act as counter co-receptors. Presence of these co-receptors in place of B7-1,B7-2 would disrupt the conventional T cell immunological synapse formation, required for T cell induction, and sets the stage for promotion of Tregs. Similarly MSCs secrete TGF-β (signal 3), one of the main cytokines responsible for driving iTreg expansion. Presence of signal 1 (MHC-TCR interaction), alternative signal 2 (PDL-1/B7H-1 – PD1) and alternative signal 3 (MSC secreted factors) on MSCs may play a counter intuitive role in promoting immunosuppression and tolerance.

In vitro suppression of mixed lymphocyte cultures have also been shown that 'third party' MSC are equally as suppressive as autologous MSC to the responder or

stimulating human peripheral blood lymphocytes[169]. Here the authors suggested that the effect of MSC suppression on peripheral blood lymphocytes was independent of MHC. However recent development in Treg tolerance has revealed that host-type Tregs may are capable of being induced by MHC-mismatched cell transplants[171]. MHC-mismatched mixed chimerism have since demonstrated autoimmunity reversal in mouse models of type 1 diabetes and EAE is accompanied by host type Tregs[172–176]. Importantly this recovery is not dependent on presence of donor-type FoxP3^{+} Tregs[175]. Given that FoxP3^{+} Treg induction, remylination and deletion of host-type autoreactive T cells are associated with both MSC and MHC-mismatched chimerism we suppose that MSC presentation of myelin antigenic determinants to T cells may play a role in initiating MSC mediated host-Treg induction in EAE mice. To promote MSC into a MHC-II^{Hi} state we stimulated our cells with 50ng/mL IFN-γ continuously for three days followed by withdrawal into a cytokine free environment. MSC were successively harvested over the course of six days and surface labeled for identification of HLA-DR using flow cytometry.

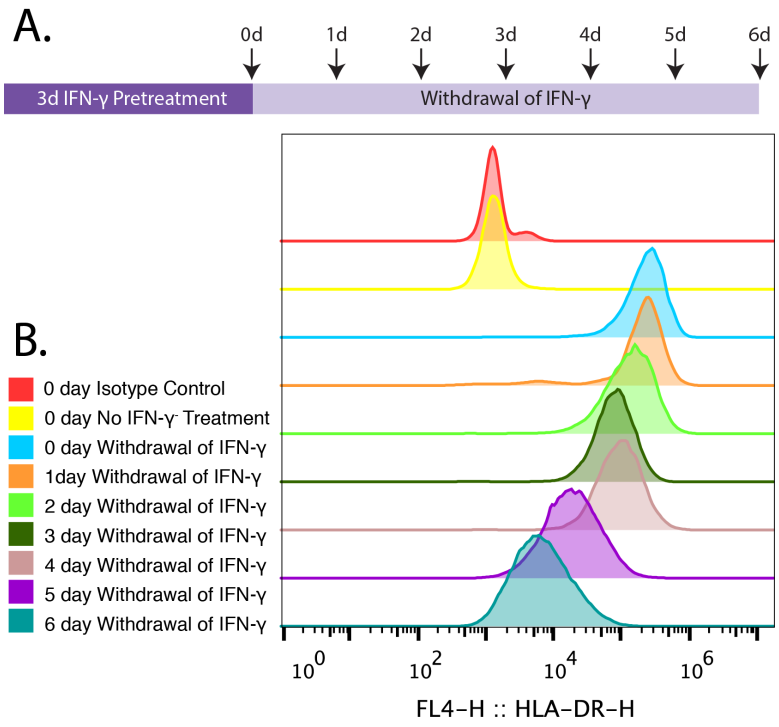

Figure 16: MSC Display prolonged HLA-DR surface presence post IFN-γ stimulation.

(A)Timeline of MSC treatment. MSC are pretreated with IFN- γ for 3 days. Inflammatory stimulus is removed and replaced with MEMα supplemented with 15% fetal bovine serum. Following stimulus withdrawal MSC are analyzed daily through flow cytometry over the course of 6 days. (B) Representative flow cytometry histograms overlays for detection of surface presence of human HLA-DR (*n=4*).

Here we observe that surface expression of HLA-DR closely follows the intracellular presence of the prototypical immunomodulatory marker IDO over the course of 6 days in the absence of initial stimulation (Figure 16B, Figure 8). In contrast immature dendritic cells, also capable of promoting Treg subsets, express relatively small amounts of MHC-II on their surface[177]. While prolonged presence of surface bound MHC-II is associated with activated dendritic cells and APC functions[178]. The stable persistence in HLA-DR progressively declined over the course of six days and was completely absent in the IFN γ^- unstimulated control. MSC were the challenged with IFN γ for 3 days and administered a model antigen, myelin proteolipid protein (PLP), known to induce EAE. The PLP amino acid sequence in the range 91-110 (YTTGAVRQIFGDYKTTICGK) is known to bind to HLA-DR epitopes[179] and was conjugated to Fluorescein isothiocyanate (FITC). MSC were allowed 24 hours to process the PLP antigen onto surface bound HLA-DR, prior to analysis though flow cytometry and immunohistochemistry. MSC stimulated with PLP-FITC showed bound presence of FITC 24 hours after initial antigen challenge and showed a correspondent increase in surface expression of HLA-DR (Figure 17).

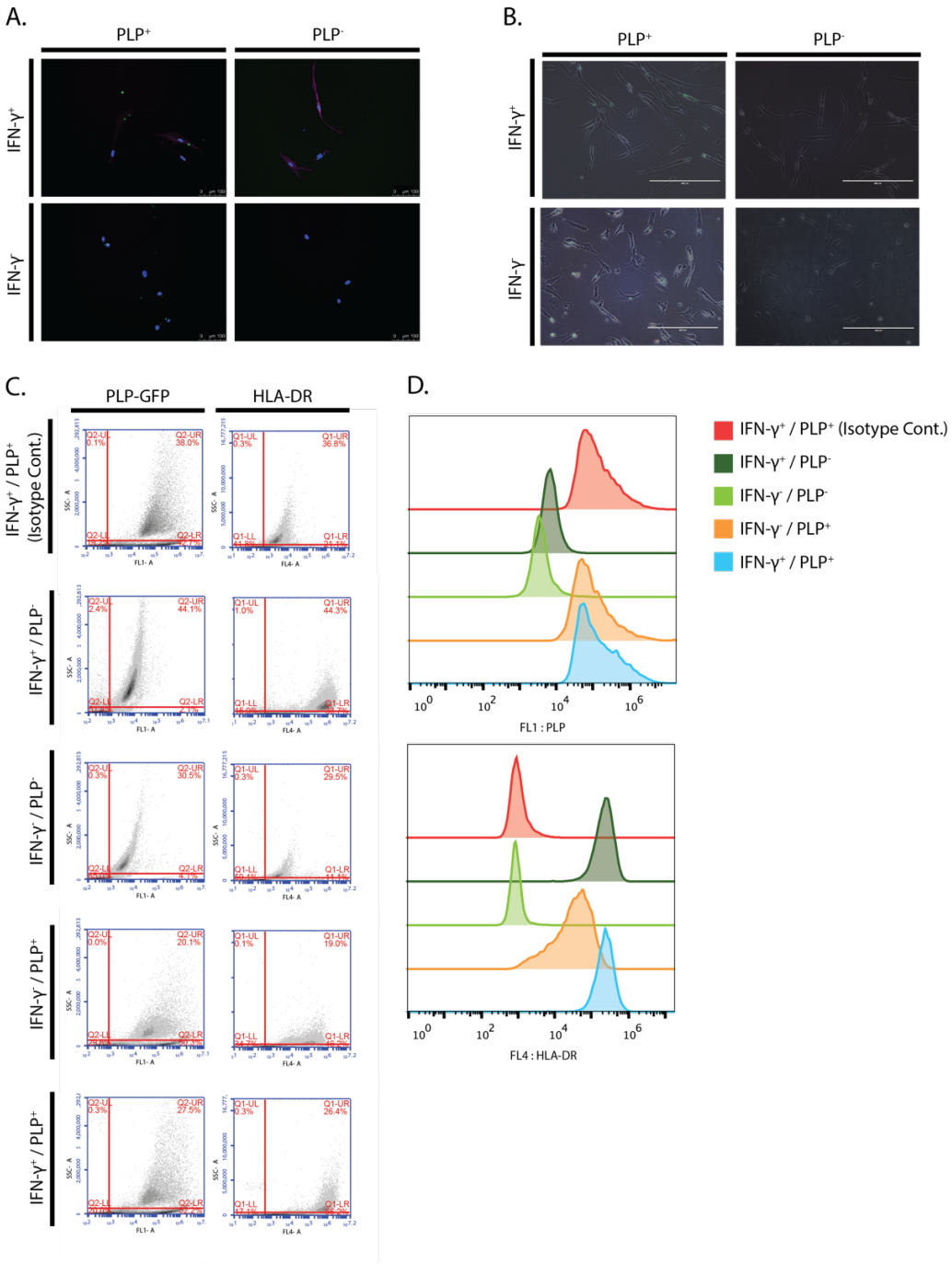

Figure 17: MSC uptake and present soluble PLP antigen on surface bound HLA-DR.

(A) MSC stained with Alexa Fluor® 647 dye tagged with anti-HLA-DR shows increase expression of HLA-DR in IFN- γ^+ conditions, (A, B) while surface bound FITC tagged PLP is present in all groups receiving 24hour PLP challenge (PLP^+). (C) Flow cytometry gating for PLP-FITC and anti-HLA-DR. (D) Population histograms of MSC challenged with IFN- γ and or PLP-FITC.

These preliminary findings of prolonged surface expression of HLA-DR and MSC ability to uptake target antigens of MS in absence of traditional T cell costimulatory molecules provides the initial support behind the hypothesis that MSC may be capable of promoting host-Treg subsets via PLP priming. In the future, this proposed mechanism of facilitated MSC mediated tolerance could be applied to *in vivo* murine models of EAE, as well as for use in ameliorating MS associated pathologies. Of specific interest would be to examine the role MSC may play in curing Optic neuritis - an associated pathology of MS, often an early sign of the disease. In fact, approximately 15-20% of patients that are diagnosed with MS have optic neuritis as a presenting feature, while the disease will manifest in 50% of all MS patients at some point in the course of their disease[180–184]. Damage to the optic nerve and bystander inflammation to the head of the unmyelinated optic nerve, lamina cribrosa sclerae, results in rapid onset of vision loss. While bilateral clinical presentation is rare, vison loss is permanent and may cause progressive visual loss. However rapid onset of visual loss allows for early detection, diagnosis, and treatment of MS associated optic neuritis. Patients with optic neritus associated MS are typically diagnosed with MS within 48 hours of initial visual symptoms, and immediately put on a treatment plan thereafter[184]. Despite our ability to detect and manage MS symptoms, there is an urgent need to understand how to translate MSC therapies from clinical trials to the treatment of the population at large.

Here, I propose to pair MSC therapies with MS associated optic neuritis to both treat optic neuritis and prevent MS. Delivery of MSC to treat optic neuritis may increase the clinical efficacy of these treatments, as early treatment of MS with daily high dose glucocorticoids or corticosteroids is associated with reduced disease progression[185,186].

Moreover, MSC have been shown to be most effective in preventing the progression of MS when administered at early stages of disease progression in mice[187]. Early treatment of MS in humans, recently diagnosed with optic neuritis, may allow MSC to have a more substantial impact on reversing the progression of MS, compared to late stage relapse remittent patients[188]. Furthermore, rapid early detection and treatment of optic neuritis make it a strong candidate therapy to pair with an "off the shelf" cryopreserved MSC.

Long term studies of visual prognosis in MS patients with clinical manifestations of optic neuritis have shown a progressive loss in retinal nerve fiber layer which is directly linked to retinal ganglion cell (RGC) loss[189–191]. Importantly vision loss in optic neuritis has been directly linked to this RGC death[192]. Autoimmune triggered inflammation on the optic nerve results in deleterious stress on resident oligodendrocytes, leading to dysfunction of mitochondrial oxidative metabolism in the retina[192]. An important anatomical feature to consider is that RGC axons located in the pre-laminar region of the optic nerve are unmyelinated. Thus, the generation and propagation of action potentials in this region is inefficient and requires greater energy input to properly transmit visual signals[193,194]. Histological studies of human optic nerves have reviled that mitochondrial COX and succinate dehydrogenase (SDH) enzyme activities are concentrated at the prelaminar unmyelinated optic nerve[195]. These histological studies suggest that approximately 90% of mitochondria of the optic nerve are concentrated in RGC resident to the pre-laminar region[195]. Retrograde axoplasmic transport across the optic nerve concentrates this mitochondria to the RGC[194]. Disruption of this mitochondrial transport leads to energy failure of the RGC and eventual RGC loss and death. The prelaminar segment of the optic nerve can then be considered a vulnerable

"choke point" that could be rescued through restoring energy balance to the RGC. Emerging evidence suggest that MSC also employ mitochondrial transferring tunneling microtubules, which could be exploited to restore energy balance in inflammatory environments[196,197]. Our previous study using MSC to rescue RGC survival in a murine ischemia reperfusion stroke model as well as in glaucoma[44] lead us to believe that mitochondrial transfer from MSC to injured RGC plays an important role in the RGC rescue we observe. To further investigate the possible use of MSC as a treatment in optic neuritis I propose using a PLP based experimental autoimmune encephalomyelitis (EAE) mouse model. Administration of PLP and complete fruends adjuvant leads to reliable development of optic neuritis in C57B6 mice and Lewis rats.

In this study we would be specifically interested in using MSC for optic neuritis treatment while subsequently curing EAE in mice. We suspect MSC are capable of transferring mitochondria to restore energy balance in RGC and this transfer would correlate with improved outcomes. If successful this experiment could be paired with a priming of MSC with PLP antigen to increase the effective ability of MSC to promote tolerance and EAE recovery.

APPENDIX B: ENGINEERING ORGANOID SYSTEMS TO MODEL HEALTH AND DISEASE

In addition to optimizing and modifying a MSC immunomodulatory phenotype, my work has also supported the development of 3D culture systems to guide assembly of MSC into spheres or biodegradable spheroid scaffold constructs. These approaches have several advantages over traditional 2D culture systems, and have application far beyond just MSC research. Sophisticated self-assembling 3D culture systems are being developed across the field of tissue engineering and have considerable promise to model health and disease states.

Much of the *in vitro* study of organs relies on responses from monolayers composed of one or more cell types, however in many cases this simplistic modeling of the organ system does not replicate how cells behave *in vivo* in the context of their organ and organism. While many useful cell characteristics can be deduced from 2D cell cultures, a full understanding of organ systems and biology requires studying cells in the context of their native environment. Traditionally, animal models have fulfilled this role, however, in the past decade techniques and technologies to grow 3D tissue organoids in culture have been developed as an intermediate or replacement for *in vivo* studies. In this chapter, we review the genesis of organoid culture systems and provide an in-depth view of several fields that have been significantly impacted by organoid technology. Finally, we summarize emerging applications of organoids in modeling health and disease, treating patients, and discovering novel pharmaceuticals.

The following chapter is an excerpt of sections I have written for a review chapter entitled “Engineering Organoid Systems to Model Health and Disease”. This work has

accepted for publication in the following book though Springer Publishing Company "Cell Therapy: Current Status and Future Directions". Edited by, Dwaine Emerich and Gorka Orive.

Authors: James Ankrum, Thomas Bartosh, Xiaolei Yin, Alexander Brown, Anthony Burand, Lauren Boland

Keywords: Matrigel, Spheroid, Organ on a chip, stem cells, niche, model system, drug discovery, regenerative medicine, paracrine signaling.

Introduction

The ability to propagate cells *in vitro* revolutionized biology and medicine in the mid-twentieth century enabling the study of individual cell types and cell clones independent of their complex *in vivo* environment. Cell culture also proved immensely useful in the reproducibility of results, as cell lines could be generated and shared amongst laboratories. Perhaps most famously, the HeLa cell lines ushered in a new paradigm for cancer research and drug discovery[198]. While critical to the advancement of science to date, *in vitro* systems have not been without significant shortcomings. Discoveries in cell culture have been notoriously difficult to successfully translate to *in vivo* animal models[199,200]. What is beneficial to a specific cell type in culture may prove toxic to other cell types in the body. Furthermore, the pharmacokinetics of drugs cannot be appreciated with simple *in vitro* systems as they are dependent on the metabolism of drugs by the liver and the kinetics of drug excretion[200]. In addition, the artificial nature of cell culture systems in which cells are rapidly dividing and bathed in growth factors and nutrients can create biological scenarios that would rarely, if ever, be observed if the cell where in its native environment. Without discounting the immense utility of cell culture systems, it is important to understand the similarities and differences between the *in vitro* and *in vivo* environment.

Multicellular organisms are by nature, systems, in which each cell interacts and impacts the fate and function of the surrounding cells. Such systems quickly grow in complexity as they form distinct tissues, organs, and regulatory networks. Embedded into the fiber of every model system is an assumption or allowance of approximation to

reality. As novel technologies are developed, this allowance of approximation must necessarily decrease as our models more closely approach the true value of the subject being modeled. The environment of a cell in traditional *in vitro* culture systems is distinct from its natural *in vivo* environment in multiple aspects as outlined in Table 1. *In vivo* environments exist in 3-dimensions, are exposed to endocrine signaling from distant tissues, thrive in low oxygen tensions, and receive paracrine signaling from both similar and distinct cell types in their local vicinity. In contrast, purified cultures *in vitro* lack the physical architecture and signaling from their neighbors and are instead sustained by growth factors and metabolites supplemented in culture media. Such signaling sustains the viability of the cells in culture allowing the culture to be propagated and studied in a highly controlled fashion. However, the *in vitro* phenotype of cells can easily be altered causing *in vitro* cultures to fall short of recapitulating *in vivo* biology.

Table 1: Differences Among 2D and 3D Culture Systems.

Variable	*2D*	*3D*
Transport	Gradients absent	Diffusional transport limitations
Focal adhesions	Basal surface only	distributed in 3D
Cell junctions	Integrin-ECM	Integrin-ECM
		adhesion juctions
		gap junctions
		tight junctions
		desmosomes
Mechanical properties	Single stiffness, typically high kPa	Potential for variable stiffness
Organization	Uncontrolled organization	Sptatially Distinct Zones
Platforms	Culture flasks	scaffolds
	Transwell cocultre inserts	scaffold free speroids
	matrix coated 2D	fluidics systems
	fluidic systems	spinning flask bioreactors
		organotype explant culture
		micropattered surface microplates
		microcarrier culture
		gels
Polarity	Forced apical-basal polarity	no prescribed polarity
Cell interface	50% cell-surface (plastic / matrix)	80% cell-cell & cell-matrix
	50% cell-liquid	20% cell-liquid

While *in vitro* systems lose the systems-level regulation seen *in vivo*, they also provide critical advantages over *in vivo* systems that make them of immense utility for both research and the development of new therapies. Cell culture systems are cheaper and more accessible than animal or human studies. For example, cell culture systems enable high throughput screening of hundreds or thousands of drugs to identify new candidates to treat cancer. The analogous experiment in an *in vivo* system, whether small

animal or human, would be both cost-prohibitive and ethically questionable. In addition, many culture systems are amenable to culture expansion, in which billions of cells can be generated from a common source. Thus, the cells in each well of an experiment or even in experiments performed on opposite sides of the world can be of a common source. Such expansion potential, makes culture systems highly reproducible and distributable. Finally, cell culture systems are highly controllable, as their environment is completely controlled by the researcher. Virtually every aspect of the cell's environment including its extracellular matrix, pH, and exposure to oxygen, glucose, nutrients, growth factors, and cytokines can be tightly monitored and controlled. This control enables robust identification of specific pathways and mechanisms that control cell phenotype and has led to the discovery of protocols that drive the differentiation of progenitor cells and pluripotent stem cells. Such strategies are now being leveraged to generate large pools of cells that can be used for drug screening as well as the development of cell-based therapies. Two-dimensional *in vitro* cell culture has been a vital tool cultivated in research labs to probe and model questions of cellular biology without the complexity of the multivariate *in vivo* environment. However, 2D cell culture scenarios are rife with assumptions that make translation of scientific discovery to medical therapies that much more complicated, motivating the development if the next generation of *in vitro* models.

Organoid systems under development today seek to combine the advantages of *in vitro* systems including their reproducibility, scalability, and cost with the systems level communication cells are accustom to experiencing *in vivo* to better recapitulate *in vivo* biology in a dish. Herein we will highlight progress to date in organoid development in key fields including mesenchymal stem cells (MSC), mini-brains, insulin producing cells,

and intestinal stem cells, and look at the future prospect of organoid systems in research and therapy.

Multicellular Organoids

While spheroids composed of a single cell type can dramatically alter the phenotype of the cells, 3D culture systems can also replicate *in vivo* anatomical relationships of different types of cells. These multi-cell-type assemblies are called organoids and techniques to develop them have been developed to aid in the study of many fields including neuroscience and stem cell niches. Multicellular organoids are inherently more complicated, as they require different cell types to be supported by a common culture media and to be arranged in such a way that the spatial relationship of different types of cells are maintained. In this section we highlight advances over the last decade in the development of *in vitro* organoid systems.

Development of a Mini-Brain in a Dish

Neurons and glial cells that give rise to the brain heavily rely on an orderly composition of mechanical, biochemical, and spatial queues to coordinate differentiation, migration, survival, gene expression, and synaptic transmission. Given the complexity of the brain, studying neuronal development and disease has proven to be challenging in living organisms. These important structural and microenvironment ques become dismantled when neurons are grown in 2D planar cultures, making it difficult to accurately characterize neuronal behavior. Driven from the need to develop better *in vitro* models capable of recapitulating brain tissue, neuronal spheroids have emerged as a

novel research platform to interrogate neuronal development, drug transport, and pathogenesis of neuronal disease.

Initial development of 3D neuronal constructs relied on scaffold based structures composed of collagen, Matrigel, alginate, and silk derivations[201–205]. More sophisticated strategies which utilize composite biomaterials constructed of alternating mechanical properties allowed for use of a stiff scaffold to provide neuronal anchoring while softer gel matrixes promoted axonal connectivity. This strategy demonstrated that modular 3D architectures are capable of being created and can be used to mimic relevant biomechanical stimuli needed to support neuronal development. Despite this, biomaterials still present degradation and structural challenges that can limit the size, complexity, and viable time window an individual organoid can be studied. Alternative approaches to neuronal organoid development include biomaterial-free architectures that promote spontaneous neurogenesis, akin to central nervous system (CNS) processes that naturally occur during development. At this time there are a number of emerging methods to generate ordered 3D tissue using neural progenitor cell aggregates[206–211]. The serum-free floating culture of embryoid body-like aggregates with quick re-aggregation (SFEBq) method has been widely used to generate discrete CNS regions such as cerebral cortex[211–214], pituitary[215], and retina[211,216]. Similar methods relying on poly(dimethylsiloxane) (PDMS) microwells to facilitate aggregation of neural progenitor cells, have demonstrated functional connectivity and transmission of electrical stimulus propagated through a 2D array of bundled spheroids[217]. Future implementations of a microchanneled network could conceivably tether discrete CNS organoids in an

interconnected and modular 2D array. Linking neural organoids in this manner could allow for sophisticated models for drug screening and neurophysiology.

Importantly, Lancaster *et al.* has also reported a method to generate self-organized organoids composed of discrete, yet interdependent, multiregional subunits (Figure 18)[207,218].

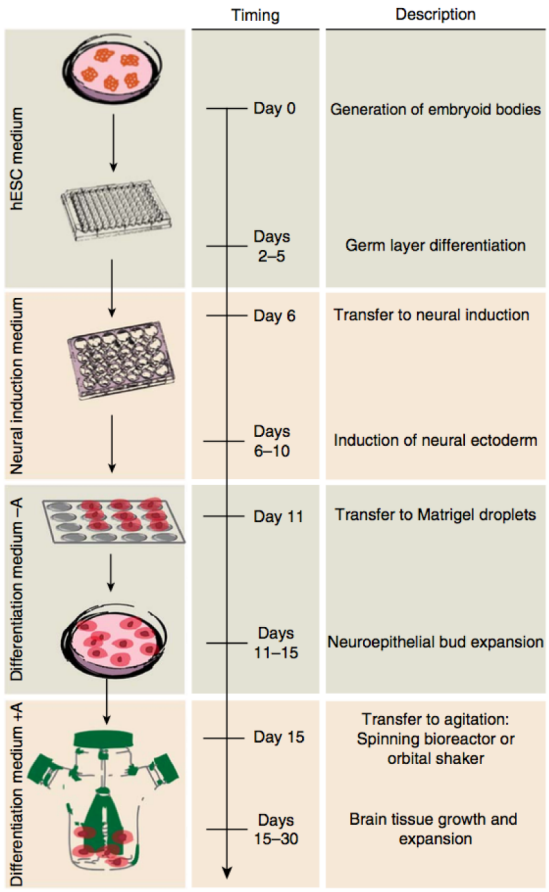

Figure 18: Schematic diagram of the cerebral organoid production method and timing. Figure adapted from Lancaster et al.[207] with permission from Nature Publishing Group.

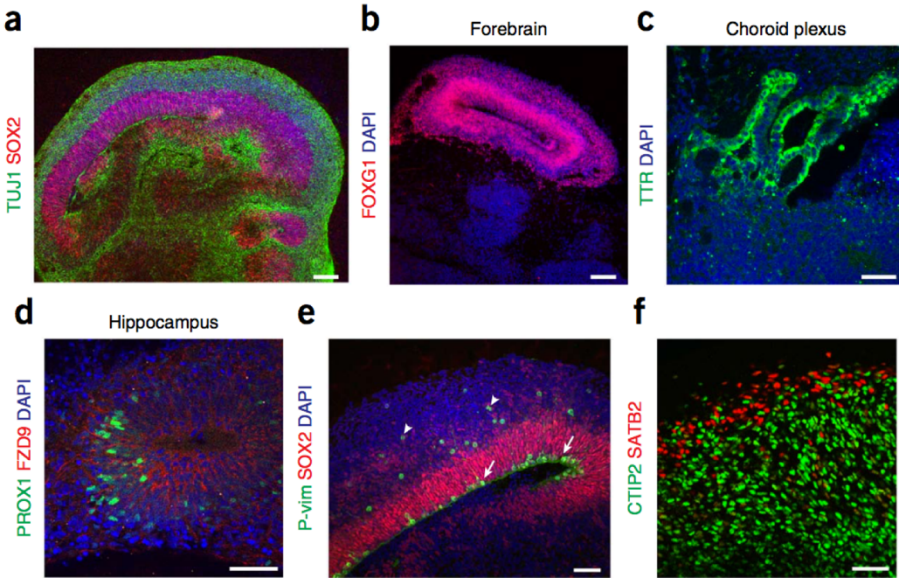

Figure 19: Staining for brain regions and neuronal cell identities in in vitro grown mini-brains.

Organoids grown in the lab can be stained to reveal numerous distinct regions of brain ranging from (**A**) cortical tissue composed of neurons (TUJ1, green) and progenitors (SOX2, red), (**B**) forebrain identified by positive staining for FOXG1 (red), (**C**) Choroid plexus identified by TTR staining and convoluted cuboidal epithelium and (**D**) Hippocampal regions identified by PROX1 (green) and FZD9 (red) staining. (**E**) Staining for mitotic radial glia (P-vimentin (P-vim), green) in a cortical region reveals inner radial glia undergoing mitosis at the apical membrane (arrows), whereas outer radial glia undergo mitosis outside the ventricular zone (arrowheads). All radial glia are marked by SOX2 (red). (**F**) Staining for cortical layer identities of advanced organoids (75 d). Later-born superficial-layer identity (SATB2, red) neurons populate more superficial regions of the organoid, whereas early-born deep-layer identity (CTIP2, green) neurons populate deeper regions of the organoid. DAPI in **A-E** labels nuclei (blue). Samples in **A-E** are 30–35 d after initiation of the protocol. Scale bars, 100 µm (**A,B**) and 50 µm (**C-F**). Figure and description adapted from Lancaster et al.[207] with permission from Nature Publishing Group.[207] with permission from Nature Publishing Group.

Both the SFEBq and former organoid methods show high similarity in development of pallium tissues, yet they maintain distinct differences in media formulations, and developmental timings. Notably the method developed by Lancaster et al. incorporates a 3D Matrigel to facilitate growth of embroid bodies into continuous neuroepithelial tissue. Whereas adaptations to the SFEBq approaches have attempted to utilize addition of dissolved extracellular matrix proteins to expand growth of this tissue[219–222]. Using a spinning bioreactor, suspended 3D Matrigel constructs were able to spontaneously generate cerebral organoids with discrete hippocampus, forebrain, chordid plexus, Dorsal cortex, Prefrontal lobe, retina, and cortical interneurons after two months (Figure 19). Furthermore, the cerebral organoids could be maintained for over a year and grew up to 4mm in diameter[207]. Next generation cerebral organoids might employ engineered vascular networks capable of delivering nutrients to the inner cell mass to improve survival maturation of these structures.

While numerous groups have reported on the structural similarities of these neuronal organoid systems, Camp *et al.* identified close genomic similarity of cortical processes like progenitor cell proliferation, production of extracellular matrix, migration, adherence, delamination and differentiation between structured fetal neocortex and their organoid culture system counterparts[223]. Given their functional and near-physiologic structural similarities to brain tissue, cerebral neuronal organoids are emerging as an essential tool for basic neuroscience investigations in neuronal development[211,212,216,223].

Pancreatic organoids for insulin production

Development of mulitcelluler organoids represents an exciting cell replacement tool that could modernize organ transplantation for degenerative diseases like type one diabetes (T1D). Pancreatic islet transplants based off the "Edmonton protocol" relied on transplantation of allogenic islets to restore insulin independence. Despite the relative success of this therapy, serious issues including the massive loss of islets post-transplantation due to instant blood-mediated inflammatory reaction and a limited donor supply have limited the therapeutic reach of this procedure. Pancreatic organ donations alone are insufficient to meet the demand of patients waiting for a curative treatment for T1D. This has prompted numerous groups to develop alternative sources of insulin producing cells.

The pancreas is a glandular organ serving both exocrine and endocrine functions. The endocrine functions of the pancreas are primarily mediated through beta, delta, alpha, and PP cells resident in the Islets of Langerhans. The embryonic cells that generate the islets of Langerhans are traditionally characterized by presence of the transcription factors PDX1, PTF1a, SOX9, and HNF1b[224]. 3D self-organization, and commitment of these cells to a terminal duct or acinus fate requires a highly regulated series of intra- and inter-cellular signaling events compounded with spatial-temporal environmental cues during foregut development. Differentiation capacity and origin of adult pancreatic stem cells, however remains an openly debated topic. In fact several sophisticated linage tracking studies have argued for and against the idea of adult multipotent stem cells capable of being sourced from ductal and acinar cells[225–230]. Although several adult and

iPS derived sources have been employed, the generation of 3D organoids in culture has primarily been accomplished using embryonic progenitors.

The earliest instances of pancreatic organoid research utilized neonatal rat pancreatic endocrine cells which were found to reorganize into a smooth-contoured 3D structure on a collagen gel[231]. This reorganized structure also resembled topographical patterns of the islets of Langerhans seen *in vivo*. Since then, multiple culture conditions have been reported to successfully generate pancreatic organoid like structures from disassociated E10.5-E11.5 embriod progenitors, including spheres, clustered ductal networks, and mini-pancreatic tissues. Similarly, a number of culture conditions for pancreatic endocrine spheroids expanded from adult mouse and human ductal sources have been developed to generate pancreatic endocrine spheroids[232–234]. For a comprehensive review on the developmental techniques and culture conditions used to generate many of these pancreatic organoids we refer the reader to the excellent review described by Greggio et al[235]. Matrigel has been widely employed as the material substrate of choice to facilitate the spontaneous generation of a multicellular pancreatic environment. Laminin is a major component of Matrigel, and has been shown to play an important role in facilitating endocrine differentiation of adult and embryonic derived cell types. Similarly stiffness of these hydrogels has been shown to play an important role in pancreatic organoid clustering, as only hydrogels with low modulus of elasticity (~250Pa) were capable of maintaining these structures[236]. While gel composition and structure appear to be playing clear roles in the engineered pancreatic niche, advancement of differentiation protocols will likely require development of new materials with tunable

structural properties and integrated lineage directing cues to better dictate cell fate in pancreatic organogenesis.

While embryonic cells remain the standard for generating insulin producing cells (IPC), ethical and immunogenic HLA barriers surrounding these cell sources have put increased pressure on identifying alternative sources of IPC. Mouse fibroblast derived induced pluripotent stem cells (iPS) derived IPC have been shown to effectively reverse hyperglycemia in a diabetic mouse model[237]. Human iPS derived IPC were also shown to form a vascularized organoid when injected under kidney capsules of $Rag2^{-/-}$ $\gamma c^{-/-}$ streptozotocin induced diabetic mice[238]. No biomaterial scheme was implemented in this model, yet transplanted IPC still showed tissue adhesion at the sight of injection, and neovascular development. This strategy showed that iPS derived IPCs secreted insulin and were able to reduce resting serum glucose levels over the course of 150 days. However, it is unclear whether the spontaneous development of these iPS derived islet like structures *in vivo* results in organized or randomly distributes endocrine beta, alpha, and delta cells.

Corporate and academic interests alike have already begun to work together on pancreatic organoid technology transfer. For instance, the consortium "LFM4LIFE" brings corporations and academic institutions from six European countries for the development of large scale organoid therapies in T1D. The groups primarily aim is to source adult human progenitor cells from pancreatic ductal cells. Injury by partial ligation has been shown to be naturally associated with Wnt pathway activation and $Lgr5^{+}$ cell emergence during ductal regeneration[233]. Facilitated by a Wnt agonist RSPO1, pancreatic

organoids produced in these culture conditions allows for unlimited expansion of ductal fragments; capable for use in large commercial scale up applications.

Alternative adult sources for renewable beta cells include intestinal and stomach epithelial tissue reprogramed for ubiquitous expression of Ngn3, Pdx1, and Mafa[239,240]. While islets showed highest levels of insulin response and secretion, stomach antrum derived tissue showed highest reprogramming efficiency and more closely mimicked beta cell functionality than cells derived from the colon, ileum, or duodenum[240]. Using a Matrigel support, reprogramed stomach antrum spheroids where capable of reversing hyperglycemia after transplantation. This work highlights the potential of engineered gastric and intestinal derived tissues to serve as novel sources of insulin producing cells.

Applying Organoids in Disease Models

While healthy organoid function can provide useful information about normal organ function, advances in gene editing such as CRISPR/Cas9 and viral transduction in addition to the availability of disease tissue samples have allowed for *in vitro* modeling of many diseases while retaining much of the structural relationships seen *in vivo*. Perhaps the most well developed disease in organoid systems are various forms of cancer. Pre-cancerous transformations such as Barrett's esophagus, *helicobacter pylori* infection, and irritable bowel disease allow for interrogation of mechanisms of cancer formation. Cancerous lesions such as lingual carcinoma, stomach, intestinal, colon, pancreatic, and prostate have been modeled in organoid systems[241]. Not only does this give insight into progression of cancerous lesions and potential therapeutic screens, but these models also allow for interrogation of the etiology of each malignancy in the context of its 3D

multicellular environment. Such systems are critical as our understanding of cancer moves beyond the cancer cells themselves to understanding the role of the tumor stroma that supports the survival and propagation of the cancer cells[242].

Other disease models developed using organoid techniques include models of cystic fibrosis. Dekkers et al. developed a CF intestinal organoid model where they can screen for CFTR function in CF by measuring organoid swelling due to forskolin treatment, a molecule which causes chloride influx in non-CF tissues. Demonstrating the potential utility of organoids, CF organoids treated with CF correcting drugs had normal swelling characteristics after treatment[243]. Another disease model using organoid techniques is a model of hyposalivation, a condition where patients' salivary glands do not produce adequate amounts of saliva. It has been reported that isolated stem cells highly expressing CD24 and CD29 could restore function to irradiated salivary glands in mice[244]. Bacterial and viral infection models in both the stomach and intestines have been developed to study formation of ulcers and understand bacterial interactions with epithelial cells of the gut[241]. Enteric bacteria normally do not pose a problem to their human host, but there is a complex regulation of bacterial colonization by the gut which when disrupted can result in severe sickness. Wilson et al. and Zhang et al. have studied the antimicrobial α-defensins produced by Paneth cells and bacterial disruption of epithelial tight junctions, induction of inflammation, and depopulation of regenerative stem cells respectively in intestinal organoid systems[245,246]. Huch et al. demonstrated that organoids derived from patient samples with α1-antitrypsin (A1AT) deficiency undergo similar pathology to the original biopsied samples as demonstrated by A1AT aggregation in cells, decreased secretion of A1AT, decreased elastin blocking activity, increased ER

stress, eIF2α phosphorylation, and increased cell apoptosis[247]. Cerebral organoids like those described in detail above are also being used as analytic tools to probe disease mechanisms in autism[248] and Zika virus associated microcephaly[218,249,250]. As in the brain, 3D ductal pancreatic organoid systems are emerging as a promising tool to model disease development, function, and as drug screening tools. While these platforms have been used to model pancreatic abnormalities in cystic fibrosis, the primary application has been in modeling pancreatic cancer[251–255]. 3D tumor organoids promise to be an incredibly powerful tool in cancer research. Biopsies of human pancreatic neoplasms can be used to generate organoids that maintain differentiation status, tumor architecture, and retain patient specific physiological changes (Figure 20). Once these cancer organoids have been grown in culture, they can be transplanted into mouse models, and screened against drugs to better understand patient specific disease progression and treatment options. Transcriptional and proteomic analysis of these transplanted neoplastic organoids have uncovered important genes and pathways involved in the development of the disease[254]. Use of these models may help uncover patient specific biomarkers and characteristics involved in malignancy. Overall, organoid systems provide superior in vitro models of many diseases compared to conventional 2D cultures and continue to gain prominence as a research tool.

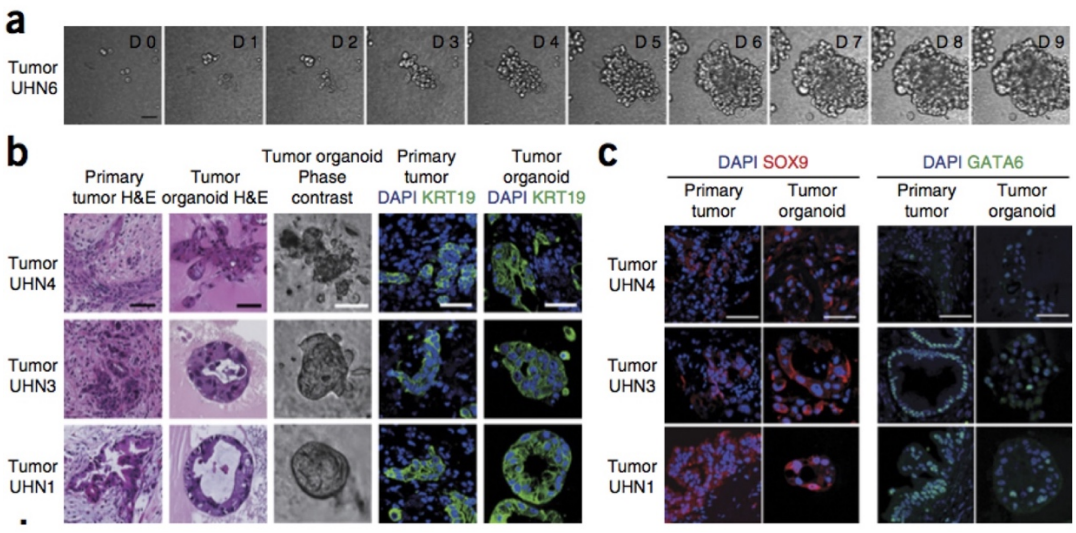

Figure 20: Establishment of tumor organoids that conserve patient-specific traits.

(**A**) Time-lapse imaging sequence of UHN6 organoids. Scale bars, 50 μm. (**B**) H&E, phase and immunofluorescence images of KRT19 (green) and DAPI (blue) staining of tumor organoids and matched primary tumors. Scale bars, 50 μm. (**C**) SOX9 (red) and GATA6 (green) staining in primary tumors and tumor organoids. Scale bars, 50 μm. Figure and caption reproduced from –Huang et al.[255] with permission from Nature Publishing Group.

Conclusion

Just as the advent of *in vitro* systems catalyzed the last century of biology, 3D organoid systems that recapitulate and maintain mature phenotypes of a large variety of cell types will drive discoveries over the next few decades. Success in organoid systems have demonstrated the importance of moving past the convenience and simplicity of 2D cultures, which often fail to recapitulate relevant biology, and turn our focus instead toward creating *in vitro* systems that maintain phenotype and functionality, even if it requires more challenging techniques and technologies. While strategies to create organoids for different tissue types have their own key characteristics, there are

commonalities. Most systems employ either a scaffold free induced aggregation technique, as seen in MSC spheroid formation and neuronal SFEBq strategies, while others employ scaffolds, most commonly matrigel, to facilitate 3D development and outgrowth of the organoid. Another key factor driving organoid protocol development is the identification of signaling factors that drive and maintain cell fate. These cues take a variety of forms including mechanical cues from the substrate, presentation of factors from neighboring cells (Notch) or the substrate (ECM), and soluble secreted factors. Once identified, these factors can be engineered into the system, through inclusion of the producing cells themselves, or by substituting the cues with small molecules and recombinant factors that stimulate the same pathways. Thus, as more is discovered about the pathways that regulate and maintain cell fate decisions in different tissues, more precise and predictable organoid systems can be designed and made available for research and therapeutic uses.

The applications of organoids are many, from understanding development, to generating therapeutic cells to repair damaged organs, to creating drug discovery systems that recapitulate multi-system human physiology. The future success of organoid systems will likely depend on collaboration between biologists and engineers from diverse backgrounds from both academia and industry in order to implement basic biology discoveries into scalable and predictable systems. If the early years of organoid development are any indication, the future of engineered organoid systems is bright.

REFERENCES

(1) Friedenstein, A. J.; Petrakova, K. V.; Kurolesova, A. I.; Frolova, G. P. *Transplantation* **1968**, *6* (2), 230–247.

(2) Friedenstein, A. J.; Piatetzky-Shapiro, I. I.; Petrakova, K. V. *Development* **1966**, *16* (3), 381–390.

(3) Elahi, K. C.; Klein, G.; Avci-Adali, M.; Sievert, K. D.; MacNeil, S.; Aicher, W. K. *Stem Cells Int.* **2015**, *2016*.

(4) Friedenstein, A. J.; Gorskaja, J. F.; Kulagina, N. N. *Exp. Hematol.* **1976**, *4* (5), 267–274.

(5) Friedenstein, A. J. *Exp. Hematol.* **1978**, *2*, 83–92.

(6) Kyurkchiev, D. *World J. Stem Cells* **2014**, *6* (5), 552.

(7) Lalu, M. M.; McIntyre, L.; Pugliese, C.; Fergusson, D.; Winston, B. W.; Marshall, J. C.; Granton, J.; Stewart, D. J.; Canadian Critical Care Trials, G. *PLoS One* **2012**, *7* (10), e47559.

(8) Song, Y.; Dou, H.; Li, X.; Zhao, X.; Li, Y.; Liu, D.; Ji, J.; Liu, F.; Ding, L.; Ni, Y.; Hou, Y. *Stem Cells* **2017**, 1–18.

(9) Wang, Q.; Sun, B.; Wang, D.; Ji, Y.; Kong, Q.; Wang, G.; Wang, J.; Zhao, W.; Jin, L.; Li, H. *Scand. J. Immunol.* **2008**, *68* (6), 607–615.

(10) Ivanova-Todorova, E.; Bochev, I.; Mourdjeva, M.; Dimitrov, R.; Bukarev, D.; Kyurkchiev, S.; Tivchev, P.; Altunkova, I.; Kyurkchiev, D. S. *Immunol. Lett.* **2009**, *126* (1), 37–42.

(11) Jiang, X.-X.; Zhang, Y.; Liu, B.; Zhang, S.-X.; Wu, Y.; Yu, X.-D.; Mao, N. *Blood* **2005**, *105* (10), 4120–4126.

(12) Nauta, A. J.; Kruisselbrink, A. B.; Lurvink, E.; Willemze, R.; Fibbe, W. E. *J. Immunol.* **2006**, *177* (4), 2080–2087.

(13) Amorin, B.; Alegretti, A. P.; Valim, V.; Pezzi, A.; Laureano, A. M.; da Silva, M. A. L.; Wieck, A.; Silla, L. *Hum. Cell* **2014**, *27* (4), 137–150.

(14) Bochev, I.; Elmadjian, G.; Kyurkchiev, D.; Tzvetanov, L.; Altankova, I.; Tivchev, P.; Kyurkchiev, S. *Cell Biol. Int.* **2008**, *32* (4), 384–393.

(15) Corcione, A.; Benvenuto, F.; Ferretti, E.; Giunti, D.; Cappiello, V.; Cazzanti, F.; Risso, M.; Gualandi, F.; Mancardi, G. L.; Pistoia, V. *Blood* **2006**, *107* (1), 367–372.

(16) Hsu, W.; Lin, C.; Chiang, B. *J. Immunol.* **2013**, *190*, 2372–2380.

(17) Prevosto, C.; Zancolli, M.; Canevali, P.; Zocchi, M. R.; Poggi, A. *Haematologica* **2007**, *92* (7), 881–888.

(18) Yan, Z.; Zhuansun, Y.; Chen, R.; Li, J.; Ran, P. *Exp. Cell Res.* **2014**, *324* (1), 65–74.

(19) Keating, A. *Cell Stem Cell* **2012**, *10* (6), 709–716.

(20) Trounson, A.; McDonald, C. *Cell Stem Cell* **2015**, *17* (1), 11–22.

(21) Le Blanc, K.; Rasmusson, I.; Sundberg, B.; Gotherstrom, C.; Hassan, M.; Uzunel, M.; Ringden, O. *Lancet* **2004**, *363* (9419), 1439–1441.

(22) Tan, J.; Wu, W.; Xu, X.; Liao, L.; Zheng, F.; Messinger, S.; Sun, X.; Chen, J.; Yang, S.; Cai, J.; Gao, X.; Pileggi, A.; Ricordi, C. *JAMA* **2012**, *307* (11), 1169–1177.

(23) Ge, W.; Jiang, J.; Baroja, M. L.; Arp, J.; Zassoko, R.; Liu, W.; Bartholomew, A.; Garcia, B.; Wang, H. *Am. J. Transplant.* **2009**, *9* (8), 1760–1772.

(24) Xia, X.; Chen, W.; Ma, T.; Xu, G.; Liu, H.; Liang, C.; Bai, X.; Zhang, Y.; He, Y.; Liang, T. *Liver Transplant.* **2012**, *18* (6), 696–706.

(25) Mohamadnejad, M.; Alimoghaddam, K.; Mohyeddin-Bonab, M.; Bagheri, M.; Bashtar, M.; Ghanaati, H.; Baharvand, H.; Ghavamzadeh, A.; Malekzadeh, R. *Arch. Iran. Med.* **2007**, *10* (4), 459–466.

(26) Li, Y.; Liu, W.; Liu, F.; Zeng, Y.; Zuo, S.; Feng, S.; Qi, C.; Wang, B.; Yan, X.; Khademhosseini, A.; Bai, J.; Du, Y. *Proc. Natl. Acad. Sci. U. S. A.* **2014**, *111* (37), 13511–13516.

(27) Berman, D. M.; Willman, M. A.; Han, D.; Kleiner, G.; Kenyon, N. M.; Cabrera, O.; Karl, J. A.; Wiseman, R. W.; O'Connor, D. H.; Bartholomew, A. M.; Kenyon, N. S. *Diabetes* **2010**, *59* (10), 2558–2568.

(28) Ankrum, J. a; Dastidar, R. G.; Ong, J. F.; Levy, O.; Karp, J. M. *Sci. Rep.* **2014**, *4*, 4645.

(29) Zhukareva, V.; Obrocka, M.; Houle, J. D.; Fischer, I.; Neuhuber, B. *Cytokine* **2010**, *50* (3), 317–321.

(30) Lee, R. H.; Yu, J. M.; Foskett, A. M.; Peltier, G.; Reneau, J. C.; Bazhanov, N.; Oh, J. Y.; Prockop, D. J. *Proc. Natl. Acad. Sci. U. S. A.* **2014**, *111* (47), 16766–16771.

(31) von Bahr, L.; Sundberg, B.; Lönnies, L.; Sander, B.; Karbach, H.; Hägglund, H.; Ljungman, P.; Gustafsson, B.; Karlsson, H.; Le Blanc, K.; Ringdén, O. *Biol. Blood Marrow Transplant.* **2012**, *18* (4), 557–564.

(32) François, M.; Copland, I. B.; Yuan, S.; Romieu-Mourez, R.; Waller, E. K.; Galipeau, J. *Cytotherapy*. 2012.

(33) Chinnadurai, R.; Garcia, M. A.; Sakurai, Y.; Lam, W. A.; Kirk, A. D.; Galipeau, J.; Copland, I. B. *Stem cell reports* **2014**, *3* (1), 60–72.

(34) Kuçi, Z.; Bönig, H.; Kreyenberg, H.; Bunos, M.; Jauch, A.; Janssen, J. W. G.; Skific, M.; Michel, K.; Eising, B.; Lucchini, G. *Haematologica* **2016**, haematol-2015.

(35) Bianco, P.; Cao, X.; Frenette, P. S.; Mao, J. J.; Robey, P. G.; Simmons, P. J.; Wang, C.-Y. *Nat. Med.* **2013**, *19* (1), 35–42.

(36) Le Blanc, K.; Frassoni, F.; Ball, L.; Locatelli, F.; Roelofs, H.; Lewis, I.; Lanino, E.; Sundberg, B.; Bernardo, M. E.; Remberger, M.; Dini, G.; Egeler, R. M.; Bacigalupo, A.; Fibbe, W.; Ringden, O. *Lancet (London, England)* **2008**, *371* (9624), 1579–1586.

(37) Ringdén, O.; Uzunel, M.; Rasmusson, I.; Remberger, M.; Sundberg, B.; Lönnies, H.; Marschall, H.-U.; Dlugosz, A.; Szakos, A.; Hassan, Z. *Transplantation* **2006**, *81* (10), 1390–1397.

(38) Jin, P.; Zhao, Y.; Liu, H.; Chen, J.; Ren, J.; Jin, J.; Bedognetti, D.; Liu, S.; Wang, E.; Marincola, F.; Stroncek, D. *Sci. Rep.* **2016**, *6* (April), 26345.

(39) Sudan, B.; Wacker, M. A.; Wilson, M. E.; Graff, J. W. *Frontiers in Immunology* . 2015, p 253.

(40) Ranganath, S. H.; Tong, Z.; Levy, O.; Martyn, K.; Karp, J. M.; Inamdar, M. S. *Stem Cell Reports* **2016**, *6* (6), 926–939.

(41) Moll, G.; Alm, J. J.; Davies, L. C.; Von Bahr, L.; Heldring, N.; Stenbeck-Funke, L.; Hamad, O. A.; Hinsch, R.; Ignatowicz, L.; Locke, M.; Lönnies, H.; Lambris, J. D.; Teramura, Y.; Nilsson-Ekdahl, K.; Nilsson, B.; Le Blanc, K. *Stem Cells* **2014**, *32* (9), 2430–2442.

(42) Galipeau, J. *Cytotherapy* **2013**, *15* (1), 2–8.

(43) Quimby, J. M.; Webb, T. L.; Habenicht, L. M.; Dow, S. W. *Stem Cell Res. Ther.* **2013**, *4* (2), 48.

(44) Gramlich, O. W.; Burand, A. J.; Brown, A. J.; Deutsch, R. J.; Kuehn, M. H.; Ankrum, J. A. *Sci. Rep.* **2016**, *6* (May), 26463.

(45) Burand, A. J.; Gramlich, O. W.; Brown, A. J.; Ankrum, J. A. *Stem Cells* **2016**, 0–2.

(46) Luetzkendorf, J.; Nerger, K.; Hering, J.; Moegel, A.; Hoffmann, K.; Hoefers, C.; Mueller-Tidow, C.; Mueller, L. P. *Cytotherapy* **2015**, *17* (2), 186–198.

(47) Ankrum, J.; Karp, J. M. *Trends Mol. Med.* **2010**, *16* (5), 203–209.

(48) Ankrum, J. a; Ong, J. F.; Karp, J. M. *Nat. Biotechnol.* **2014**, *32* (3), 252–260.

(49) da Silva Meirelles, L.; Chagastelles, P. C.; Nardi, N. B. *J. Cell Sci.* **2006**, *119* (Pt 11), 2204–2213.

(50) Stolzing, A.; Jones, E.; McGonagle, D.; Scutt, A. *Mech. Ageing Dev.* **2008**, *129* (3), 163–173.

(51) Murphy, M. B.; Moncivais, K.; Caplan, A. I. *Exp. Mol. Med.* **2013**, *45* (11), e54.

(52) Luetzkendorf, J.; Nerger, K.; Hering, J.; Moegel, A.; Hoffmann, K.; Hoefers, C.; Mueller-Tidow, C.; Mueller, L. P. *Cytotherapy* **2015**, *17* (2), 186–198.

(53) He, F.; Liu, W.; Zheng, S.; Zhou, L.; Ye, B.; Qi, Z. *Mol. Membr. Biol.* **2012**, *29* (3–4), 107–113.

(54) Fallarino, F.; Grohmann, U.; You, S.; McGrath, B. C.; Cavener, D. R.; Vacca, C.; Orabona, C.; Bianchi, R.; Belladonna, M. L.; Volpi, C.; Fioretti, M. C.; Puccetti, P. *Transpl. Immunol.* **2006**, *17* (1), 58–60.

(55) Van der Sluijs, K.; Singh, R.; Dijkhuis, A.; Snoek, M.; Lutter, R. *Crit. care* **2011**, *15* (S1), P208.

(56) Nauta, A. J.; Fibbe, W. E. *Blood* **2007**, *110* (10), 3499–3506.

(57) Deng, Y. Bin; Ye, W. B.; Hu, Z. Z.; Yan, Y.; Wang, Y.; Takon, B. F.; Zhou, G.-Q.; Zhou, Y. F. *Neurol. Res.* **2010**, *32* (2), 148–156.

(58) Johnson, T. V; DeKorver, N. W.; Levasseur, V. A.; Osborne, A.; Tassoni, A.; Lorber, B.; Heller, J. P.; Villasmil, R.; Bull, N. D.; Martin, K. R. *Brain* **2014**, *137* (2), 503–519.

(59) Paradisi, M.; Alviano, F.; Pirondi, S.; Lanzoni, G.; Fernandez, M.; Lizzo, G.; Giardino, L.; Giuliani, A.; Costa, R.; Marchionni, C. *Int. J. Immunopathol. Pharmacol.* **2014**, *27* (3), 391–402.

(60) Moriscot, C.; de Fraipont, F.; Richard, M.-J.; Marchand, M.; Savatier, P.; Bosco, D.; Favrot, M.; Benhamou, P.-Y. *Stem Cells* **2005**, *23* (4), 594–603.

(61) Tucker, B. A.; Mullins, R. F.; Streb, L. M.; Anfinson, K.; Eyestone, M. E.; Kaalberg, E.; Riker, M. J.; Drack, A. V; Braun, T. A.; Stone, E. M. *Elife* **2013**, *2*, e00824.

(62) Chinnadurai, R.; Copland, I. B.; Garcia, M. A.; Petersen, C. T.; Lewis, C. N.; Waller, E. K.; Kirk, A. D.; Galipeau, J. *Stem Cells* **2016**, *34* (9), 2429–2442.

(63) Kuehn, M. H.; Kim, C. Y.; Jiang, B.; Dumitrescu, A. V.; Kwon, Y. H. *Exp. Eye Res.* **2008**, *87* (2), 89–95.

(64) Yong, K. W.; Wan Safwani, W. K. Z.; Xu, F.; Wan Abas, W. A. B.; Choi, J. R.; Pingguan-Murphy, B. *Biopreserv. Biobank.* **2015**, *13* (4), 231–239.

(65) Yong, K. W.; Safwani, W. K. Z. W.; Xu, F.; Zhang, X.; Choi, J. R.; Abas, W. A. B. W.; Omar, S. Z.; Azmi, M. A. N.; Chua, K. H.; Pingguan-Murphy, B. *J. Tissue Eng. Regen. Med.* **2016**.

(66) Yong, K. W.; Pingguan-Murphy, B.; Xu, F.; Abas, W. A. B. W.; Choi, J. R.; Omar, S. Z.; Azmi, M. A. N.; Chua, K. H.; Safwani, W. K. Z. W. *Sci. Rep.* **2015**, *5*, 9596.

(67) Tokumoto, S.; Sotome, S.; Torigoe, I.; Omura, K.; Shinomiya, K. *J. Med. Dent. Sci.* **2008**, *55*, 137–143.

(68) Liu, G.; Shu, C.; Cui, L.; Liu, W.; Cao, Y. *Cryobiology* **2008**, *56* (3), 209–215.

(69) Zhu, X.; Yuan, F.; Li, H.; Zheng, Y.; Xiao, Y.; Yan, F. *Zoolog. Sci.* **2013**, *30* (12), 1032–1037.

(70) Horwitz, E. M.; Prockop, D. J.; Fitzpatrick, L. A.; Koo, W. W. K.; Gordon, P. L.; Neel, M.; Sussman, M.; Orchard, P.; Marx, J. C.; Pyeritz, R. E.; Brenner, M. K. *Nat. Med.* **1999**, *5* (3), 309–313.

(71) Shen, H.; Kreisel, D.; Goldstein, D. R. *J. Immunol.* **2013**, *191* (6), 2857–2863.

(72) Rock, K. L.; Latz, E.; Ontiveros, F.; Kono, H. *Annu. Rev. Immunol.* **2010**, *28*, 321–342.

(73) Iyer, S. S.; Pulskens, W. P.; Sadler, J. J.; Butter, L. M.; Teske, G. J.; Ulland, T. K.; Eisenbarth, S. C.; Florquin, S.; Flavell, R. A.; Leemans, J. C.; Sutterwala, F. S. *Proc. Natl. Acad. Sci. U. S. A.* **2009**, *106* (48), 20388–20393.

(74) Chen, G. Y.; Nuñez, G. *Nat. Rev. Immunol.* **2010**, *10* (12), 826–837.

(75) Kono, H.; Rock, K. L. *Nat. Rev. Immunol.* **2008**, *8* (4), 279–289.

(76) Marquez-Curtis, L. A.; Janowska-Wieczorek, A.; McGann, L. E.; Elliott, J. A. W. *Cryobiology* **2015**, *71* (2), 181–197.

(77) Farance, I.; Lock, L. T.; Baraniak, P.; Rowley, J. A. *Cytotherapy* **2015**, *17* (6), S67–S68.

(78) Sanes, J. R.; Masland, R. H. *Annu. Rev. Neurosci.* **2015**, *38*, 221–246.

(79) Kaur, C.; Foulds, W. S.; Ling, E.-A. *Clin Ophthalmol* **2008**, *2* (4), 879–889.

(80) Osborne, N. N.; Casson, R. J.; Wood, J. P. M.; Chidlow, G.; Graham, M.; Melena, J. *Progress in Retinal and Eye Research*. 2004, pp 91–147.

(81) D'onofrio, P. M.; Koeberle, P. D. *Acta Pharmacol. Sin.* **2013**, *34* (1), 91–103.

(82) Baker, M. L.; Hand, P. J.; Wang, J. J.; Wong, T. Y. *Stroke* **2008**, *39* (4), 1371–1379.

(83) Chamberlain, G.; Wright, K.; Rot, A.; Ashton, B.; Middleton, J. *PLoS One* **2008**, *3* (8).

(84) Ren, G.; Su, J.; Zhang, L.; Zhao, X.; Ling, W.; L'huillie, A.; Zhang, J.; Lu, Y.; Roberts, A. I.; Ji, W. *Stem Cells* **2009**, *27* (8), 1954–1962.

(85) Ranganath, S. H.; Levy, O.; Inamdar, M. S.; Karp, J. M. *Cell Stem Cell* **2012**, *10* (3), 244–258.

(86) Islam, M. N.; Das, S. R.; Emin, M. T.; Wei, M.; Sun, L.; Westphalen, K.; Rowlands, D. J.; Quadri, S. K.; Bhattacharya, S.; Bhattacharya, J. *Nat. Med.* **2012**, *18* (5), 759–765.

(87) Castelo-Branco, M. T. L.; Soares, I. D. P.; Lopes, D. V.; Buongusto, F.; Martinusso, C. A.; do Rosario, A.; Souza, S. A. L.; Gutfilen, B.; Fonseca, L. M. B.; Elia, C.; Madi, K.; Schanaider, A.; Rossi, M. I. D.; Souza, H. S. P. *PLoS One* **2012**, *7* (3).

(88) Cruz, F. F.; Borg, Z. D.; Goodwin, M.; Sokocevic, D.; Wagner, D.; McKenna, D. H.; Rocco, P. R. M.; Weiss, D. J. *Stem Cells Transl. Med.* **2015**, *4* (6), 615–624.

(89) Otsuru, S.; Hofmann, T. J.; Raman, P.; Olson, T. S.; Guess, A. J.; Dominici, M.; Horwitz, E. M. *Cytotherapy* **2015**, *17* (3), 262–270.

(90) Gupta, P. K.; Chullikana, A.; Parakh, R.; Desai, S.; Das, A.; Gottipamula, S.; Krishnamurthy, S.; Anthony, N.; Pherwani, A.; Majumdar, A. S. *J. Transl. Med.* **2013**, *11* (1), 143.

(91) Moll, G.; Alm, J. J.; Davies, L. C.; Von Bahr, L.; Heldring, N.; Stenbeck-Funke, L.; Hamad, O. A.; Hinsch, R.; Ignatowicz, L.; Locke, M.; Lönnies, H.; Lambris, J. D.; Teramura, Y.; Nilsson-Ekdahl, K.; Nilsson, B.; Le Blanc, K. *Stem Cells* **2014**, *32* (9), 2430–2442.

(92) Johnson, T. V; Bull, N. D.; Hunt, D. P.; Marina, N.; Tomarev, S. I.; Martin, K. R. *Invest Ophthalmol Vis Sci* **2010**, *51* (4), 2051–2059.

(93) Dominici, M.; Le Blanc, K.; Mueller, I.; Slaper-Cortenbach, I.; Marini, F. .; Krause, D. S.; Deans, R. J.; Keating, A.; Prockop, D. J.; Horwitz, E. M. *Cytotherapy* **2006**, *8* (4), 315–317.

(94) Davies, L. C.; Lönnies, H.; Locke, M.; Sundberg, B.; Rosendahl, K.; Götherström, C.; Le Blanc, K.; Stephens, P. *Stem Cells Dev.* **2012**, *21* (9), 1478–1487.

(95) Kambhampati, S. P.; Clunies-Ross, A. J. M.; Bhutto, I.; Mishra, M. K.; Edwards, M.; McLeod, D. S.; Kannan, R. M.; Lutty, G. *Invest. Ophthalmol. Vis. Sci.* **2015**, *56* (8), 4413–4424.

(96) Joachim, S. C.; Jehle, T.; Boehm, N.; Gramlich, O. W.; Lagreze, W. A.; Pfeiffer, N.; Grus, F. H. *Ophthalmic Res.* **2012**, *48* (2), 67–74.

(97) Ding, Q. J.; Cook, A. C.; Dumitrescu, A. V; Kuehn, M. H. *Invest. Ophthalmol. Vis. Sci.* **2012**, *53* (10), 6370–6377.

(98) Gramlich, O. W.; Ding, Q. J.; Zhu, W.; Cook, A.; Anderson, M. G.; Kuehn, M. H. *Acta Neuropathol. Commun.* **2015**, *3* (1), 56.

(99) Krampera, M. *Leukemia* **2011**, *25* (9), 1408–1414.

(100) Nicola, M. Di; Carlo-stella, C.; Magni, M.; Milanesi, M.; Longoni, P. D.; Grisanti, S.; Gianni, A. M.; Matteucci, P. **2002**, *99* (10), 3838–3843.

(101) Liu, H.; Kemeny, D. M.; Heng, B. C.; Ouyang, H. W.; Melendez, A. J.; Cao, T. *J. Immunol.* **2006**, *176* (5), 2864–2871.

(102) Tse, W. T.; Pendleton, J. D.; Beyer, W. M.; Egalka, M. C.; Guinan, E. C. *Transplantation* **2003**, *75* (3), 389–397.

(103) Krampera, M.; Cosmi, L.; Angeli, R.; Pasini, A.; Liotta, F.; Andreini, A.; Santarlasci, V.; Mazzinghi, B.; Pizzolo, G.; Vinante, F.; Romagnani, P.; Maggi, E.; Romagnani, S.; Annunziato, F. *Stem Cells* **2006**, *24* (2), 386–398.

(104) Krampera, M.; Sartoris, S.; Liotta, F.; Pasini, A.; Angeli, R.; Cosmi, L.; Andreini, A.; Mosna, F.; Bonetti, B.; Rebellato, E.; Testi, M. G.; Frosali, F.; Pizzolo, G.; Tridente, G.; Maggi, E.; Romagnani, S.; Annunziato, F. *Stem Cells Dev.* **2007**, *16* (5), 797–810.

(105) Meisel, R.; Zibert, A.; Laryea, M.; Göbel, U.; Däubener, W.; Dilloo, D. *Blood* **2004**, *103* (12), 4619–4621.

(106) Xu, G.; Zhang, Y.; Zhang, L.; Ren, G.; Shi, Y. *Biochem. Biophys. Res. Commun.* **2007**, *361* (3), 745–750.

(107) Djouad, F.; Charbonnier, L.-M.; Bouffi, C.; Louis-Plence, P.; Bony, C.; Apparailly, F.; Cantos, C.; Jorgensen, C.; Noël, D. *Stem Cells* **2007**, *25* (8), 2025–2032.

(108) Zhang, W.; Ge, W.; Li, C.; You, S.; Liao, L.; Han, Q.; Deng, W.; Zhao, R. C. *Stem Cells Dev.* **2004**, *13* (3), 263–271.

(109) Aggarwal, S.; Pittenger, M. F. *Blood* **2005**, *105* (4), 1815–1822.

(110) Zafranskaya, M.; Nizheharodava, D.; Yurkevich, M.; Ivanchik, G.; Demidchik, Y.; Kozhukh, H.; Fedulov, A. *Scand. J. Immunol.* **2013**, *78* (5), 455–462.

(111) Di Nicola, M.; Carlo-Stella, C.; Magni, M.; Milanesi, M.; Longoni, P. D.; Matteucci, P.; Grisanti, S.; Gianni, A. M. *Blood* **2002**, *99*, 3838–3843.

(112) Bai, L.; Lennon, D. P.; Caplan, A. I.; Dechant, A.; Hecker, J. *Nat. Neurosci.* **2012**, *15* (6), 862–870.

(113) Sato, K.; Ozaki, K.; Oh, I.; Meguro, A.; Hatanaka, K.; Nagai, T.; Muroi, K.; Ozawa, K. *Blood* **2007**, *109* (1), 228–234.

(114) Chabannes, D.; Hill, M.; Merieau, E.; Rossignol, J.; Brion, R.; Soulillou, J. P.; Anegon, I.; Cuturi, M. C. *Blood* **2007**, *110* (10), 3691–3694.

(115) Bouffi, C.; Bony, C.; Courties, G.; Jorgensen, C.; Noël, D. *PLoS One* **2010**, *5* (12), e14247.

(116) Beegle, J.; Lakatos, K.; Kalomoiris, S.; Stewart, H.; Isseroff, R. R.; Nolta, J. A.; Fierro, F. A. *Stem Cells* **2015**, *33* (6), 1818–1828.

(117) Mougiakakos, D.; Jitschin, R.; Johansson, C. C.; Okita, R.; Kiessling, R.; Le Blanc, K. *Blood* **2011**, *117* (18), 4826–4835.

(118) Selmani, Z.; Naji, A.; Zidi, I.; Favier, B.; Gaiffe, E.; Obert, L.; Borg, C.; Saas, P.; Tiberghien, P.; Rouas-Freiss, N.; Carosella, E. D.; Deschaseaux, F. *Stem Cells* **2008**, *26* (1), 212–222.

(119) Yang, H.-M.; Sung, J.-H.; Choi, Y.-S.; Lee, H.-J.; Roh, C.-R.; Kim, J.; Shin, M.; Song, S.; Kwon, C.-H.; Joh, J.-W.; Kim, S.-J. *Cytotherapy* **2012**, *14* (1), 70–79.

(120) Lee, R. H.; Pulin, A. a.; Seo, M. J.; Kota, D. J.; Ylostalo, J.; Larson, B. L.; Semprun-Prieto, L.; Delafontaine, P.; Prockop, D. J. *Cell Stem Cell* **2009**, *5* (1), 54–63.

(121) Kota, D. J.; Wiggins, L. L.; Yoon, N.; Lee, R. H. *Diabetes* **2013**, *62* (6), 2048–2058.

(122) DelaRosa, O.; Lombardo, E. *Mediators Inflamm.* **2010**, *2010*, 865601.

(123) Raicevic, G.; Rouas, R.; Najar, M.; Stordeur, P.; Id Boufker, H.; Bron, D.; Martiat, P.; Goldman, M.; Nevessignsky, M. T.; Lagneaux, L. *Hum. Immunol.* **2010**, *71* (3), 235–244.

(124) Prockop, D. J.; Youn Oh, J. *Mol. Ther.* **2012**, *20* (1), 14–20.

(125) Duijvestein, M.; Wildenberg, M. E.; Welling, M. M.; Hennink, S.; Molendijk, I.; van Zuylen, V. L.; Bosse, T.; Vos, A. C. W.; de Jonge-Muller, E. S. M.; Roelofs, H. *Stem Cells* **2011**, *29* (10), 1549–1558.

(126) Polchert, D.; Sobinsky, J.; Douglas, G. W.; Kidd, M.; Moadsiri, A.; Reina, E.; Genrich, K.; Mehrotra, S.; Setty, S.; Smith, B. *Eur. J. Immunol.* **2008**, *38* (6), 1745–1755.

(127) Lan, Y.-W.; Choo, K.-B.; Chen, C.-M.; Hung, T.-H.; Chen, Y.-B.; Hsieh, C.-H.; Kuo, H.-P.; Chong, K.-Y. *Stem Cell Res. Ther.* **2015**, *6* (1), 97.

(128) Sarkar, D.; Spencer, J. A.; Phillips, J. A.; Zhao, W.; Schafer, S.; Spelke, D. P.; Mortensen, L. J.; Ruiz, J. P.; Vemula, P. K.; Sridharan, R. *Blood* **2011**, *118* (25), e184–e191.

(129) Sackstein, R.; Merzaban, J. S.; Cain, D. W.; Dagia, N. M.; Spencer, J. A.; Lin, C. P.; Wohlgemuth, R. *Nat. Med.* **2008**, *14* (2), 181–187.

(130) François, M.; Romieu-Mourez, R.; Li, M.; Galipeau, J. *Mol. Ther.* **2012**, *20* (1), 187–195.

(131) von Bahr, L.; Sundberg, B.; Lönnies, L.; Sander, B.; Karbach, H.; Hägglund, H.; Ljungman, P.; Gustafsson, B.; Karlsson, H.; Le Blanc, K. *Biol. Blood Marrow Transplant.* **2012**, *18* (4), 557–564.

(132) Sekiya, I.; Larson, B. L.; Smith, J. R.; Pochampally, R.; Cui, J.; Prockop, D. J. *Stem Cells* **2002**, *20* (6), 530–541.

(133) Su, J.; Chen, X.; Huang, Y.; Li, W.; Li, J.; Cao, K.; Cao, G.; Zhang, L.; Li, F.; Roberts, A. I. *Cell Death Differ.* **2014**, *21* (3), 388–396.

(134) Coudriet, G. M.; He, J.; Trucco, M.; Mars, W. M.; Piganelli, J. D. *PLoS One* **2010**, *5* (11), e15384.

(135) Pallotta, M. T.; Orabona, C.; Volpi, C.; Vacca, C.; Belladonna, M. L.; Bianchi, R.; Servillo, G.; Brunacci, C.; Calvitti, M.; Bicciato, S.; Mazza, E. M. C.; Boon, L.; Grassi, F.; Fioretti, M. C.; Fallarino, F.; Puccetti, P.; Grohmann, U. *Nat. Immunol.* **2011**, *12* (9), 870–878.

(136) Shi, Y.; Massague, J. *Cell* **2003**, *113* (6), 685–700.

(137) Wang, D.; Saga, Y.; Sato, N.; Nakamura, T.; Takikawa, O.; Mizukami, H.; Matsubara, S.; Fujiwara, H. *Int. J. Oncol.* **2016**, 2303–2309.

(138) Lewis, C.; Chinnadurai, R.; Galipeau, J. *J. Immunol.* **2015**, *194* (1 Supplement), 130.7-130.7.

(139) Nguyen, N. T.; Kimura, A.; Nakahama, T.; Chinen, I.; Masuda, K.; Nohara, K.; Fujii-Kuriyama, Y.; Kishimoto, T. *Proc Natl Acad Sci U S A* **2010**, *107* (46), 19961–19966.

(140) Noakes, R. *Int. J. Tryptophan Res.* **2015**, *8* (1), 7–18.

(141) Bessede, A.; Gargaro, M.; Pallotta, M. T.; Matino, D.; Servillo, G.; Brunacci, C.; Bicciato, S.; Mazza, E. M. C.; Macchiarulo, A.; Vacca, C.; Iannitti, R.; Tissi, L.; Volpi, C.; Belladonna, M. L.; Orabona, C.; Bianchi, R.; Lanz, T. V; Platten, M.; Della Fazia, M. a; Piobbico, D.; Zelante, T.; Funakoshi, H.; Nakamura, T.; Gilot, D.; Denison, M. S.; Guillemin, G. J.; DuHadaway, J. B.; Prendergast, G. C.; Metz, R.; Geffard, M.; Boon, L.; Pirro, M.; Iorio, A.; Veyret, B.; Romani, L.; Grohmann, U.; Fallarino, F.; Puccetti, P. *Nature* **2014**, *511* (7508), 184–190.

(142) Quintana, F.; Sherr, D. *Pharmacol. Rev.* **2013**, *65* (October), 1148–1161.

(143) Braun, D.; Longman, R. S.; Albert, M. L. *Cancer* **2005**, *33* (0), 2375–2382.

(144) Girdlestone, J.; Pido-Lopez, J.; Srivastava, S.; Chai, J.; Leaver, N.; Galleu, A.; Lombardi, G.; Navarrete, C. V. *Cytotherapy* **2015**, *17* (9), 1188–1199.

(145) Sarkar, D.; Ankrum, J. A.; Teo, G. S. L.; Carman, C. V.; Karp, J. M. *Biomaterials* **2011**, *32* (11), 3053–3061.

(146) Lee, M. J.; Kim, J.; Kim, M. Y.; Bae, Y.-S.; Ryu, S. H.; Lee, T. G.; Kim, J. H. *J. Proteome Res.* **2010**, *9* (4), 1754–1762.

(147) Ivanova-Todorova, E.; Mourdjeva, M.; Kyurkchiev, D.; Bochev, I.; Stoyanova, E.; Dimitrov, R.; Timeva, T.; Yunakova, M.; Bukarev, D.; Shterev, A.; Tivchev, P.; Kyurkchiev, S. *Am. J. Reprod. Immunol.* **2009**, *62* (1), 25–33.

(148) Blanco, O.; Tirado, I.; Munoz-Fernandez, R.; Abadia-Molina, A. C.; Garcia-Pacheco, J. M.; Pena, J.; Olivares, E. G. *Hum Reprod* **2008**, *23* (1), 144–152.

(149) Yie, S. M.; Li, L. H.; Li, G. M.; Xiao, R.; Librach, C. L. *Hum Reprod* **2006**, *21* (1), 46–51.

(150) Ito, S.; Osaka, M.; Edamatsu, T.; Itoh, Y.; Yoshida, M. *J. Atheroscler. Thromb.* **2016**, *23* (8), 960–975.

(151) Schroeder, J. C.; DiNatale, B. C.; Murray, I. A.; Flaveny, C. A.; Liu, Q.; Laurenzana, E. M.; Lin, J. M.; Strom, S. C.; Omiecinski, C. J.; Amin, S. *Biochemistry* **2009**, *49* (2), 393–400.

(152) Le Blanc, K.; Mougiakakos, D. *Nat. Rev. Immunol.* **2012**, *12* (5), 383–396.

(153) Harden, J. L.; Egilmez, N. K. *Immunol Invest.* **2013**, *41* (0).

(154) Obermajer, N.; Popp, F. C.; Soeder, Y.; Haarer, J.; Geissler, E. K.; Schlitt, H. J.; Dahlke, M. H. *J. Immunol.* **2014**, *193* (10), 4988–4999.

(155) Rovira Gonzalez, Y. I.; Lynch, P. J.; Thompson, E. E.; Stultz, B. G.; Hursh, D. A. *Cytotherapy* **2016**, *18* (9), 1114–1128.

(156) Quintana, F. J.; Basso, A. S.; Iglesias, A. H.; Korn, T.; Farez, M. F.; Bettelli, E.; Caccamo, M.; Oukka, M.; Weiner, H. L. *Nature* **2008**, *453* (7191), 65–71.

(157) Gramatzki, D.; Pantazis, G.; Schittenhelm, J.; Tabatabai, G.; Köhle, C.; Wick, W.; Schwarz, M.; Weller, M.; Tritschler, I. *Oncogene* **2009**, *28* (28), 2593–2605.

(158) Soshilov, A. A.; Denison, M. S. *Mol. Cell. Biol.* **2014**, *34* (9), 1707–1719.

(159) Connick, P.; Kolappan, M.; Crawley, C.; Webber, D. J.; Patani, R.; Michell, A. W.; Du, M.-Q.; Luan, S.-L.; Altmann, D. R.; Thompson, A. J. *Lancet Neurol.* **2012**, *11* (2), 150–156.

(160) Mohajeri, M.; Farazmand, A.; Mohyeddin Bonab, M.; Nikbin, B.; Minagar, A. *Iran J Allergy Asthma Immunol* **2011**, *10* (3), 155–161.

(161) Li, J.; Chen, Y.; Chen, Z.; Huang, Y.; Yang, D.; Su, Z.; Weng, Y.; Li, X.; Zhang, X. *Sci. Rep.* **2017**, *7*.

(162) Kleinewietfeld, M.; Hafler, D. A. *Semin. Immunol.* **2013**, *25* (4), 305–312.

(163) Basu, R.; Hatton, R. D.; Weaver, C. T. *Immunol. Rev.* **2013**, *252* (1), 89–103.

(164) Sharma, M. D.; Baban, B.; Chandler, P.; Hou, D.; Singh, N.; Yagita, H.; Azuma, M.; Blazar, B. R.; Mellor, A. L.; Munn, D. H. *J. Clin. Invest.* **2007**, *117* (9), 2570–2582.

(165) Chan, J. L.; Tang, K. C.; Patel, A. P.; Bonilla, L. M.; Pierobon, N.; Ponzio, M.; Rameshwar, P.; Dc, W.; Ponzio, N. M. *Blood* **2006**, *107* (12), 4817–4824.

(166) Francois, M.; Romieu-Mourez, R.; Stock-Martineau, S.; Boivin, M.; Bramson, J.; Galipeau, J. *Blood* **2009**, *114* (13), 1–25.

(167) Wen, L.; Zhu, M.; Madigan, M. C.; You, J.; King, N. J. C.; Billson, F. a.; McClellan, K.; Sutton, G.; Petsoglou, C. *PLoS One* **2014**, *9* (7), 1–12.

(168) Klyushnenkova, E.; Mosca, J. D.; Zernetkina, V.; Majumdar, M. K.; Beggs, K. J.; Simonetti, D. W.; Deans, R. J.; McIntosh, K. R. *J. Biomed. Sci.* **2005**, *12* (1), 47–57.

(169) Le Blanc, K.; Tammik, L.; Sundberg, B.; Haynesworth, S. E.; Ringden, O. *Scand. J. Immunol.* **2003**, *57* (1), 11–20.

(170) Majumdar, M. K.; Keane-Moore, M.; Buyaner, D.; Hardy, W. B.; Moorman, M. A.; McIntosh, K. R.; Mosca, J. D. *J. Biomed. Sci.* **2003**, *10* (2), 228–241.

(171) Sachs, D. H.; Kawai, T.; Sykes, M. *Cold Spring Harb. Perspect. Med.* **2014**, *4* (1), a015529.

(172) Racine, J. J.; Zhang, M.; Wang, M.; Morales, W.; Shen, C.; Zeng, D. *J. Immunol.* **2015**, *194* (1), 407–417.

(173) Nikolic, B.; Takeuchi, Y.; Leykin, I.; Fudaba, Y.; Smith, R. N.; Sykes, M. *Diabetes* **2004**, *53* (2), 376–383.

(174) Beilhack, G. F.; Landa, R. R.; Masek, M. A.; Shizuru, J. A. *Diabetes* **2005**, *54* (6), 1770–1779.

(175) Zhang, M.; Racine, J.; Liu, Y.; Lin, Q.; Qi, T.; Wang, T.; Riggs, A. D.; Zeng, D. *J. Immunol.* **2016**, *196* (1 Supplement), 186.19 LP-186.19.

(176) Wu, L.; Li, N.; Zhang, M.; Xue, S.-L.; Cassady, K.; Lin, Q.; Riggs, A. D.; Zeng, D. *Proc. Natl. Acad. Sci.* **2015**, *112* (52), 15994–15999.

(177) Lutz, M. B.; Schuler, G. *Trends Immunol.* **2002**, *23* (9), 445–449.

(178) Cho, K.-J.; Walseng, E.; Ishido, S.; Roche, P. A. *Proc. Natl. Acad. Sci.* **2015**, *112* (33), 10449–10454.

(179) Paulino, L. V. UMass Medical School 2015.

(180) Arnold, A. C. *Am. J. Ophthalmol.* **2005**, *139* (6), 1101–1108.

(181) Frohman, E. M.; Frohman, T. C.; Zee, D. S.; McColl, R.; Galetta, S. *Lancet. Neurol.* **2005**, *4* (2), 111–121.

(182) Balcer, L. J. *N. Engl. J. Med.* **2006**, *354* (12), 1273–1280.

(183) Foroozan, R.; Buono, L. M.; Savino, P. J.; Sergott, R. C. *Curr. Opin. Ophthalmol.* **2002**, *13* (6), 375–380.

(184) Osborne, B.; Balcer, L. J. Optic neuritis: Pathophysiology, clinical features, and diagnosis.

(185) Qizilbash, N.; Mendez, I.; Sanchez-de la Rosa, R. *Clin. Ther.* **2012**, *34* (1), 159–176.

(186) Freedman, M. S. *Neurology* **2011**, *76* (1 Supplement 1), S26–S34.

(187) Liao, W.; Pham, V.; Liu, L.; Riazifar, M.; Pone, E. J.; Zhang, S. X.; Ma, F.; Lu, M.; Walsh, C. M.; Zhao, W. *Biomaterials* **2016**, *77* (September 2015), 87–97.

(188) Karussis, D.; Karageorgiou, C.; Vaknin-Dembinsky, A.; Gowda-Kurkalli, B.; Gomori, J. M.; Kassis, I.; Bulte, J. W. M.; Petrou, P.; Ben-Hur, T.; Abramsky, O.; Slavin, S. *Arch. Neurol.* **2010**, *67* (10), 1187–1194.

(189) Frohman, E. M.; Fujimoto, J. G.; Frohman, T. C.; Calabresi, P. A.; Cutter, G.; Balcer, L. J. *Nat. Clin. Pract. Neurol.* **2008**, *4* (12), 664–675.

(190) Zaveri, M. S.; Conger, A.; Salter, A.; Frohman, T. C.; Galetta, S. L.; Markowitz, C. E.; Jacobs, D. A.; Cutter, G. R.; Ying, G.-S.; Maguire, M. G. *Arch. Neurol.* **2008**, *65* (7), 924–928.

(191) Talman, L. S.; Bisker, E. R.; Sackel, D. J.; Long, D. A.; Galetta, K. M.; Ratchford, J. N.; Lile, D. J.; Farrell, S. K.; Loguidice, M. J.; Remington, G. *Ann. Neurol.* **2010**, *67* (6), 749–760.

(192) Yu-Wai-Man, P.; Griffiths, P. G.; Chinnery, P. F. *Prog. Retin. Eye Res.* **2011**, *30* (2), 81–114.

(193) Morgan, J. E. *Eye* **2004**, *18* (11), 1089–1095.

(194) Carelli, V.; Ross-Cisneros, F. N.; Sadun, A. A. *Prog. Retin. Eye Res.* **2004**, *23* (1), 53–89.

(195) Bristow, E. A.; Griffiths, P. G.; Andrews, R. M.; Johnson, M. A.; Turnbull, D. M. *Arch. Ophthalmol.* **2002**, *120* (6), 791–796.

(196) Jiang, D.; Gao, F.; Zhang, Y.; Wong, D. S. H.; Li, Q.; Tse, H.-F.; Xu, G.; Yu, Z.; Lian, Q. *Cell Death Dis.* **2016**, *7* (11), e2467.

(197) Jackson, M. V; Morrison, T. J.; Doherty, D. F.; McAuley, D. F.; Matthay, M. A.; Kissenpfennig, A.; O'Kane, C. M.; Krasnodembskaya, A. D. *Stem Cells* **2016**, 2210–2223.

(198) Masters, J. R. *Nat. Rev. Cancer* **2002**, *2* (4), 315–319.

(199) Scannell, J. W.; Bosley, J. *PLoS One* **2016**, *11* (2), e0147215.

(200) Wienkers, L. C.; Heath, T. G. *Nat. Rev. Drug Discov.* **2005**, *4* (10), 825–833.

(201) O'Shaughnessy, T. J.; Lin, H. J.; Ma, W. *Neurosci. Lett.* **2003**, *340* (3), 169–172.

(202) Cullen, D. K.; Stabenfeldt, S. E.; Simon, C. M.; Tate, C. C.; LaPlaca, M. C. *J. Neurosci. Res.* **2007**, *85* (16), 3642–3651.

(203) Li, G. N.; Livi, L. L.; Gourd, C. M.; Deweerd, E. S.; Hoffman-Kim, D. *Tissue Eng.* **2007**, *13* (5), 1035–1047.

(204) Frampton, J. P.; Hynd, M. R.; Shuler, M. L.; Shain, W. *Biomed. Mater.* **2011**, *6* (1), 15002.

(205) Tang-Schomer, M. D.; White, J. D.; Tien, L. W.; Schmitt, L. I.; Valentin, T. M.; Graziano, D. J.; Hopkins, A. M.; Omenetto, F. G.; Haydon, P. G.; Kaplan, D. L. *Proc. Natl. Acad. Sci. U. S. A.* **2014**, *111* (38), 13811–13816.

(206) Paşca, A. M.; Sloan, S. A.; Clarke, L. E.; Tian, Y.; Makinson, C. D.; Huber, N.; Kim, C. H.; Park, J.-Y.; O'Rourke, N. A.; Nguyen, K. D.; Smith, S. J.; Huguenard, J. R.; Geschwind, D. H.; Barres, B. A.; Paşca, S. P. *Nat Methods.* **2015**, *12* (7), 671–678.

(207) Lancaster, M. A.; Knoblich, J. A. *Nat. Protoc.* **2014**, *9* (10), 2329–2340.

(208) Kraus, D.; Boyle, V.; Leibig, N.; Stark, G. B.; Penna, V. *J. Neurosci. Methods* **2015**, *246*, 97–105.

(209) Dingle, Y.-T. L.; Boutin, M. E.; Chirila, A. M.; Livi, L. L.; Labriola, N. R.; Jakubek, L. M.; Morgan, J. R.; Darling, E. M.; Kauer, J. a.; Hoffman-Kim, D. *Tissue Eng. Part C Methods* **2015**, *0* (0), ten.TEC.2015.0135.

(210) Waugh, C. E.; Shing, E.; Avery, B. *Emot. Rev.* **2015**, No. 434.

(211) Eiraku, M.; Watanabe, K.; Matsuo-Takasaki, M.; Kawada, M.; Yonemura, S.; Matsumura, M.; Wataya, T.; Nishiyama, A.; Muguruma, K.; Sasai, Y. *Cell Stem Cell* **2008**, *3* (5), 519–532.

(212) Kadoshima, T.; Sakaguchi, H.; Nakano, T.; Soen, M.; Ando, S.; Eiraku, M.; Sasai, Y. *Proc. Natl. Acad. Sci. U. S. A.* **2013**, *110* (50), 20284–20289.

(213) Mariani, J.; Vittoria, M.; Palejev, D.; Tomasini, Livia; Coppola, G.; Szekely, A.M.; Horvath, T.L.; Vaccarino, M. V. *Proc. Natl. Acad. Sci.* **2012**, *109* (31), 12770–12775.

(214) Danjo, T.; Eiraku, M.; Muguruma, K.; Watanabe, K.; Kawada, M.; Yanagawa, Y.; Rubenstein, J. L. R.; Sasai, Y. *J. Neurosci.* **2011**, *31* (5), 1919–1933.

(215) Suga, H.; Kadoshima, T.; Minaguchi, M.; Ohgushi, M.; Soen, M.; Nakano, T.; Takata, N.; Wataya, T.; Muguruma, K.; Miyoshi, H.; Yonemura, S.; Oiso, Y.; Sasai, Y. *Nature* **2011**, *480* (7375), 57–62.

(216) Eiraku, M.; Takata, N.; Ishibashi, H.; Kawada, M.; Sakakura, E.; Okuda, S.; Sekiguchi, K.; Adachi, T.; Sasai, Y. *Nature* **2011**, *472* (7341), 51–56.

(217) Jeong, G. S.; Chang, J. Y.; Park, J. S.; Lee, S.-A.; Park, D.; Woo, J.; An, H.; Lee, C. J.; Lee, S.-H. *Mol. Brain* **2015**, *8*, 17.

(218) Lancaster, M. A.; Renner, M.; Martin, C.-A.; Wenzel, D.; Bicknell, L. S.; Hurles, M. E.; Homfray, T.; Penninger, J. M.; Jackson, A. P.; Knoblich, J. A. *Nature* **2013**, *501* (2), 185–185.

(219) Nasu, M.; Takata, N.; Danjo, T.; Sakaguchi, H.; Kadoshima, T.; Futaki, S.; Sekiguchi, K.; Eiraku, M.; Sasai, Y. *PLoS One* **2013**, *7* (12), e53024.

(220) Kadoshima, T.; Sakaguchi, H.; Nakano, T.; Soen, M.; Ando, S.; Eiraku, M.; Sasai, Y. *Proc. Natl. Acad. Sci.* **2014**, *111* (20), 7498–7498.

(221) Koch, P.; Opitz, T.; Steinbeck, J. A.; Ladewig, J.; Brustle, O. *Proc. Natl. Acad. Sci. U. S. A.* **2009**, *106* (9), 3225–3230.

(222) Gaspard, N.; Bouschet, T.; Hourez, R.; Dimidschstein, J.; Naeije, G.; van den Ameele, J.; Espuny-Camacho, I.; Herpoel, A.; Passante, L.; Schiffmann, S. N.; Gaillard, A.; Vanderhaeghen, P. *Nature* **2008**, *455* (7211), 351–357.

(223) Camp, J. G.; Badsha, F.; Florio, M.; Kanton, S.; Gerber, T.; Wilsch-Bräuninger, M.; Lewitus, E.; Sykes, A.; Hevers, W.; Lancaster, M.; Knoblich, J. a; Lachmann, R.; Pääbo, S.; Huttner, W. B.; Treutlein, B. *Proc. Natl. Acad. Sci. U. S. A.* **2015**, *112* (51), 15672–15677.

(224) Pan, F. C.; Wright, C. *Dev. Dyn.* **2011**, *240* (3), 530–565.

(225) Kopp, J. L.; Dubois, C. L.; Schaffer, A. E.; Hao, E.; Shih, H. P.; Seymour, P. A.; Ma, J.; Sander, M. *Development* **2011**, *138* (4), 653–665.

(226) Solar, M.; Cardalda, C.; Houbracken, I.; Martín, M.; Maestro, M. A.; De Medts, N.; Xu, X.; Grau, V.; Heimberg, H.; Bouwens, L.; Ferrer, J. *Dev. Cell* **2009**, *17* (6), 849–860.

(227) Furuyama, K.; Kawaguchi, Y.; Akiyama, H.; Horiguchi, M.; Kodama, S.; Kuhara, T.; Hosokawa, S.; Elbahrawy, A.; Soeda, T.; Koizumi, M.; Masui, T.; Kawaguchi, M.; Takaori, K.; Doi, R.; Nishi, E.; Kakinoki, R.; Deng, J. M.; Behringer, R. R.; Nakamura, T.; Uemoto, S. *Nat. Genet.* **2011**, *43* (1), 34–41.

(228) Kopinke, D.; Brailsford, M.; Shea, J. E.; Leavitt, R.; Scaife, C. L.; Murtaugh, L. C. *Development* **2011**, *138* (3), 431–441.

(229) Inada, A.; Nienaber, C.; Katsuta, H.; Fujitani, Y.; Levine, J.; Morita, R.; Sharma, A.; Bonner-Weir, S. *Proc. Natl. Acad. Sci. U. S. A.* **2008**, *105* (50), 19915–19919.

(230) Thorel, F.; Népote, V.; Avril, I.; Kohno, K.; Desgraz, R.; Chera, S.; Herrera, P. L. *Nature* **2010**, *464* (7292), 1149–1154.

(231) Montesano, R.; Mouron, P.; Amherdt, M.; Orci, L. *J. Cell Biol.* **1983**, *97* (3).

(232) Jin, L.; Feng, T.; Shih, H. P.; Zerda, R.; Luo, A.; Hsu, J.; Mahdavi, A.; Sander, M.; Tirrell, D. A.; Riggs, A. D.; Ku, H. T. *Proc. Natl. Acad. Sci. U. S. A.* **2013**, *110* (10), 3907–3912.

(233) Huch, M.; Bonfanti, P.; Boj, S. F.; Sato, T.; Loomans, C. J. M.; van de Wetering, M.; Sojoodi, M.; Li, V. S. W.; Schuijers, J.; Gracanin, A.; Ringnalda, F.; Begthel, H.; Hamer, K.; Mulder, J.; van Es, J. H.; de Koning, E.; Vries, R. G. J.; Heimberg, H.; Clevers, H. *EMBO J.* **2013**, *32* (20), 2708–2721.

(234) Lee, J.; Sugiyama, T.; Liu, Y.; Wang, J.; Gu, X.; Lei, J.; Markmann, J. F.; Miyazaki, S.; Miyazaki, J.-I.; Szot, G. L.; Bottino, R.; Kim, S. K.; Al-Hasani, K.; Pfeifer, A.; Courtney, M.; Dodge, R. J.; Anderson, W.; Gray, P.; Melton, D. *Elife* **2013**, *2*, e00940.

(235) Greggio, C.; De Franceschi, F.; Grapin-Botton, A. *Stem Cells* **2015**, *33* (1), 8–14.

(236) Greggio, C.; De Franceschi, F.; Figueiredo-Larsen, M.; Gobaa, S.; Ranga, A.; Semb, H.; Lutolf, M.; Grapin-Botton, A. *Development* **2013**, *140* (21).

(237) Alipio, Z.; Liao, W.; Roemer, E. J.; Waner, M.; Fink, L. M.; Ward, D. C.; Ma, Y. *Proc. Natl. Acad. Sci. U. S. A.* **2010**, *107* (30), 13426–13431.

(238) Raikwar, S. P.; Kim, E. M.; Sivitz, W. I.; Allamargot, C.; Thedens, D. R.; Zavazava, N. *PLoS One* **2015**, *10* (1), 1–15.

(239) Chen, Y.-J.; Finkbeiner, S. R.; Weinblatt, D.; Emmett, M. J.; Tameire, F.; Yousefi, M.; Yang, C.; Maehr, R.; Zhou, Q.; Shemer, R.; Dor, Y.; Li, C.; Spence, J. R.; Stanger, B. Z.; Rankin, S. A.; Kuhar, M. F.; Vallance, J. E.; Tolle, K.; Hoskins, E. E.; Kalinichenko, V. V.; Wells, S. I.; Zorn, A. M.; Al., E.; Szymczak, A. L.; Workman, C. J.; Greenbaum, L. E.; Stanger, B. Z.; Yechoor, V.; Liu, V.; Espiritu, C.; Paul, A.; Oka, K.; Kojima, H.; Chan, L.; Zhou, Q.; Brown, J.; Kanarek, A.; Rajagopal, J.; Melton, D. A. *Cell Rep.* **2014**, *6* (6), 1046–1058.

(240) Ariyachet, C.; Tovaglieri, A.; Xiang, G.; Lu, J.; Shah, M. S.; Richmond, C. A.; Verbeke, C.; Melton, D. A.; Stanger, B. Z.; Mooney, D.; Shivdasani, R. A.; Mahony, S.; Xia, Q.; Breault, D. T.; Zhou, Q. *Cell Stem Cell* **2016**, *18* (3), 410–421.

(241) Fatehullah, A.; Tan, S. H.; Barker, N. *Nat. Cell Biol.* **2016**, *18* (3), 246–254.

(242) Hanahan, D.; Weinberg, R. A. *Cell* **2011**, *144* (5), 646–674.

(243) Dekkers, J. F.; Wiegerinck, C. L.; De Jonge, H. R.; Bronsveld, I.; Janssens, H. M.; De Winter-de Groot, K. M.; Brandsma, A. M.; De Jong, N. W. M.; Bijvelds, M. J. C.; Scholte, B. J. *Nat. Med.* **2013**, *19* (7), 939–945.

(244) Nanduri, L. S. Y.; Baanstra, M.; Faber, H.; Rocchi, C.; Zwart, E.; de Haan, G.; van Os, R.; Coppes, R. P. *Stem cell reports* **2014**, *3* (6), 957–964.

(245) Zhang, Y.; Wu, S.; Xia, Y.; Sun, J. *Physiol. Rep.* **2014**, *2* (9), e12147.

(246) Wilson, S. S.; Tocchi, A.; Holly, M. K.; Parks, W. C.; Smith, J. G. *Mucosal Immunol.* **2015**, *8* (2), 352–361.

(247) Huch, M.; Gehart, H.; Van Boxtel, R.; Hamer, K.; Blokzijl, F.; Verstegen, M. M. A.; Ellis, E.; Van Wenum, M.; Fuchs, S. A.; de Ligt, J. *Cell* **2015**, *160* (1), 299–312.

(248) Mariani, J.; Coppola, G.; Zhang, P.; Abyzov, A.; Provini, L.; Tomasini, L.; Amenduni, M.; Szekely, A.; Palejev, D.; Wilson, M.; Gerstein, M.; Grigorenko, E. L.; Chawarska, K.; Pelphrey, K. A.; Howe, J. R.; Vaccarino, F. M. *Cell* **2015**, *162* (2), 375–390.

(249) Dang, J.; Tiwari, S. K.; Lichinchi, G.; Qin, Y.; Patil, V. S.; Eroshkin, A. M.; Rana, T. M. *Cell Stem Cell* **2016**, *19* (2), 1–8.

(250) Nowakowski, T. J.; Pollen, A. A.; Di Lullo, E.; Sandoval-Espinosa, C.; Bershteyn, M.; Kriegstein, A. R. *Cell Stem Cell* **2016**, *18* (5), 591–596.

(251) Hohwieler, M.; Illing, A.; Hermann, P. C.; Mayer, T.; Stockmann, M.; Perkhofer, L.; Eiseler, T.; Antony, J. S.; Müller, M.; Renz, S.; Kuo, C.-C.; Lin, Q.; Sendler, M.; Breunig, M.; Kleiderman, S. M.; Lechel, A.; Zenker, M.; Leichsenring, M.; Rosendahl, J.; Zenke, M.; Sainz, B.; Mayerle, J.; Costa, I. G.; Seufferlein, T.; Kormann, M.; Wagner, M.; Liebau, S.; Kleger, A. *Gut* **2016**, gutjnl-2016-312423.

(252) Baker, L. A.; Tiriac, H.; Clevers, H.; Tuveson, D. A. *Trends in Cancer* **2016**, *2* (4), 176–190.

(253) Baker, L. A.; Tiriac, H.; Corbo, V.; Boj, S. F.; Hwang, C.; Chio, I. I. C.; Engle, D. D.; Jager, M.; Ponz-Sarvise, M.; Spector, M. S.; Gracanin, A.; Oni, T.; Yu, K. H.; Boxtel, R. van; Huch, M.; Rivera, K. D.; Wilson, J. P.; Feigin, M. E.; Öhlund, D.; Handly-Santana, A.; Ardito-Abraham, C. M.; Ludwig, M.; Elyada, E.; Alagesan, B.; Biffi, G.; Yordanov, G. N.; Delcuze, B.; Creighton, B.; Wright, K.; Park, Y.; Morsink, F. H. M.; Molenaar, I. Q.; Rinkes, I. H. B.; Cuppen, E.; Hao, Y.; Jin, Y.; Nijman, I. J.; Iacobuzio-Donahue, C.; Leach, S. D.; Pappin, D. J.; Hammell, M.; Klimstra, D. S.; Basturk, O.; Hruban, R. H.; Offerhaus, G. J.; Vries, R. G. J.; Clevers, H.; Tuveson, D. A. *Clin. Cancer Res.* **2016**, *22* (16 Supplement).

(254) Boj, S. F.; Hwang, C.-I.; Baker, L. A.; Chio, I. I. C.; Engle, D. D.; Corbo, V.; Jager, M.; Ponz-Sarvise, M.; Tiriac, H.; Spector, M. S.; Gracanin, A.; Oni, T.; Yu, K. H.; van Boxtel, R.; Huch, M.; Rivera, K. D.; Wilson, J. P.; Feigin, M. E.; Öhlund, D.; Handly-Santana, A.; Ardito-Abraham, C. M.; Ludwig, M.; Elyada, E.; Alagesan, B.; Biffi, G.; Yordanov, G. N.; Delcuze, B.; Creighton, B.; Wright, K.; Park, Y.; Morsink, F. H. M.; Molenaar, I. Q.; Borel Rinkes, I. H.; Cuppen, E.; Hao, Y.; Jin, Y.; Nijman, I. J.; Iacobuzio-Donahue, C.; Leach, S. D.; Pappin, D. J.; Hammell, M.; Klimstra, D. S.; Basturk, O.; Hruban, R. H.; Offerhaus, G. J.; Vries, R. G. J.; Clevers, H.; Tuveson, D. A. *Cell* **2015**, *160* (1), 324–338.

(255) Huang, L.; Holtzinger, A.; Jagan, I.; BeGora, M.; Lohse, I.; Ngai, N.; Nostro, C.; Wang, R.; Muthuswamy, L. B.; Crawford, H. C.; Arrowsmith, C.; Kalloger, S. E.; Renouf, D. J.; Connor, A. A.; Cleary, S.; Schaeffer, D. F.; Roehrl, M.; Tsao, M.-S.; Gallinger, S.; Keller, G.; Muthuswamy, S. K. *Nat. Med.* **2015**, *21* (11), 1364–1371.